OPTIMAL STEADY STATE AND TRANSIENT OPERATION OF SIMULATED MOVING BED CHROMATOGRAPHIC PROCESSES

vorgelegt von

M.Eng. Suzhou Li

aus China

von der Fakultät IV - Elektrotechnik und Informatik

der Technischen Universität Berlin

zur Erlangung des akademischen Grades

Doktor der Ingenieurwissenschaften

Dr.-Ing.

genehmigte Dissertation

Promotionsausschuss:

Vorsitzender: Prof. Dr.-Ing. Roland Thewes

Gutachter: Prof. Dr.-Ing. Jörg Raisch

Gutachter: Prof. Dr.-Ing. Andreas Seidel-Morgenstern

Tag der wissenschaftlichen Aussprache: 21.12.2011

Berlin 2012

D 83

To my wife Fuhong Dong

Acknowledgements

No research is done in a vacuum. My research work at Max Planck Institute for Dynamics of Complex Technical Systems Magdeburg has been influenced by and benefited from many distinguished people I fortunately met.

A good boss is absolutely an asset to a PhD student. I feel incredibly lucky to have an opportunity to be supervised by two excellent advisors. I would like to express my deep gratitude towards Prof. Jörg Raisch, who initially accepted me as a PhD student in his group at MPI, and who has, over the past several years, given me a good chance and the sufficient freedom to collaborate with other MPI groups. I could always get his helpful advice at every key step of my PhD work. I am very grateful for his complete confidence, continuous guidance and full support for the joint projects I have been involved in. I highly appreciate Prof. Andreas Seidel-Morgenstern for allowing me to get involved in his projects and providing a wonderful cooperating platform for me. His energy, enthusiasm, patience and scholarship encouraged me to conquer any difficulty I encountered during my PhD studies. The discussions with him were always sources of new ideas. His perfect balance between freedom and constraint has enabled me to exploit my full research potential and to appreciate the fun of doing scientific work.

I would like to acknowledge Assistant Prof. Yoshiaki Kawajiri from the School of Chemical & Biomolecular Engineering in Georgia Institute of Technology for the fruitful collaboration over the years. It was really a great pleasure to work with Yoshi. He spent countless time and effort discussing with me, addressing my problems and giving me useful suggestions. His patience, hard work and vast expertise left a deep impression on me. I also thank his support and help during his postdoctoral stay at MPI, which created a good start for our later collaboration. Yoshi, we have done an excellent team work

together! Furthermore, I am particularly indebted to Dr. Malte Kaspereit from MPI Magdeburg, Prof. Marco Mazzotti from ETH Zurich, Assistant Prof. Arvind Rajendran from NTU Singapore and Prof. Sebastian Engell from TU Dortmund for their constructive suggestions for my work.

I want to thank all the group members with whom I had the fortune to work. In particular, special thanks to the former group member Dmitry Gromov. We had worked on the first DFG project together for more than one year and I learned a lot from him. Many thanks to my officemate Naim Bajcinca, a "paper killer" previously working at DLR, for sharing his experience with me. His hard work with great enthusiasm set an example for me. My sincere gratitude also goes to the group secretary Janine Holzmann. Reading a letter written in German sometimes was a big headache. You always made everything easier. Thanks, Janine, for your endless help during my stay in Magdeburg.

Being a wife of a PhD student is not easy. It is even more difficult if she is also a PhD student. My deepest appreciation to my wife, Fuhong, who needs not only to do her work but also to take care of the life. Thanks for putting up with such a terrible man during these years and for always being there to share all of life's gifts and challenges with me. Without your everyday love, patience and inspiration, this work would not have been possible.

Finally, I thank my parents and my grandparents for their selfless love, constant understanding and encouragement throughout my research.

Suzhou Li

Magdeburg, August 2011

Abstract

The dissertation deals with the optimal steady state and transient operation problems of simulated moving bed (SMB) chromatographic processes. For the first topic that is discussed in the first part of the thesis, we optimize the steady state operation of one newly developed SMB variant, called fractionation and feedback SMB (FF-SMB). We aim to demonstrate the effectiveness of this advanced operating mode, to evaluate its optimal potential systematically and to explore its practical applicability. In the second part of the thesis, we turn our research endeavors to optimal startup and shutdown issues of conventional SMB. The aim is to develop efficient startup and shutdown procedures with the ability to overcome drawbacks of conventional schemes and to improve the transient performance of SMB.

For the optimization of FF-SMB, we concentrate our attention firstly on the case where only one outlet is used for fractionation. A rigorous model-based optimization approach is adopted to optimize this fractionation mode. The effectiveness of the concept is demonstrated and its relative potentials over the classical SMB are assessed quantitatively. The results reveal that the new operating regime significantly outperforms SMB in terms of maximum feed throughput and minimum desorbent consumption for both linear and Langmuir isotherms.

We then extend the previous concept to the general scenario that fractionates both outlet streams simultaneously. The optimization strategy proposed is also extended to deal with this more flexible fractionation policy. To evaluate its superiority over the existing two single fractionation options and the SMB concept, extensive optimization studies are carried out for these process alternatives. The performance comparison shows that the double fractionation regime is most productive, although each single fractionation scheme is

clearly superior to SMB. The effectiveness of the extension is also illustrated in terms of commonly used performance parameters. Besides, the practical applicability of FF-SMB is analyzed in detail by examining the effect of different parameters on its relative advantages. The studies show that FF-SMB has more potential for difficult separations characterized by high purity requirements, low column efficiency, small selectivity and a small number of columns. For such kind of applications, FF-SMB is a highly competitive alternative to SMB and its other derivatives.

Furthermore, we also explore the possibility of exploiting the potential of FF-SMB by enriching the recycled fractions before feeding them back into the unit. It is found that this enrichment operation allows to create more concentrated recyclates. Recycling the resulting enriched fractions is proven advantageous for FF-SMB and leads to further performance enhancement.

Efficient startup and shutdown procedures are highly advantageous for SMB regardless of production scale. The complex mixed discrete and continuous dynamics of SMB poses a significant challenge for the development of efficient transient strategies. The conventional startup and shutdown approaches, which simply specify steady state operating conditions as transient policies, are very often used in practice. However, they suffer from a few shortcomings, such as long transient duration and high desorbent consumption. Moreover, the products collected during transient periods may not be necessarily guaranteed to respect required specifications. They have to be discarded or subject to reprocessing in the case of off-spec production, leading to an extremely adverse impact upon the overall process economics and efficiency. These drawbacks become particularly serious for small-scale separation campaigns.

To surmount these limitations and to improve the transient performance,

the thesis presents new multistage optimal startup and shutdown procedures in the second part. Compared to the conventional operation, the proposed concept allows for a stage-wise modulation of transient operating conditions and is able to take the product quality specifications into account. The optimal transient operation is then formulated as a dynamic optimization problem. The inherent periodic nature of the process dynamics largely complicates the direct solution of the original problem. We suggest a specially tailored decomposition algorithm to guarantee the computational tractability. This solution strategy decomposes the overall problem into a sequence of stage-wise sub-problems, each of which is of reduced complexity and thus easier to deal with. The procedure then solves these problems sequentially until some given convergence criterion for steady state is fulfilled. By examining a separation example with Langmuir isotherm, the feasibility of the solution algorithm is demonstrated, and the performance of the conventional and multistage optimal schemes is compared systematically. The results show that the newly suggested regimes not only significantly shorten transient time, but also drastically reduce desorbent usage. Another attractive advantage of the multistage approach lies in its capability of optimizing the transient performance while respecting the product quality requirements. Aided by this strength, the process can achieve on-spec production of both extract and raffinate products even over the startup and shutdown periods, which is proven infeasible with the conventional methods. The developed startup and shutdown strategies not only are advantageous for continuous large-volume purifications, but also can expand the applicability of SMB to small batch productions.

Contents

List of Figures

List of Tables

1

Introduction

1.1 Overview of SMB chromatography

Efficient separation and purification technologies are of crucial importance in process industries. Chromatography, among various unit operations, has been regarded as one of the flexible and powerful tools for the isolation of valuable products at different production scales. Conventionally, such processes are operated in a batch mode, where the separation is performed by repeatedly injecting samples of the feed mixture into a stream of mobile phase which flows through a chromatographic column packed with a suitable stationary phase. Because the solutes to be resolved exhibit different adsorption affinities to the stationary phase, they move with different velocities in the column, and thus separate from each other as they exit the column. The batch chromatography provides the distinct advantages of being flexible and easy to operate, requiring a low investment cost, and being able to realize multicomponent separations. However, due to its batchwise nature, the process usually suffers from limited productivity and high solvent consumption, resulting in highly diluted products. In order to overcome these

limitations, the continuous simulated moving bed (SMB) process was developed and patented by Universal Oil Products (UOP, USA) in the early 1960s [1]. It is a practical implementation of the hypothetical true moving bed (TMB) concept where a real countercurrent movement between the mobile and solid phases is involved but proven to be technically infeasible. The SMB process consists of multiple chromatographic columns connected in series, and the continuous countercurrent movement is achieved approximately by periodically shifting the inlet and outlet ports in the direction of the liquid flow. By using such an ingenious way of simulating countercurrent motion, SMB benefits from the desired countercurrent operation but avoids the practical shortcomings caused by moving the solid phase directly. A more detailed description of the process is presented in Chapter 2.

With the widely acknowledged advantages over batch separation, SMB chromatography has been used with tremendous success in the petrochemical and sugar industries over the last several decades. In the past few years, it has emerged as a promising technology for the complex and difficult separations that are often encountered in the fine chemical, pharmaceutical and biotechnology industries [4, 5]. In particular, triggered by the first example of chiral separation [3], SMB has attracted growing interest in the area of enantioseparations using chiral stationary phases [2, 6].

Currently, SMB has been consolidating its position as a separation and purification tool in the aforementioned areas. The increasing demands and challenging applications in these industries in turn place higher requirements on the process performance, and have constituted a strong driving force for the continuously emerging modifications to the conventional SMB operation. Representative extensions and developments include the use of supercritical fluid [9], temperature [10] or solvent gradient [11] on SMB units, and variation

of certain operating parameters which are kept constant in the classical mode. Examples for this later approach include VariCol [12], PowerFeed [13] and ModiCon [14]. Many attempts were also exploited to either reduce or increase the number of zones in the unit [15, 16, 17, 18]. More sophisticated operating regimes using only a single column to reproduce the SMB principle have already emerged and been subject to intensive research [19, 20, 21, 22]. In addition, several efforts which introduce on-off characteristics at either the inlet or the outlet streams have been made. The "Partial Feed" [23], "Partial Discard" [24], and fractionation and feedback SMB (FF-SMB) [26] fall into this category. For a more complete overview of various variants of SMB chromatography, we refer to the review given by Seidel-Morgenstern et al. [7]. It can be expected that more new processes will emerge in the near future as the research advances.

Recently, Rajendran et al. [8] gave a rather comprehensive review of SMB chromatography and its related subjects, and summarized future research challenges and open issues.

1.2 Relevance and motivation

The newly emerging concepts reviewed in the previous section offer the potential to further enhance the performance of the conventional process but often at the expense of additional complexity. Thus, the determination of design and operating parameters for these variants as to exploit their superiority is an important and challenging topic. The traditional simulation based trial-and-error procedures are more or less straightforward, but time-consuming and cannot guarantee to find the optimal operating condition. Furthermore, the short-cut design approaches developed for SMB are not

applicable to the non-standard processes. These facts clearly motivate us to employ rigorous model-based optimization strategies for the process design and operation. They not only allow to handle the flexibility of the operation alternatives, but provide the capability to realize the full process potential. With highly efficient and robust solution strategies, the performance evaluation of a new concept can be performed systematically. Such theoretical assessments are particularly relevant, since they can help identify relative advantages of the variant over the conventional mode and also reveal its potential operational limitations, before the detailed experimental validation and application begin.

On the other hand, for the conventional SMB and its derivatives, significant research efforts currently focus on the cyclic steady state (CSS). By contrast, systematic studies of the transient processes (e.g., startup and shutdown) remain largely unexplored and efficient transient procedures are rarely reported in the SMB community. Frequently conventional startup and shutdown approaches are used in practical applications at various scales. These operating policies, although being simple to implement, usually lead to long transient duration and a large amount of desorbent consumption. Moreover, the products obtained during the transient phases are often off-spec and have to be discarded or reprocessed, which gives rise to a loss of valuable products and additional separation costs. For large-scale separations where the steady state production typically occupies most of the operational time, these shortcomings may be tolerated to some degree but they are always harmful and unwanted. As SMB is increasingly extended to the fine chemical, biotechnology and pharmaceutical industries, small-scale campaigns, such as those in the stage of drug development, have become extremely ubiquitous nowadays. They are characterized by small batch sizes and last a short campaign

cycle. The transient period is also comparable to the production time. Obviously, in such a context the poor transient performance would result in more detrimental effects upon the overall process efficiency and economics. The above aspects give us a strong motivation for developing efficient startup and shutdown strategies for SMB processes.

1.3 Objectives and thesis structure

The thesis has two main objectives. The first objective is to develop an efficient model-based optimization tool and to systematically evaluate the optimum potential of a novel process variant FF-SMB, which has been suggested recently [26] and introduces the outlet fractionation and feedback scheme to the classical SMB operation. The second objective of the thesis is devoted to the development of new multistage optimal startup and shutdown procedures for the conventional SMB process.

We organize the thesis into ten chapters. The first chapter gives a short overview of SMB chromatography and its development, highlights the relevance and motivation of this work, defines our objectives and clarifies the structure of the thesis. The second chapter includes a brief description on the principles of TMB and SMB chromatography and discusses the related issues of mathematical modeling and numerical simulation. A basic introduction of the popular short-cut design tool, i.e., the triangle theory, is also presented. This chapter provides the essential research background for the next chapters.

After the two introductory chapters, the thesis then focuses on addressing the performance optimization and evaluation of FF-SMB. This first part is organized in Chapters 3–6 and based on the following published contribu-

tions:

- S. Li, Y. Kawajiri, J. Raisch, A. Seidel-Morgenstern, Optimization of simulated moving bed chromatography with fractionation and feedback: Part I. Fractionation of one outlet, J. Chromatogr. A 1217 (2010) 5337-5348.

- S. Li, Y. Kawajiri, J. Raisch, A. Seidel-Morgenstern, Optimization of simulated moving bed chromatography with fractionation and feedback: Part II. Fractionation of both outlets, J. Chromatogr. A 1217 (2010) 5349-5357.

- S. Li, Y. Kawajiri, J. Raisch, A. Seidel-Morgenstern, Optimization of simulated moving bed chromatography with fractionation and feedback incorporating an enrichment step, Computer Aided Chemical Engineering 29 (2011) 818-822.

Chapter 3 presents an overview regarding exploitation of various recycling techniques in both conventional batch chromatography and continuous SMB operation. Chapter 4 deals with the optimization of FF-SMB realizing one outlet fractionation. In this chapter, we lay particular emphasis on the technical details including the principle of fractionation and feedback, its mathematical modeling, the resulting nonlinear programming problems and solution algorithms. In Chapter 5, the concept examined in the previous chapter is extended to the general case where both outlets are fractionized simultaneously. The focus of this chapter is concentrated on evaluating the optimal performance of various fractionation policies and addressing the general applicability problem of the new process. Chapter 6 details a further development that incorporates an enrichment step into FF-SMB. The effectiveness of such modification is evaluated with the aid of the optimization

tool developed in the preceding chapters.

The second part of the thesis is aimed to address the optimal startup and shutdown problems of SMB. This part involves three chapters and describes the work recently published in the following papers:

- S. Li, Y. Kawajiri, J. Raisch, A. Seidel-Morgenstern, Optimal startup operation of simulated moving bed chromatographic processes, in: Proc. of the 9th International Symposium on Dynamics and Control of Process Systems, Leuven, Belgium, 2010, 725-730.

- S. Li, Y. Kawajiri, J. Raisch, A. Seidel-Morgenstern, Optimization of startup and shutdown operation of simulated moving bed chromatographic processes, J. Chromatogr. A 1218 (2011) 3876-3889.

We begin this part with a short introduction to the transient operation of SMB in Chapter 7, with special emphasis on the relevance and advantages of investigating this challenging topic. A fairly comprehensive review of the previous related work in the area is then given. Chapter 8 firstly deals with the issue of mathematical modeling of transient behavior. It then outlines various design methods developed for the steady state operation of SMB chromatography, followed by a detailed discussion concerning the conventional transient operation schemes. Their advantages and shortcomings are pointed out at the end of the chapter. Chapter 9 describes our new multistage optimal startup and shutdown regimes and presents the corresponding problem formulations. Due to significant difficulties in addressing the resulting dynamic optimization problems, we develop a specially tailored decomposition solution algorithm to ensure the computational tractability. By examining the transient operation of a case study with nonlinear Langmuir isotherm, the feasibility of the proposed solution strategy is illustrated and the systematic

performance evaluation of different transient operating regimes is carried out.

Chapter 10 concludes the thesis and suggests some perspectives for future work.

2

Background

2.1 Simulated moving bed chromatographic processes

As reviewed in Chapter 1, batch chromatography is one of the widely used separation techniques. However, the inherent drawbacks of low productivity and high operating cost restrict its applicability and motivate to develop more efficient continuous chromatographic separation units. Continuous countercurrent operations are adopted in many chemical processes, such as distillation, gas adsorption and heat exchange, since they allow to maximize the driving force for mass or heat transfer. This concept has been also exploited in the chromatographic process, leading to the suggestion of the true moving bed (TMB) operation schematically shown in Fig. 2.1. Here the classical four-zone configuration for the separation of a binary mixture of A and B is considered for illustrative purposes. The process has two inlets (feed, desorbent) and two outlets (extract, raffinate), which divide the unit into four zones that operate with different liquid flow-rates and fulfill distinct roles.

The feed stream is continuously supplied to the system between two central zones, i.e., zone II and III, where the separation occurs. The desorbent is introduced continuously from the inlet of zone I. The extract and raffinate products are withdrawn at the outlet of zone I and III, respectively. With an appropriate choice of operating conditions, complete resolution of the feed mixture can be achieved so as the less retained component A is carried by the liquid phase and collected at the raffinate outlet, while the more retained component B is conveyed by the solid phase towards the opposite direction and withdrawn at the extract outlet. Furthermore, the less retained component A entering zone IV is adsorbed to regenerate the solvent, which can then be mixed with the fresh solvent and recycled to zone I. Similarly, the more retained component B is desorbed in zone I to regenerate the solid phase before it is recycled to zone IV.

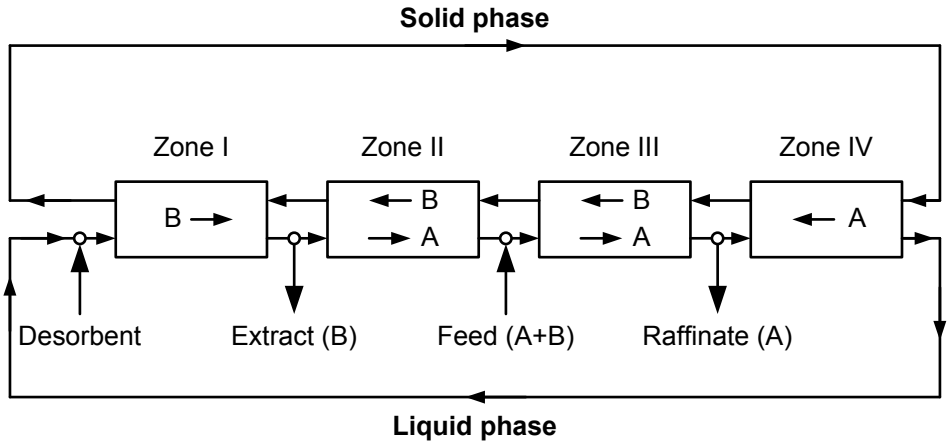

Figure 2.1: Schematic of a four-zone true moving bed (TMB) unit for the separation of a binary mixture of A and B.

The TMB process is of continuous nature and allows for continuous processing of the feed. The recycling of the mobile phase results in a relatively low solvent consumption. Furthermore, the countercurrent contact of two

phases significantly improves the mass transfer characteristics and enables more efficient utilization of the adsorbent capacity. With these distinctive features, the process provides unique advantages over the conventional batch chromatography in terms of productivity, recovery, and solvent economy. In addition, contrary to batch chromatography, overlapping of the solute profiles in TMB is not a concern, provided that the solute concentration profiles are resolved enough to provide high purity products at the outlets. This makes TMB ideally suited for difficult separations with low selectivity. Unfortunately, the TMB process suffers from difficulties in maintaining a continuous and stable circulation of the particulate solid phase, since moving the solid imposes many formidable technical problems, such as particle abrasion and back-mixing. As a result, TMB chromatography is only a theoretical concept and not used in reality.

To overcome the inherent drawbacks of the TMB process, simulated moving bed (SMB) chromatography was introduced by Broughton and Gerhold from UOP in 1961 [1], where the continuous separation is achieved by simulating the countercurrent movement of the solid adsorbent in a discrete manner. The schematic diagram of a standard four-zone SMB unit is shown in Fig. 2.2. The process consists of multiple fixed bed chromatographic columns which are connected to each other to form a closed circle. Like TMB, it has two inlet (feed, desorbent) and two outlet (extract, raffinate) ports which divide the unit into four zones. Each zone can arrange one or more columns. The continuous movement of the solid phase in the TMB process is simulated by synchronously advancing the inlet and outlet lines by one column in the direction of the liquid flow after a certain switching period t_s (see Fig. 2.2). Such movement is better approximated when each zone has a large number of columns and the port switching occurs at high frequency. Due

to the cyclic port shifting along the circularly arranged columns, the SMB process never reaches a steady state with constant profiles of the process variables. Alternatively, after an initial transient startup stage, the so-called cyclic steady state (CSS) is attained, where the process variables exhibit the same time-dependent but periodic behavior over each switching interval.

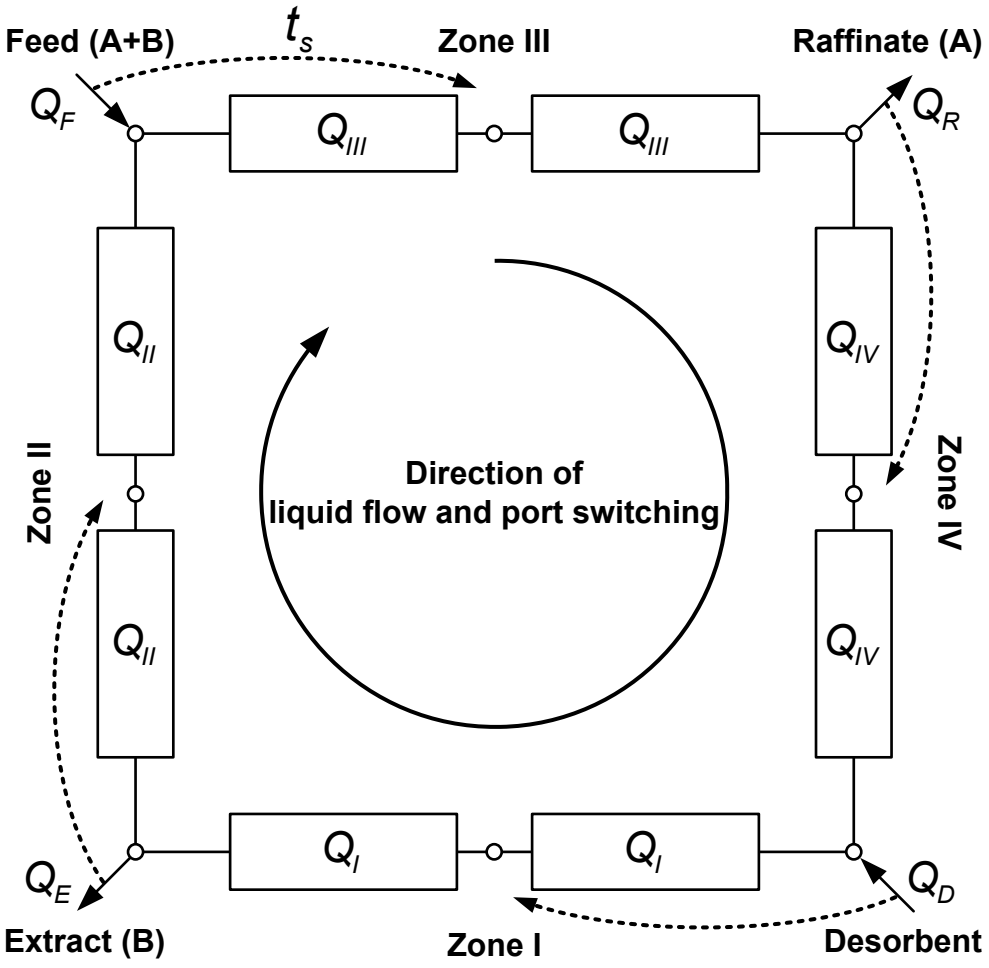

Figure 2.2: Schematic of a four-zone simulated moving bed (SMB) unit with 2 columns in each zone. The dashed arrows indicate the periodic port switching.

2.2 Mathematical modeling and simulation

In order to quantitatively characterize the dynamic behavior of the SMB process, an effective mathematical model capable of capturing both continuous chromatographic separation and periodical port switching is required. Such a model can be assembled from the chromatographic column models and the node equations. The column models describe the material balance of the single columns, and the node equations consider the mass conservation around the inlet and outlet nodes.

2.2.1 Modeling chromatographic columns

The dynamics of the single chromatographic columns can be modeled at different degrees of complexity, depending on how many physical phenomena they account for. An overview of various models with varying complexity is given by Guiochon in [27]. In this work, the well-established equilibrium dispersive model [27, 28] was used to characterize the single column dynamics. The model offers a good compromise between accuracy and computational efficiency and thus has been extensively exploited for the design, optimization and control of SMB processes [14, 26, 29, 30, 31]. In this model the differential mass balance of component i in each column can be written as

$$\frac{\partial c_i}{\partial t} + \frac{1-\epsilon}{\epsilon}\frac{\partial q_i}{\partial t} + v\frac{\partial c_i}{\partial z} = D_{ap,i}\frac{\partial^2 c_i}{\partial z^2}, \quad i = A,\, B \tag{2.1}$$

with the following initial and Danckwerts boundary conditions

$$c_i(t,z)|_{t=t_0} = c_{i,0}(z) \tag{2.2}$$

$$D_{ap,i}\frac{\partial c_i}{\partial z}\Big|_{z=0} - v(c_i|_{z=0} - c_i^{in}(t)) = 0, \quad D_{ap,i}\frac{\partial c_i}{\partial z}\Big|_{z=L} = 0 \tag{2.3}$$

where c_i and q_i are the concentrations of component i in the liquid and solid phases, respectively, v the interstitial liquid velocity, t the time, z the ax-

ial coordinate along the column, ϵ the total porosity of the column, L the column length, t_0 the initial time, $c_{i,0}$ the initial concentration of component i, and c_i^{in} the concentration of component i at the column inlet. The model assumes an instantaneous equilibrium between the liquid and solid phases. The contributions to band broadening due to axial dispersion and mass transfer resistances are lumped into the apparent dispersion coefficients $D_{ap,i}$. For simplicity, the same coefficient was assumed for both components in this work and determined by using [28]:

$$D_{ap,i} = \frac{vL}{2N_p} \tag{2.4}$$

with N_p being the number of theoretical plates per column, which is commonly used to measure the column efficiency.

2.2.2 Adsorption isotherms

For the above model, an adsorption isotherm model which characterizes the equilibrium of the components between the two phases is needed. Such a model should be accurate enough to describe the adsorption behavior of the mixture to be separated. A number of different isotherm models for liquid-solid equilibrium are discussed in [28]. Here only linear and nonlinear competitive Langmuir equilibrium isotherms were considered:

Linear isotherm:

$$q_i = H_i c_i, \quad i = A,\, B \tag{2.5}$$

where H_i is the Henry constant of component i.

Nonlinear isotherm:

$$q_i(c_A, c_B) = \frac{H_i c_i}{1 + K_A c_A + K_B c_B}, \quad i = A,\, B \tag{2.6}$$

with K_i being the thermodynamic coefficient of component i. Note that the linear isotherm can be considered as a special case of the Langmuir isotherm, since the latter converges to the linear case when the concentrations of both components in the liquid phase are sufficiently small.

2.2.3 Node balances

By considering the mass balance at the inlet and outlet ports (refer to SMB schematic diagram of Fig. 2.2), one set of node equations reads as follows:

Desorbent node:

$$Q_{IV} + Q_D = Q_I \tag{2.7}$$

$$c_{i,IV}^{out} Q_{IV} = c_{i,I}^{in} Q_I \tag{2.8}$$

Extract node:

$$Q_I - Q_E = Q_{II} \tag{2.9}$$

$$c_{i,I}^{out} = c_{i,II}^{in} = c_i^E \tag{2.10}$$

Feed node:

$$Q_{II} + Q_F = Q_{III} \tag{2.11}$$

$$c_{i,II}^{out} Q_{II} + c_i^F Q_F = c_{i,III}^{in} Q_{III} \tag{2.12}$$

Raffinate node:

$$Q_{III} - Q_R = Q_{IV} \tag{2.13}$$

$$c_{i,III}^{out} = c_{i,IV}^{in} = c_i^R \tag{2.14}$$

where $Q_j \, (j = I, II, III, IV)$ are the four internal flow-rates, Q_D the desorbent flow-rate, Q_E the extract flow-rate, Q_F the feed flow-rate, Q_R the raffinate flow-rate, $c_{i,j}^{in}$ and $c_{i,j}^{out}$ the liquid concentrations of component i entering and leaving zone j, c_i^E and c_i^R the liquid concentrations of component

i at the extract and raffinate outlets, and c_i^F the feed concentration of component i, $i = A, B$.

The mathematical model described in Section 2.2.1 for each column can be connected by the node equations to form the nonlinear dynamic model of the SMB process, which is represented by a system of coupled partial differential equations (PDEs). The PDE system can be reduced to a system of ordinary differential equations (ODEs) or differential algebraic equations (DAEs) by efficient spatial discretization schemes. In the present work, the orthogonal collocation on finite elements (OCFE) approach [32] was employed to discretize the original dynamic system. A system of linearly-implicit index-1 DAEs of the following form was then obtained:

$$M(C(t))\,\dot{C}(t) = f(t, C(t), u) \tag{2.15}$$

$$C(t_0) = C_0 \tag{2.16}$$

where $C(t) \in \mathbb{R}^{N_C}$ is the resulting state variables which represent the concentrations in the liquid phase at the grid nodes, $C_0 \in \mathbb{R}^{N_C}$ the consistent initial conditions, and $u \in \mathbb{R}^{N_u}$ the vector of operating parameters. The above DAEs were solved by using the DASPK3.1 package [33]. The periodic port switching must be considered when integrating the model equations. Such switching mechanism was implemented by specifying the initial concentration profile of one column for the k-th switching period using the concentration profile of its neighboring downstream column at the end of the previous period $k-1$.

2.3 Triangle theory

Over the last decade, the so-called triangle theory as a graphic short-cut design tool, has achieved great popularity among SMB practitioners. The

theory is based on the simplified TMB model and developed in the framework of equilibrium theory, which assumes that axial dispersion and mass transfer resistances can be neglected, and the adsorption equilibrium between the liquid and solid phases is established instantaneously everywhere in the columns. Although neglecting the effects of non-idealities, this approach presents many advantages for the design and operation of SMB processes. It requires only the knowledge of the adsorption isotherm parameters and the feed composition, to determine optimal and robust operating conditions that can ensure complete separation of the mixture. It provides a deep insight into the dynamics exhibited by SMB separations, and in particular allows for a better understanding of how the operating conditions, e.g., feed composition and flow-rate, affect the separation performance. Furthermore, the usefulness of the tool also lies in that it gives good initial guesses for rigorous model-based optimization procedures. The triangle theory was initially developed for systems characterized by linear and Langmuir isotherms [34, 35], and has been extended to separations subject to bi-Langmuir [36] and generalized Langmuir isotherms [37]. More recently, several studies have been devoted to the development of design tools for SMB units under reduced purity requirements [38, 39]. An excellent summary of the triangle theory and its valuable extensions is given in [8].

In the triangle theory, the key operating parameters are the four dimensionless m-factors, which are defined as the net flow-rate ratios in the four zones of the SMB unit:

$$m_j = \frac{Q_j t_s - V_{Col}\epsilon}{V_{Col}(1-\epsilon)}, \quad j = I, II, III, IV \tag{2.17}$$

with t_s being the switching period and V_{Col} the column volume. In this section, the design criteria for complete separation in terms of linear and Langmuir isotherms are briefly presented.

2.3.1 Linear isotherms

For a system governed by a linear adsorption isotherm given by Eq. (2.5), the necessary and sufficient conditions for complete separation consist of the following inequalities [35]:

$$H_B < m_I < \infty \tag{2.18}$$

$$H_A < m_{II} < m_{III} < H_B \tag{2.19}$$

$$0 < m_{IV} < H_A \tag{2.20}$$

Provided that the constraints on m_I and m_{IV} are fulfilled, the operating variables m_{II} and m_{III} define a plane. The plane can be partitioned into six feasible regions each of which provides a different separation performance, as shown in Fig. 2.3. Note that the region that lies below the diagonal of the (m_{II}, m_{III}) plane is not operationally feasible, since $m_{II} < m_{III}$ must be fulfilled to ensure a positive feed flow-rate.

First, note that the region where the separation can take place is constrained by $m_{II} < H_B$ and $m_{III} > H_A$. Violation of the former (Region 1 in Fig. 2.3) or the latter inequality (Region 2) causes the extract or raffinate stream to be flooded by the solvent, respectively, and no separation can be achieved. Furthermore, the conditions given in Eq. (2.19) delimit a triangle region (Region 3) where the corresponding operating conditions lead to a complete separation of A and B. Region 4, located to the left of the triangle of complete separation, defines the operating points where the raffinate is pure while the extract outlet is polluted. Region 5 corresponds to an opposite situation where the pure extract is withdrawn whereas the raffinate stream is polluted. Finally, the operating points in region 6 determined by $m_{II} < H_A$ and $m_{III} > H_B$, lead to pollution of both streams and no pure products can be obtained.

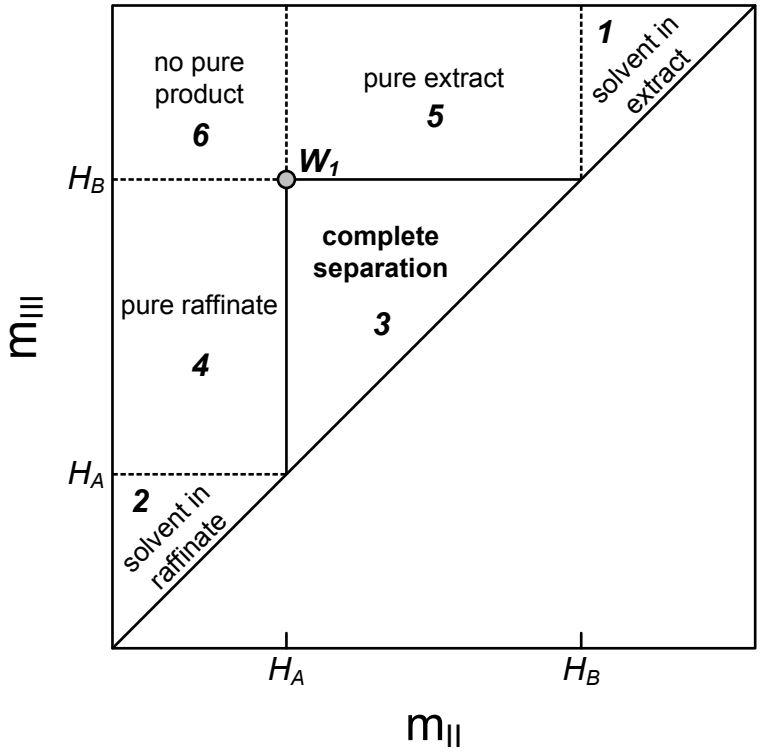

Figure 2.3: Complete separation region in the (m_{II}, m_{III}) operating parameter space for a system with linear adsorption isotherm.

On the other hand, the constraints given by Eqs. (2.18) and (2.20) delimit a rectangular region in the upper half of the (m_{IV}, m_I) plane (see Fig. 2.4) that corresponds to a complete regeneration of both the liquid and solid phases. If the constraint on the operating variable m_I is violated, incomplete regeneration of the solid phase can occur which pollutes the raffinate stream. Similarly, violation of the constraint on m_{IV} results in incomplete regeneration of the liquid phase which pollutes the extract outlet. If the inequalities imposed on m_I and m_{IV} are violated, the separation suffers from incomplete regeneration of both phases, leading to poor extract and raffinate purity. Note that only the upper half of the (m_{IV}, m_I) plane constitutes a feasible operating region because a positive desorbent flow-rate must be maintained.

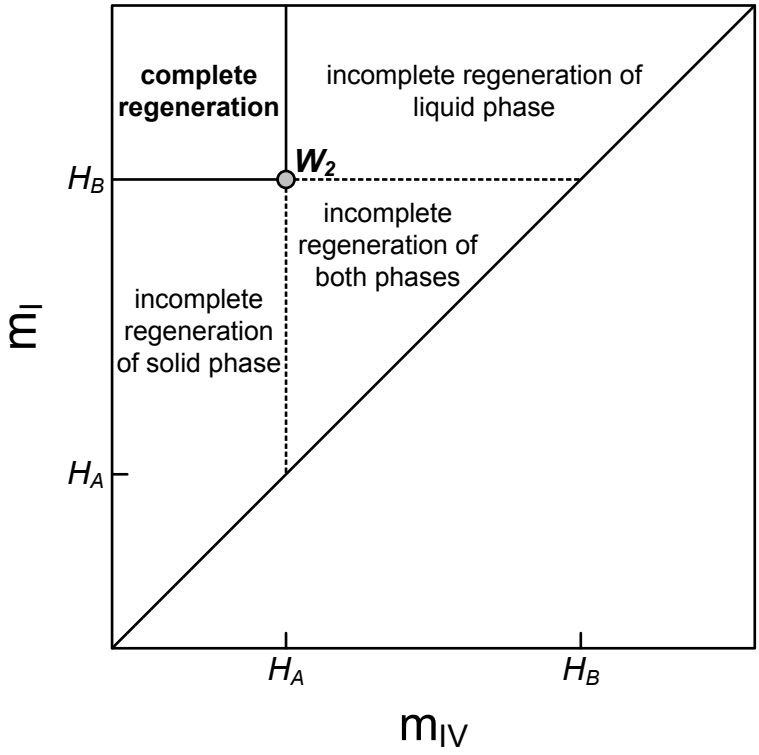

Figure 2.4: Complete regeneration region in the (m_{IV}, m_I) operating parameter space for a system with linear adsorption isotherm.

In the previous discussion, the separation performance is evaluated according to only the purity of the product streams. The triangle theory also considers how to determine the optimal operating conditions for a given performance parameter within the complete separation region. For this purpose, several performance criteria are defined in [35] as explicit functions of the flow-rate ratios m_j. One of the most important performance parameters is the productivity PR, defined as the mass of pure product recovered per unit time and unit mass of solid phase:

$$PR = \frac{Q_F\, c_T^F}{N_{Col}\, V_{Col}\, \rho_s\, (1-\epsilon)} = \frac{c_T^F\, (m_{III} - m_{II})}{N_{Col}\, \rho_s\, t_s} \tag{2.21}$$

where ρ_s is the density of the stationary phase, N_{Col} the total number of

columns in the unit and $c_T^F = c_A^F + c_B^F$ the overall feed concentration. From the definition, it can be easily observed that for a constant switching time t_s and feed concentration, the productivity is improved when the difference $(m_{III} - m_{II})$ increases. Thus, in the case of complete separation, the optimal operating point that maximizes the productivity is the vertex of the triangular region of complete separation (i.e., W_1 in Fig. 2.3).

Another key performance parameter is the desorbent requirement DR, which is defined as the mass of desorbent required to separate a unit mass of pure product:

$$DR = \frac{(Q_D + Q_F)\,\rho_D}{Q_F\,c_T^F} = \frac{\rho_D}{c_T^F}\left(1 + \frac{m_I - m_{IV}}{m_{III} - m_{II}}\right) \tag{2.22}$$

where ρ_D is the desorbent density. Note that in the above equation the feed mixture is assumed to be highly diluted so that its density is identical to the desorbent density. If this assumption does not hold, the equation is subject to modification. Obviously, the minimum desorbent consumption corresponds to the vertex of the rectangular complete regeneration region in the (m_{IV}, m_I) plane, i.e., point W_2 indicated in Fig. 2.4, since it minimizes the difference $(m_I - m_{IV})$.

However, it is worth noting that the optimal operating points identified above are not robust. Operating the unit at these conditions makes the process performance rather sensitive to various kinds of disturbances. As a result, an operating point inside the complete separation or regeneration region is often chosen alternatively in practice to create a safety margin and to ensure a robust operation. This means that there exists a compromise between robustness and separation performance.

2.3.2 Langmuir isotherms

The design criteria shown in the previous section are restricted to systems exhibiting linear adsorption behavior. The triangle theory can be also extended to derive design criteria for a rather broad class of nonlinear isotherms of great practical interest. For a separation whose adsorption equilibrium is described by the competitive Langmuir isotherm given by Eq. (2.6), the following conditions should be imposed on the flow-rate ratios m_j to achieve complete separation [35]:

$$H_B = m_{I,min} < m_I < \infty \tag{2.23}$$

$$m_{II,min} < m_{II} < m_{III} < m_{III,max} \tag{2.24}$$

$$0 < m_{IV} < m_{IV,max} \tag{2.25}$$

The results are formally similar to those obtained in the linear case. The constraints given by Eqs. (2.23) and (2.25) ensure the complete regeneration of the solid and liquid phases, respectively. The constraints on the operating parameters m_{II} and m_{III} guarantee the complete separation of the binary mixture. However, a few additional remarks are necessary at this point. First of all, the operating variables m_I and m_{IV}, as in the case of the linear isotherm, have explicit lower and upper bounds. But note that the upper bound on m_{IV} is an explicit function of the flow-rate ratios m_{II} and m_{III}:

$$\begin{aligned} m_{IV,max} = \frac{1}{2}\Big\{ & H_A + m_{III} + K_A c_A^F (m_{III} - m_{II}) \\ & - \sqrt{[H_A + m_{III} + K_A c_A^F (m_{III} - m_{II})]^2 - 4 H_A m_{III}} \Big\} \end{aligned} \tag{2.26}$$

On the other hand, the lower limit of m_I does not depend on the other flow-rate ratios. By contrast, the constraints on m_{II} and m_{III} are implicit but do not depend on m_I and m_{IV}. They delimit a distorted triangular region

of complete separation in the (m_{II}, m_{III}) plane as shown in Fig. 2.5. The boundaries of this region are determined by one set of explicit equations obtained by transforming the implicit inequality given by Eq. (2.24). As in the linear case, in addition to the complete separation region, the upper half of the (m_{II}, m_{III}) plane also includes other regions offering different separation performances, as indicated in Fig. 2.5. Note that the information about the separation regions is only valid provided that the constraints defined by Eqs. (2.23) and (2.25) are fulfilled. The vertex of the complete separation region, i.e., point W_3 in Fig. 2.5, leads to the maximum productivity, since it corresponds to the maximum difference between m_{III} and m_{II}.

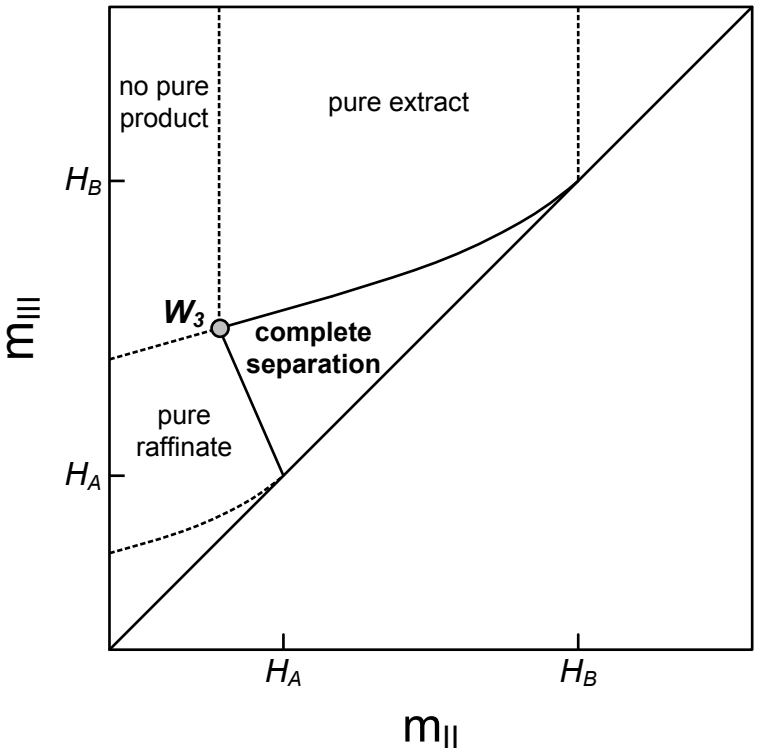

Figure 2.5: Complete separation region in the (m_{II}, m_{III}) operating parameter space for a system characterized by the Langmuir adsorption isotherm.

Furthermore, for nonlinear isotherms the region of complete separation

depends not only on the adsorption equilibrium parameters, but also on the concentration of the solutes in the feed. The impact of the total feed concentration on the complete separation region is illustrated in Fig. 2.6 for the case of the Langmuir isotherm. It is observed that as the feed concentration increases, the complete separation region shrinks and its vertex, i.e., the optimal operating point, moves towards the lower left corner of the (m_{II}, m_{III}) plane. For a limiting case where the total feed concentration approaches zero, the triangular region approximates that of the linear case.

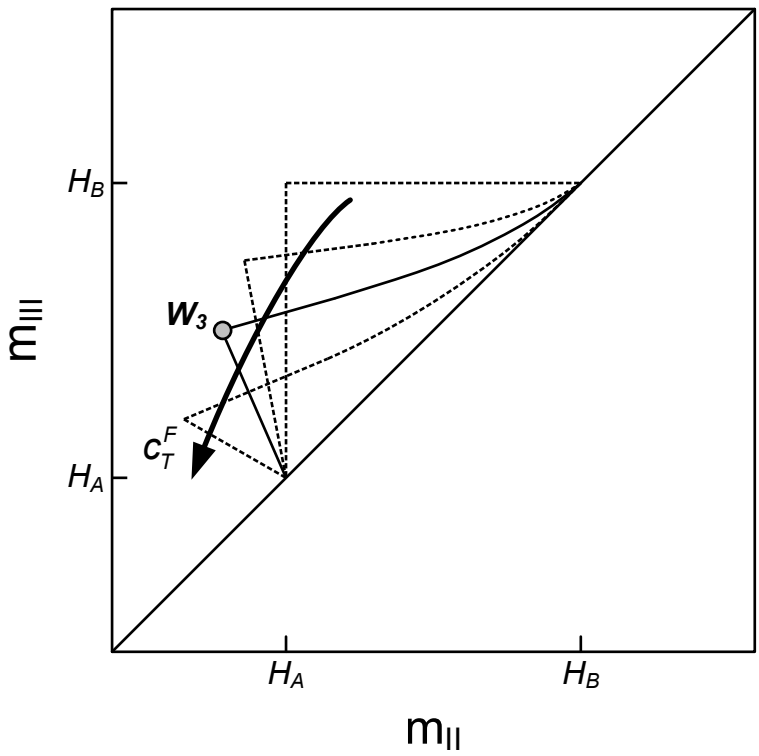

Figure 2.6: Effect of the feed concentration on the shape of the complete separation region for the case of the Langmuir isotherm. With increasing the total feed concentration c_T^F the triangular region shrinks.

2.3.3 Summary

The triangle theory reviewed above, although based on the TMB model and derived from equilibrium theory, has been proven to be an extremely useful tool in both academia and industry. It is often used to estimate optimal operating conditions, to assist in designing SMB separations and to explain experimental results. In the first part of the thesis, the triangle theory will be employed to provide a first guess for the optimization procedure developed for evaluating FF-SMB. The obtained optimization results will be also analyzed and discussed on the basis of this theory.

2.4 Nomenclature

c	liquid phase concentration [g/l]
C	liquid phase concentration state vector [g/l]
$D_{ap,i}$	apparent axial dispersion coefficient of component i [cm^2/s]
DR	desorbent requirement [g/g]
H	Henry constant [-]
K	adsorption equilibrium constant [l/g]
L	column length [cm]
m	flow-rate ratio [-]
N_C	number of concentration state variables [-]
N_{Col}	number of columns [-]
N_p	number of theoretical plates [-]
N_u	number of operating parameters [-]
PR	productivity [g/(g min)]
Q	liquid phase flow-rate [ml/min]
q	solid phase concentration [g/l]
t	time [min]
t_s	switching period [min]
u	vector of operating parameters
V_{Col}	column volume [ml]
v	interstitial velocity [cm/s]
z	axial coordinate [cm]

Greek letters

ϵ	column porosity [-]
ρ_D	desorbent density [g/l]

ρ_s	stationary phase density [g/l]

Roman letters

I, II, III, IV	zone index

Subscripts and superscripts

0	initial conditions
A	less retained component
B	more retained component
D	desorbent
E	extract
F	feed
i	component index, $i = A$, B
in	inlet of zone or column
j	zone index, $j = I, II, III, IV$
out	outlet of zone or column
R	raffinate
T	total quantity

3

Recycling in preparative liquid chromatography

Recycling is an effective operating regime and widely employed for the design and operation of many chemical processes, such as distillation and chemical reaction. In this chapter, we first provide an overview regarding the application of this technique in the conventional batch chromatography. In particular, the principles of several representative process implementations are discussed with emphasis on illustrating their essential features. After presenting these background details, we will briefly introduce FF-SMB, a novel concept that ingeniously utilizes recycling in the continuous SMB separation.

3.1 Batch chromatography

For single column batch operation, the idea of exploiting various recycling techniques to enhance the separation performance is not new, but has been subject to extensive investigation. Many technical realizations have been developed over the last few decades.

3.1.1 Closed-loop recycling chromatography

The simplest implementation of recycling is the closed-loop recycling (CLR) chromatography [40, 41, 42], which is schematically shown in Fig. 3.1. The major difference from the classical elution chromatography is that the detector outlet is connected with the pump inlet using a 4-port valve. During operation an additional recycling period is required over which the sample, after eluting from the column and passing through the detector, is reinjected to the same column with the pump several times to achieve further separation. Once the desired resolution is reached, the recycling operation can be stopped, and the sample will be collected in the appropriate fraction collectors by switching the 4-port valve. By following such recycling procedure, a longer column is simulated artificially and the separation efficiency in terms of the product purity and recovery yield can be enhanced. Furthermore, since no fresh solvent is required during recycling, the scheme allows a potential saving in solvent consumption. However, dead volumes caused by the pump, connecting tubes and valves in the recycle line can deteriorate the achieved resolution by the additional band broadening effect. Thus, recycling cannot proceed beyond the limit where the sample is spread over the whole column and begins to overlap during the successive cycles. In order to delay the undesired effect and to achieve higher yields, the so-called "peak shaving"

technique was proposed [41], where the leading and trailing edges of the peak profile containing sufficiently purified fractions are collected, while only the off-spec remainder is recycled back to the column (see Fig. 3.2).

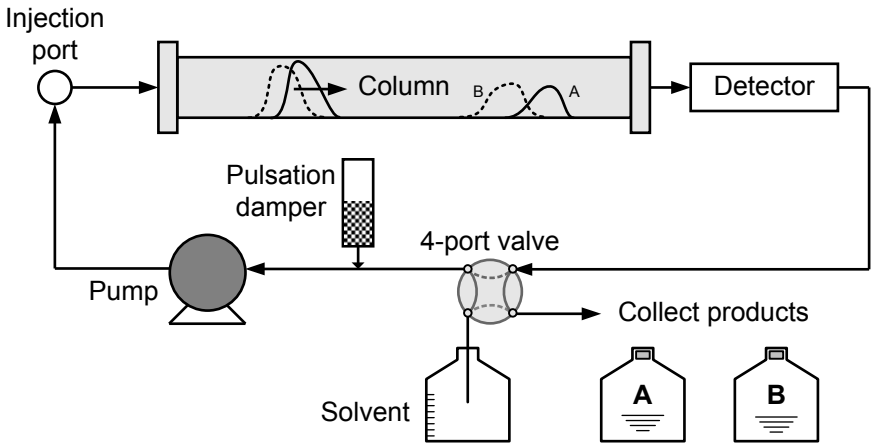

Figure 3.1: Schematic diagram of the closed-loop recycling chromatography.

3.1.2 Steady state recycling chromatography

The concepts reviewed in Section 3.1.1 are characterized by recycling the chromatogram either partially or as a whole and no fresh feed is added during recycling. Another class of recycling chromatography, referred to as steady state recycling (SSR) chromatography, has been also developed, which in addition to collecting the leading and trailing fractions of the elution profile, inserts a portion of fresh feed into the recycle fraction. Due to the repetitive introduction of fresh sample, the process eventually achieves a periodic steady state. Depending on the injection method, different operating modes can be distinguished for SSR chromatography.

Bailly and Tondeur [43] proposed a regime of "recycling with mixing" (Fig. 3.3a), in which the partially separated intermediate section of the chromatogram is collected during any given cycle and mixed with a given amount

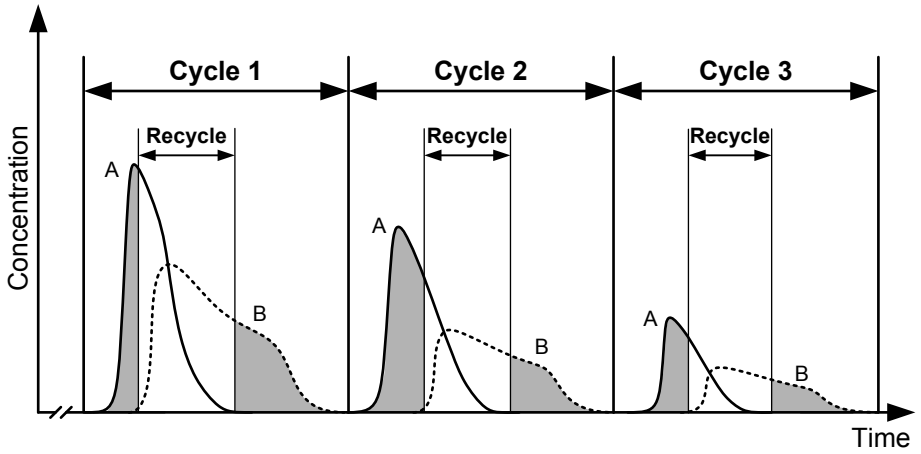

Figure 3.2: Elution profiles of closed-loop recycling chromatography with peak shaving for three recycling cycles. The shaded regions represent the "shaved" fractions which are collected as products. The intermediate unresolved fractions are recycled to the column.

of fresh feed. The resulting feed mixture is then reinjected into the column at the beginning of the next cycle. Using the equilibrium theory, the authors developed an approach for the analysis and design of the process. They showed that for a given product purity, the recycle process operated at the optimal conditions leads to more concentrated products and savings in eluent consumption with respect to the classical elution mode. However, since the recycled fraction and fresh feed differ in composition, completely mixing them prior to reinjection destroys the already developed resolution by the column. To avoid the loss of the achieved partial separation of the recycle fraction, the "segmented recycling" was suggested by the same authors [44], where the recycled fraction collected from the previous cycle is pumped into the column before the new injection of fresh feed in the next cycle (see Fig. 3.3b). In addition, Charton et al. [45] considered the possibility of recycling the tail of the second peak. This is based on the consideration that the elu-

tion profile of the more retained component usually exhibits a long tail, and the corresponding purified fraction is often dilute. Thus, it may be more advantageous to recycle the highly dilute tailing part of the fraction rather than collect it. Such a recycling procedure is shown in Fig. 3.3c. The authors also proposed to combine the two recycling policies mentioned above, as illustrated in Fig. 3.3d. In this mode, the injection is carried out by following three steps: the recycle fraction containing the dispersed tail of the second peak is injected first, followed by the intermediate partially separated fraction, and finally a portion of fresh feed. A detailed evaluation of the performance achieved by the above several recycling strategies with respect to the conventional elution mode was made in [45].

Furthermore, Grill [46] suggested another novel operating mode, called closed-loop recycling with periodic intra-profile injection (CLRPIPI) or closed-loop SSR. The process also collects the leading and tailing edges of the chromatogram during each cycle. The unresolved intermediate zone of the chromatographic profile, however, is treated in a different way. As this part elutes from the column, it is not collected, lumped into the recycle fraction and reinjected later, but rather recycled to the column inlet. At one properly selected time instant in each cycle, a certain amount of fresh sample is injected into the interior of the elution profile by switching the injection loop into the recycle stream (see Fig. 3.4). The concept is similar to SMB, since for both cases fresh sample is injected into the interior of the circulating chromatographic profile and two product streams are collected from either end of it. However, the CLRPIPI process, although repetitive, is not continuous. Using the separation of a racemic pharmaceutical intermediate, Grill and Miller [47] examined the underlying mechanisms of this process experimentally. They found that, in order to obtain high purity fractions, it

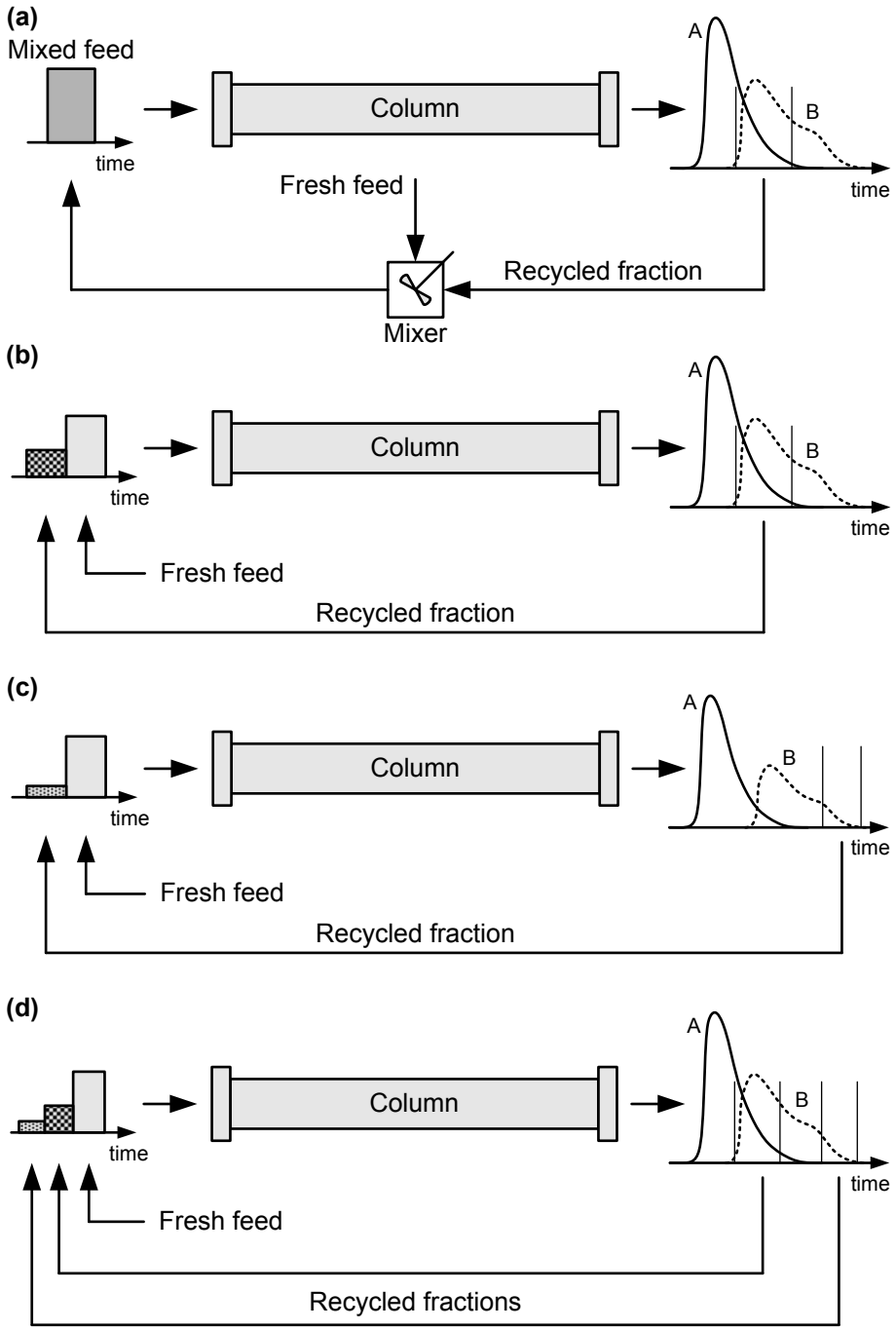

Figure 3.3: Schematic representation of (a) "recycling with mixing", (b) "segmented recycling", (c) recycling of the second peak tail and (d) combination of (b) and (c).

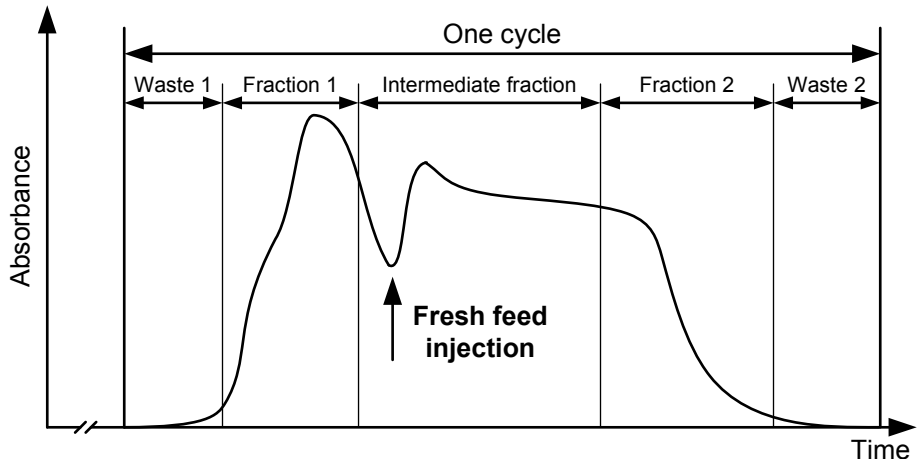

Figure 3.4: Superimposed chromatogram of closed-loop SSR at periodic steady state for one cycle [46]. The dilute parts of the leading and trailing edges of the elution profile are treated as waste fractions (Wastes 1 and 2), and the remaining parts are collected as products (Fractions 1 and 2). The intermediate fraction is recycled to the column inlet. At an appropriate time a given amount of fresh feed is injected into the interior of the profile.

is crucial to create a stable steady state chromatographic profile. This can be achieved by adjusting the size and location of the fractions collected, the position of the injection point and the amount of sample injected. They showed that these operating parameters are analogous to some parameters of SMB. The authors also compared the new concept with SMB for the separation of the same racemic mixture using the same chiral stationary phase and mobile phase. The experimental work revealed that the two techniques achieve similar performance in terms of production rate, purity and recovery. The encouraging results motivated the authors to develop a mathematical model for the process and to perform its experimental validation [48]. A detailed comparison of this process with other existing techniques for the resolution of pharmaceutical intermediates has been reported in recent experimental

studies [49, 50, 51].

Although various implementations of SSR chromatography have emerged, development of an efficient analysis and design procedure for such processes remains significantly untouched. For the closed-loop SSR process, only an empirical design approach derived from an experimental procedure is available [46]. The method, although simple and intuitive, suffers from the drawback that it provides neither a priori prediction of the steady state nor a guarantee of the fulfillment of purity requirements or optimal performance. Furthermore, for the "recycling with mixing" mode, as already mentioned, a design procedure based on the equilibrium theory was developed but restricted to the case of complete separation [43]. Recently, Sainio and Kaspereit [52] have extended this equilibrium-design method to the case of arbitrary purity or yield specifications. They used the proposed approach to analyze the "recycling with mixing" operation. It was shown that with the new design scheme, direct prediction of the steady state and the relevant design parameters can be performed, without resorting to time-consuming dynamic simulations using a column model. Thus, their work largely simplifies the optimal design of SSR processes.

3.2 SMB chromatography

The concept of recycling and reprocessing unresolved fractions can be transferred from the previous batch mode to the continuous SMB chromatography, leading to the emergence of new operating regimes. The "Partial Discard" strategy [24] can be considered as an earlier attempt made in this aspect. Compared to the permanent collection in the classical SMB operation, the partial withdrawal of one or both outlet streams is exploited by this scheme

to obtain high purity products. However, the concept does not explicitly recycle the fractions that are shaved off, but suggests either discarding or remixing with the fresh feed. Discarding the off-spec fractions leads to losses in recovery yields. Further, remixing with the fresh sample, as pointed out in Section 3.1.2, spoils the separation achieved in the fractions, and thus is not preferable. In order to circumvent these limitations, the **F**ractionation and **F**eedback SMB (FF-SMB) process has been invented [25]. In contrast to the "Partial Discard" approach, the new operating mode neither discards nor remixes the off-spec fraction(s). They are instead collected in one or more separate buffer vessel(s) and fed back into the unit alternatingly with the original fresh feed. A detailed description of the principle of FF-SMB will be presented in the next chapter.

Some preliminary results obtained from parametric simulation studies [26] revealed advantages of FF-SMB over both the conventional SMB and the "Partial Discard" scheme. However, simulation based strategies are often computationally intensive and do not guarantee to obtain optimum operating conditions. Thus, the full potential offered by FF-SMB cannot be exploited. Furthermore, the previous work [26] was restricted to a special case characterized by only one outlet fractionation. The potential of the more general concept realizing simultaneous double fractionation remains unexplored. Motivated by these facts, an efficient model-based optimization framework will be developed for FF-SMB in the following chapter, with which the optimal performance of various fractionation policies can be evaluated systematically. The possibility to further improve the process performance of FF-SMB by enriching the recycled fractions will be also investigated.

4

Fractionation of one outlet

We start this chapter by describing the principle of FF-SMB realizing one outlet fractionation, followed by a detailed mathematical model used to characterize the process dynamics. Then a model-based optimization framework developed for efficiently evaluating the fractionation and feedback regime is presented, which is able to take advantage of the flexibility of FF-SMB and to exploit its full potential. Different solution strategies for addressing the resulting nonlinear programming problem are discussed. By taking a difficult separation problem characterized by small selectivity and low column efficiency as reference, systematic optimization studies are carried out for FF-SMB and the classical SMB concept. The optimal performances that can be achieved by the two operating schemes are quantitatively compared in terms of maximizing feed throughput and minimizing desorbent consumption. The optimization results obtained are interpreted in the framework of equilibrium theory. The effect of feeding sequence on the potential of FF-SMB is also examined and the best feeding sequence is identified.

4.1 Principle of FF-SMB

4.1.1 Conventional SMB

To understand the principle of the fractionation and feedback concept, knowledge of how the conventional SMB works is vital. A detailed schematic description of SMB can be found in Chapter 2. In this section, only the information that is relevant to the following discussion is presented.

As pointed out in Chapter 2, a cyclic steady state (CSS), characterized by time-dependent periodic behavior inside the columns and at both outlets during each switching period, is attained by SMB after a startup period. The resulting dimensionless outlet concentration profiles for the case of an incomplete separation are illustrated exemplarily in Fig. 4.1a and c for the raffinate and extract ports, respectively. The product purities can then be calculated by integrating the concentration profiles over time (see Fig. 4.1b and d). Note that in Fig. 4.1, only one CSS period is considered and the dimensionless concentration values are obtained by relating the outlet concentration of each component with respect to its feed concentration. Furthermore, for convenience a dimensionless time τ is defined as

$$\tau = \frac{t}{t_s}, \quad \tau \in [0, 1] \tag{4.1}$$

with t_s being the switching period. In this classical concept, the following features are worth mentioning:

- Both raffinate and extract outlet streams are withdrawn continuously as product over one complete switching period (i.e., from $\tau = 0$ to $\tau = 1$).
- Only one feed solution with constant feed concentrations is supplied permanently.

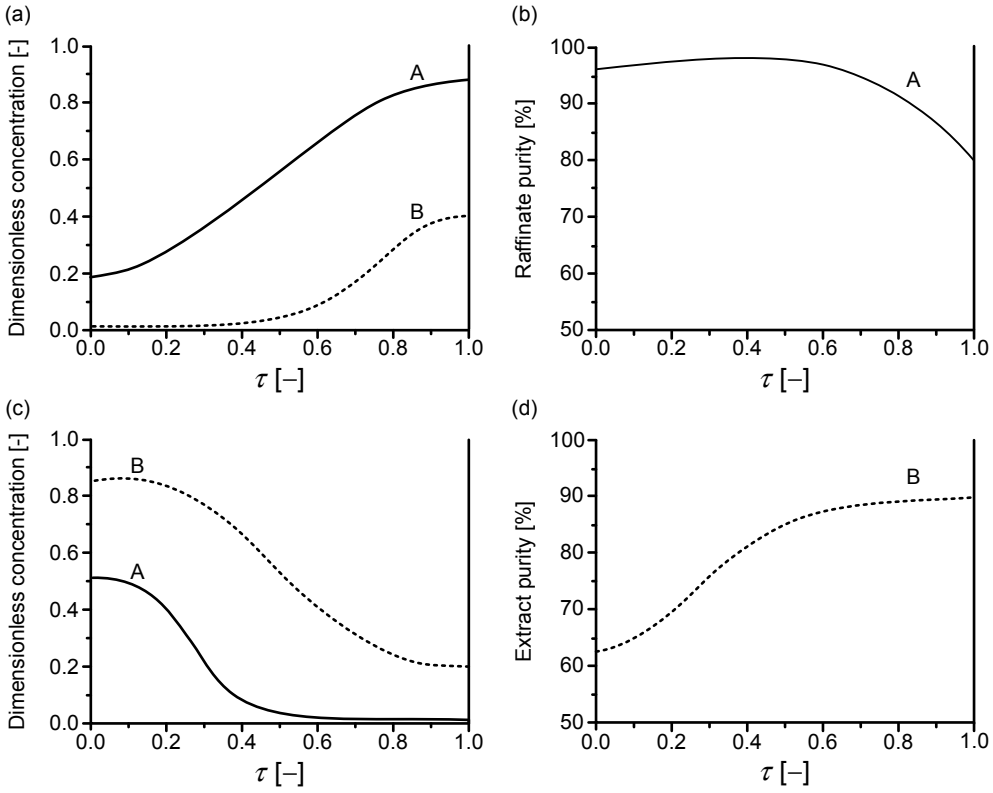

Figure 4.1: Outlet concentration profiles and integral purity profiles of conventional SMB chromatography at cyclic steady state. (a) Dimensionless raffinate concentration profiles for the less retained (solid line: A) and the more retained component (dotted line: B). (b) Raffinate integral purity profile. (c) Dimensionless extract concentration profiles for the more retained (dotted line: B) and the less retained component (solid line: A). (d) Extract integral purity profile.

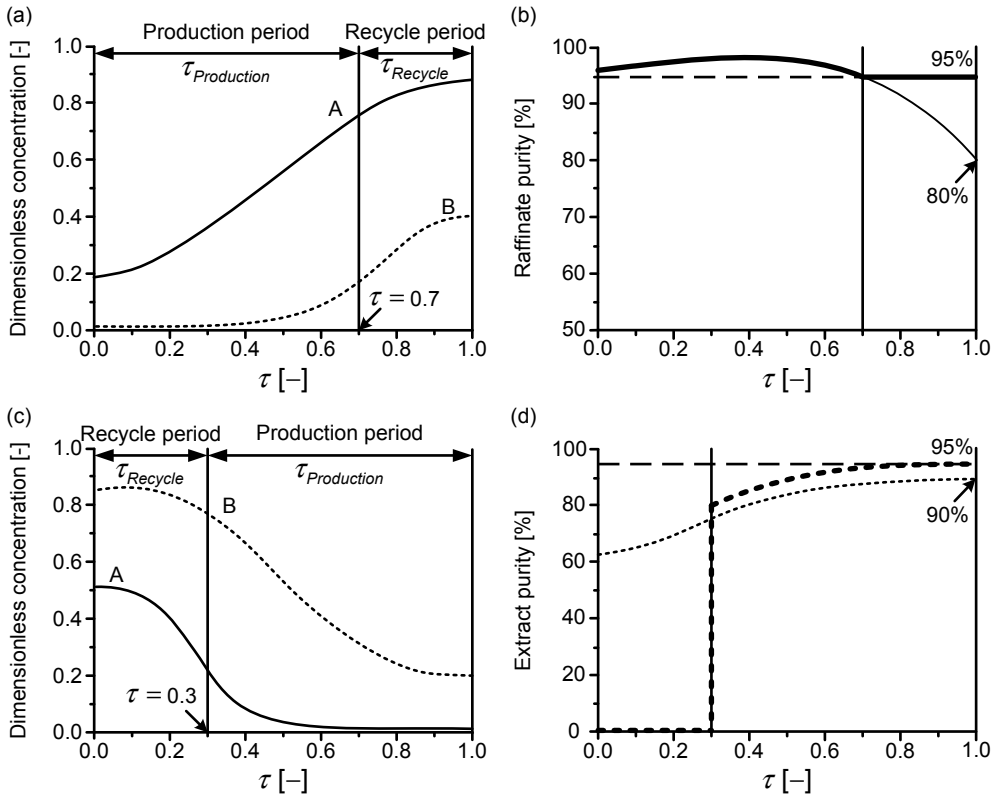

Figure 4.2: Illustration of principle of outlet fractionation and resulting integral purity profiles. (a) Raffinate outlet fractionation (solid line: A; dotted line: B). (b) Raffinate integral purity profiles (thin solid line: without outlet fractionation; thick solid line: outlet fractionation). (c) Extract outlet fractionation (solid line: A; dotted line: B). (d) Extract integral purity profiles (thin dotted line: without outlet fractionation; thick dotted line: outlet fractionation). Dashed lines in (b) and (d): hypothetical purity threshold of 95%.

4.1.2 Outlet fractionation

The outlet concentration profiles illustrated in Fig. 4.1a and c are of time-dependent nature. In the case of successful operation, the concentration profile of component A eluting from the raffinate outlet increases typically over the course of one switching period; at the same outlet, component B exhibits a similar increasing tendency but appears later (see Fig. 4.1a). On the other hand, both components at the extract outlet elute usually with higher concentrations at the beginning of each period. As time increases, the concentration drop of A is faster than that of B (see Fig. 4.1c). It is readily noted that the elution of the "unwanted" components from the outlets is most pronounced at the end (raffinate outlet, component B) or the beginning (extract outlet, component A) of one period, causing low product purity during these time periods (see Fig. 4.1b and d). This fact motivates to collect only certain fractions of the outlet streams that include less "unwanted" components to improve process performance.

The basic principle of such an outlet fractionation scheme is demonstrated in Fig. 4.2, where the example shown in Section 4.1.1 is used again for illustrative purposes. A hypothetical purity threshold of 95% for both products is assumed (see Fig. 4.2b and d, dashed lines). In the case without fractionation, collecting the outlet streams over one complete period leads to an integral purity of 80% for the raffinate and of 90% for the extract (see Fig. 4.2b and d, thin solid and dotted lines), i.e., both below the required purity. In contrast, adopting the fractionation concept and withdrawing from $\tau = 0$ to $\tau = 0.70$ at the raffinate outlet and from $\tau = 0.30$ to $\tau = 1$ at the extract outlet, allows to reach the desired purity of 95%. Note that the two dimensionless times (i.e., 0.70 and 0.30) introduce new degrees of freedom which define the "production periods" for the corresponding outlets. We will

discuss them in more detail in Sections 4.2 and 4.3.

4.1.3 Feedback regime

As shown in the previous section, fractionation of one or both outlet streams offers an advantage of enhancing product purity. However, it produces off-spec fractions in each switching period, which contain considerable amounts of components of high concentration. Obviously, effective treatment of the valuable fractions is of critical importance for process economics. The "Partial Discard" scheme advocated in [24] simply discards them and tolerates reduced recovery yields of the products. This appears not to be acceptable for the purification of highly valuable products. Another alternative option suggested also by [24] is to remix them with the fresh feed, assuming that the amount of the fractions is small enough not to change the feed concentrations. The idea is similar to the "recycling with mixing" regime previously discussed in Section 3.1.2. However, since the fractions have already been partially separated, remixing with the original feed destroys the achieved resolution.

In FF-SMB with one outlet fractionation, which is examined in this chapter, a separate buffer vessel is introduced to contain the off-spec fraction. During each switching period, the recycled fraction is fed back into the unit in an alternating manner with the fresh feed. Such an alternating use of different feed sources results in a distinct feeding regime as shown in Fig. 4.3. Further discussion of the additional degrees of freedom associated with this feeding scheme (e.g., feedback periods and feeding sequences) will be given in Sections 4.2 and 4.3.

The new concept can be easily implemented for the conventional SMB and other modifications, by just adding a buffer tank and two standard three-

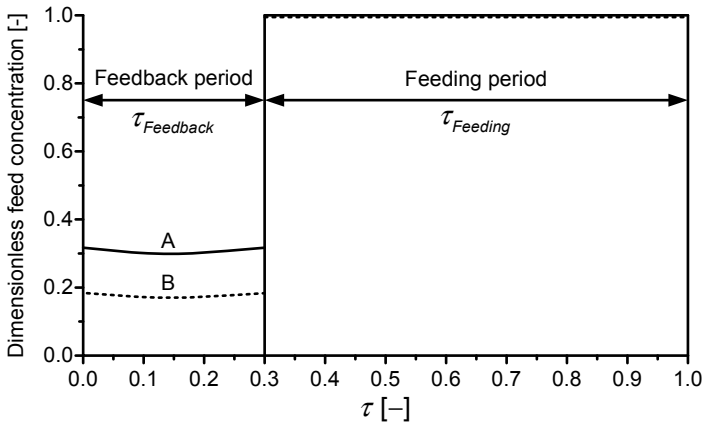

Figure 4.3: Non-constant feeding regime of FF-SMB. Solid line: dimensionless feed concentration of component A; dotted line: dimensionless feed concentration of component B. A feeding sequence of buffer vessel followed by original feed tank is used for illustrative purposes.

way valves. Thus, the additional hardware investment is rather small. A schematic illustration of an FF-SMB unit using raffinate fractionation as example is given in Fig. 4.4.

4.2 Process modeling

The basic principle outlined in the previous section reveals that the overall process model governing the dynamics of FF-SMB consists of two parts: an SMB model taking into account the continuous chromatographic separation in each column and the cyclic port switching, and the buffer vessel dynamics. The two sub-processes are closely coupled through the fractionation and feedback operation, leading to a rather complex hybrid dynamic system. The detailed model equations used to quantify the conventional SMB process are presented in Section 2.2 and not reproduced here for the sake of brevity. In this section, only the new degrees of freedom due to the fractionation and

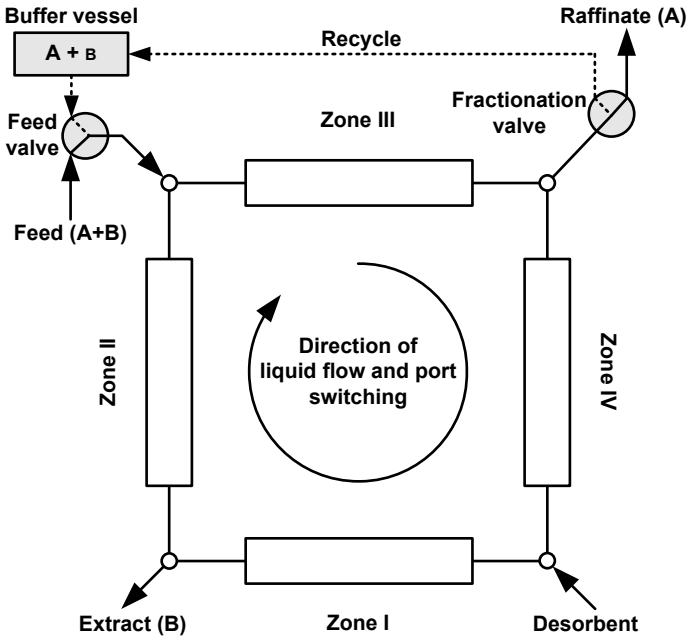

Figure 4.4: Illustration of an FF-SMB process with raffinate outlet fractionation. Two additional three-way valves and a buffer vessel are required to realize the outlet fractionation and feedback concept.

feedback regime will be introduced. Then a simplified dynamic model for the additional buffer tank is described. Finally, it will be demonstrated that classical SMB and the "Partial Discard" strategy are just special cases of the more general FF-SMB concept. It should be noted that we restrict ourselves in this chapter to the fractionation of only one outlet. An extension of the modeling framework to the simultaneous fractionation of both outlets will be discussed in the next chapter.

4.2.1 Fractionation and feedback

As pointed out above, the novel concept offers more degrees of freedom than the conventional SMB chromatography. In this section, the definitions of

these additional degrees of freedom and the resulting mass balance equations will be given.

Production and recycle periods

The outlet fractionation strategy described in Section 4.1.2 divides each switching period into a production period and a recycle period (see Fig. 4.2a and c). Within the production period of length $\tau_{Production}$, the stream from the outlet chosen for fractionation fulfills the desired integral product purity and is collected in a product tank. During the recycle period of length $\tau_{Recycle}$, however, the product withdrawal is interrupted and the outlet stream is recycled into the buffer vessel. Such a discontinuous collection regime can be implemented by periodically switching the three-way valve installed at the corresponding outlet. Obviously, the following simple relation holds for the production and recycle periods:

$$\tau_{Production} + \tau_{Recycle} = 1 \tag{4.2}$$

where $\tau_{Production} \in [0, 1]$. Accordingly, the total volume leaving the fractionated outlet is split into two portions:

$$V_{Production} = t_s \tau_{Production} Q_k \tag{4.3}$$

$$V_{Recycle} = t_s \tau_{Recycle} Q_k \tag{4.4}$$

where Q_k can be either Q_R or Q_E, depending on which port is fractionated.

It should be pointed out that a more general collection policy which allows multiple transitions between production and recycle within each switching period, could eventually lead to further improvements in process performance. However, such a regime would increase the complexity of FF-SMB, and is not taken into account here. Moreover, it is worth noting that the

optimal sequence of the above two periods depends on which outlet is fractionated and is relatively straightforward to determine. However, for those sophisticated schemes realizing multiple production and recycle operations, finding the optimum sequence is not trivial.

Feeding and feedback periods

Feeding the mixture from the buffer vessel and the feed tank in an alternating way introduces two other periods as denoted in Fig. 4.3. Over the feedback period of length $\tau_{Feedback}$, the off-spec fraction collected in the buffer vessel is fed back into the unit. Within the remainder of one switching period, i.e., the feeding period $\tau_{Feeding}$, the original feed tank is used as inlet source. Such a feeding regime can be easily realized by operating periodically the three-way feed valve. Similarly, the following set of balance equations results:

$$\tau_{Feedback} + \tau_{Feeding} = 1 \tag{4.5}$$

$$V_{Feedback} = t_s \tau_{Feedback} Q_F \tag{4.6}$$

$$V_{Feeding} = t_s \tau_{Feeding} Q_F \tag{4.7}$$

where $\tau_{Feedback} \in [0, 1]$, and $V_{Feedback}$ and $V_{Feeding}$ are the liquid volumes processed within the respective periods.

In contrast to the fixed sequence of production and recycle for an outlet port, the inlet feeding sequence is variable so that two possible options (buffer vessel followed by feed tank, or fresh feed tank followed by buffer vessel) are available. For the sequence of buffer vessel prior to fresh feed, as illustrated in Fig. 4.3, the feed concentration of component i at the feed inlet of the unit can be defined as:

$$c_i^F(t) = \begin{cases} c_i^{Buffer}(t), & \frac{t}{t_s} \in [0, \tau_{Feedback}] \\ c_i^{Feed}, & \frac{t}{t_s} \in (\tau_{Feedback}, 1] \end{cases} \qquad i = A,\ B \tag{4.8}$$

where c_i^{Feed} and c_i^{Buffer} represent the concentrations of component i in the feed tank and the buffer vessel, respectively. For the other feeding sequence, the corresponding definition is straightforward. More complex feeding regimes which incorporate multiple feedbacks and various feeding sequences are not considered here.

Furthermore, it is not obvious to determine which feeding sequence is preferable, even for the simplest case considered here. Fig. 4.5 schematically shows the development of axial concentration profiles helping to identify the best feeding sequence. In the example examined, the raffinate outlet is assumed to be fractionated. The buffer vessel is thus already enriched with the less retained component (A). In this case, the recyclate should be fed back at the beginning of each period, when the concentration of A is higher than that of the more retained component B (see Fig. 4.5a). After the corresponding concentration fronts have moved already downstream away from the feeding port, the fresh feed containing a relatively higher fraction of B, should be supplied (see Fig. 4.5b). Inverting this order would reduce the separation performance. Alternatively, if the extract outlet is used for fractionation, the recyclate is enriched in component B, and the reversed sequence is expected to be more favorable.

It should be emphasized that for a given separation problem, the best sequence may depend in a more sophisticated manner upon adsorption isotherms and feed concentrations. For nonlinear adsorption isotherms of the Langmuir type, the slope of the isotherm decreases as the concentration increases, leading to increased migration speeds. For FF-SMB, this effect could be also exploited as done in the ModiCon concept [14], which manipulates the concentration profiles by deliberately modulating the feed concentrations.

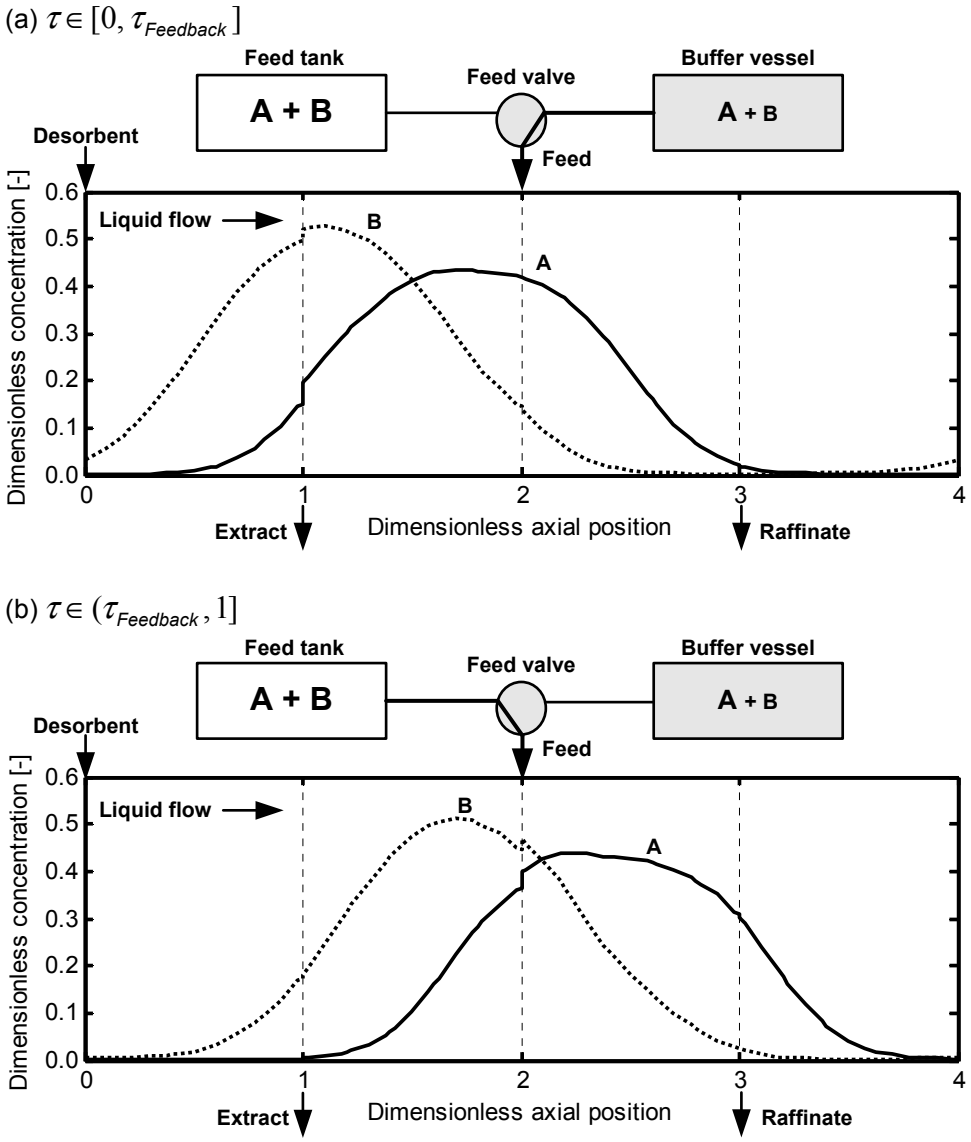

Figure 4.5: Development of axial concentration profiles and selection of optimal feeding sequence for FF-SMB. The raffinate outlet is used for fractionation. (a) For $\tau \in [0, \tau_{Feedback}]$, the buffer vessel is used as inlet source. (b) For $\tau \in (\tau_{Feedback}, 1]$, the original feed is supplied as inlet source.

4.2.2 Buffer vessel dynamics

The liquid volume and concentrations in the buffer vessel can be described by the following simple mass balance equations of a well-mixed tank:

$$\frac{dV_{Buffer}}{dt} = Q_{in}(t) - Q_{out}(t) \tag{4.9}$$

$$\frac{d(V_{Buffer}\, c_i^{Buffer})}{dt} = Q_{in}(t)\, c_i^k(t) - Q_{out}(t)\, c_i^{Buffer}(t), \quad i = A,\, B, \quad k = E \text{ or } R \tag{4.10}$$

with V_{Buffer} being the liquid volume, Q_{in} and Q_{out} the inlet and outlet flow-rates, and c_i^{Buffer} and c_i^k the concentrations of component i in the buffer vessel and at the outlet used for fractionation, respectively.

Due to the discontinuous product withdrawal and non-constant feeding, Q_{in} and Q_{out} are characterized by two piecewise constant functions. For the example of raffinate fractionation and feeding the recycled fraction first, they can be defined as:

$$Q_{in}(t) = \begin{cases} 0 & \frac{t}{t_s} \in [0, \tau_{Production}] \\ Q_R & \frac{t}{t_s} \in (\tau_{Production}, 1] \end{cases} \tag{4.11}$$

$$Q_{out}(t) = \begin{cases} Q_F & \frac{t}{t_s} \in [0, \tau_{Feedback}] \\ 0 & \frac{t}{t_s} \in (\tau_{Feedback}, 1] \end{cases} \tag{4.12}$$

For the other feeding sequence and extract fractionation, the definitions are straightforward.

In addition, initial conditions should be specified in order to predict the buffer vessel behavior:

$$V_{Buffer}(t = 0) = V_{Buffer,0} \tag{4.13}$$

$$c_i^{Buffer}(t = 0) = c_{i,0}^{Buffer},\ i = A,\, B \tag{4.14}$$

During the operation of FF-SMB, three different states for the liquid level of the buffer vessel exist. A dimensionless factor ρ, defined as a volume ratio between $V_{Recycle}$ and $V_{Feedback}$, was introduced in [26] to characterize these scenarios:

$$\rho = \frac{V_{Recycle}}{V_{Feedback}} = \frac{(1 - \tau_{Production})\, Q_k}{\tau_{Feedback}\, Q_F},\ k = E \text{ or } R \tag{4.15}$$

If $\rho = 1$, the volume accumulated in the buffer vessel within each period is zero and the liquid level remains cyclically constant. If $\rho > 1$, the level increases continuously, leading to the risk of overflow. If $\rho < 1$, a gradual decrease occurs and the buffer vessel eventually "runs dry".

It is worth noting that the buffer vessel may have an impact on the dynamics of the process. For example, the simulation studies [26] showed that the initial conditions of the buffer vessel (Eqs. (4.13)–(4.14)) affect the transient behavior and thus the resulting time required to reach the cyclic steady state. However, a detailed analysis of the effect of the buffer tank on the dynamics is beyond the scope of this work.

4.2.3 Special cases of FF-SMB

By fixing one or more degrees of freedom, the conventional SMB and the "Partial Discard" operation can be regarded as two special cases of the FF-SMB process. The "Partial Discard" concept can be interpreted as the case where the "unwanted" fraction is discarded to the buffer vessel which has no feedback connection with the unit:

$$\tau_{Feedback} = 0,\ Q_{out}(t) = 0,\ \forall t \in [0, t_s] \tag{4.16}$$

For the standard SMB chromatography realizing the continuous product collection and permanent supply of fresh feed, obviously the following conditions

hold:

$$\tau_{Feedback} = 0,\ \tau_{Production} = 1,\ Q_{in}(t) = Q_{out}(t) = 0,\ \forall t \in [0, t_s] \tag{4.17}$$

4.3 Optimization

In this section, we will present a framework developed for the optimization of FF-SMB with one outlet fractionation. The additional degrees of freedom and constraints are underlined during formulating the nonlinear programming (NLP) problem. An efficient solution strategy for the resulting optimization problem will be described. The framework given here can also deal with the classical SMB and the "Partial Discard" operation. Thus, systematic investigations and comparisons of these regimes can be carried out within it.

4.3.1 Problem formulation

Objective function

For the optimization of SMB and its various derivatives, the cost functions of interest typically differ from case to case. In [54], the authors suggested minimizing the specific separation costs directly if the detailed cost data exist. If such information is not available, those dominant factors, such as the feed throughput, or the desorbent consumption for a given throughput, can be optimized. This single objective approach was used very frequently to optimize the conventional SMB [53], SMB reactor [54] and VariCol process [55, 56]. On the other hand, multi-objective optimization has been comprehensively studied [57, 58, 59, 60, 61, 65, 66], where multiple competing performance criteria were optimized simultaneously under given constraints. Both ap-

proaches reviewed above can be applied also to the optimization of FF-SMB. It is worth noting that in the context of the fractionation and feedback concept, some of the performance parameters used to evaluate the classical SMB operation must be properly adapted, in order to correctly reflect the discontinuous product collection and non-constant feeding scheme. Such adjusted parameters are detailed in [26] and omitted here for brevity.

In the present work, the single objective optimization problem with two different objective functions will be examined. For the feed throughput maximization problem, the modified feed flow-rate introduced in [26] was chosen as the objective function:

$$\overline{Q}_F = (1 - \tau_{Feedback})\, Q_F \tag{4.18}$$

where $\overline{Q}_F$ represents the average rate of processing fresh feed. Obviously, for an FF-SMB process to be more productive, $\overline{Q}_F$ must be larger than Q_F of the conventional SMB operation. In the second case study, the desorbent flow-rate Q_D is minimized at a given $\overline{Q}_F$. If FF-SMB is more economical, a smaller Q_D should be achievable. It must be emphasized that such comparison of desorbent consumption is meaningful only provided that $\overline{Q}_F$ takes the same value as Q_F in the classical SMB.

Degrees of freedom

For the classical SMB process, the dimensionless m-values defined in Eq. (2.17), were considered as the optimization variables. The same selection has been made in many previous optimization studies [59, 61, 68, 69]. Besides the four m-values, one additional operating parameter must be specified. The feed flow-rate Q_F was chosen in this work. In the case of FF-SMB, the dimensionless parameters $\tau_{Production}$ and $\tau_{Feedback}$ become two additional degrees of

freedom. As discussed in Section 4.2.2, depending on whether $V_{Recycle}$ exactly matches $V_{Feedback}$, the buffer tank level undergoes three different situations. For the case where mismatch occurs, special care must be taken to prevent the buffer vessel from "running dry" or overflowing. For example, an external compensation stream consisting of either eluent or feed can be periodically pumped into the buffer vessel to avoid "running dry" [26]. The undesired overflow can be averted by regularly removing a certain amount of the recycled fraction from the buffer vessel. In this study, we restrict our attention to the case where $V_{Recycle} = V_{Feedback}$ and $\rho = 1$ (see Eq. (4.15)), leaving other possibilities to future work. As a result, $\tau_{Production}$ and $\tau_{Feedback}$ are not independent any more but related by the equality:

$$(1 - \tau_{Production})\, Q_k = \tau_{Feedback}\, Q_F,\ k = E \text{ or } R \tag{4.19}$$

In the optimization studies carried out below, the dimensionless production period $\tau_{Production}$ was specified as the independent variable, and $\tau_{Feedback}$ was determined through one of the following two equations, depending on which outlet is used for fractionation:

$$\tau_{Feedback} = \begin{cases} \frac{(m_{III}-m_{IV})(1-\tau_{Production})}{m_{III}-m_{II}}, & \text{raffinate fractionation} \\ \frac{(m_{I}-m_{II})(1-\tau_{Production})}{m_{III}-m_{II}}, & \text{extract fractionation} \end{cases} \tag{4.20}$$

In addition, the feeding sequence (i.e., the order of fresh feed supply and recyclate feedback, see Fig. 4.3) was also considered as a degree of freedom.

Constraints

In this work, the purity constraints for both extract and raffinate products were simultaneously taken into account:

$$Pu_E \geq Pu_{E,min} \tag{4.21}$$

$$Pu_R \geq Pu_{R,min} \tag{4.22}$$

where $Pu_{E,min}$ and $Pu_{R,min}$ are the pre-specified minimum purity requirements.

In order to respect the maximum allowable internal flow-rate Q_{max} caused by the limited pressure drop in the unit or the finite capacity of the pump, an additional inequality constraint is imposed on the highest flow-rate occurring typically in zone I:

$$Q_I \leq Q_{max} \tag{4.23}$$

In addition, the following obvious constraint on the feedback period is also required:

$$0 \leq \tau_{Feedback} \leq 1 \tag{4.24}$$

The resulting NLP problem is summarized in Table 4.1 for reference.

4.3.2 Solution strategy

Depending upon how to deal with CSS, generally two mainstream optimization strategies can be distinguished in the open literature. The first is the so-called sequential approach, where the PDEs describing the dynamics of the system are discretized only in space and the resulting ODEs or DAEs are integrated for a certain number of switching periods until the CSS is obtained. Then the values of the objective function and constraints are calculated and given back to an external optimizer. The entire procedure is repeated until the optimal solution is located. Compared to other solution algorithms, the approach does not require any other special numerical techniques except for the solution of differential equations, and thus is robust and easy to use. It also allows to deal with rather detailed and complicated first principles models. With these advantages, the sequential strategy has been

Table 4.1: Summary of the nonlinear optimization problem for FF-SMB with one outlet fractionation.

Objective function:

$\max\ \overline{Q}_F \quad$ or $\quad \min\ Q_D$ at a given $\overline{Q}_F$

Optimization variables:

$m_I, m_{II}, m_{III}, m_{IV}, Q_F, \tau_{Production}$

Purity requirements:

Raffinate fractionation:
$$Pu_E = \frac{\int_0^1 c_B^E(\tau)\,d\tau}{\int_0^1 (c_A^E(\tau)+c_B^E(\tau))\,d\tau} \geq Pu_{E,min}$$
$$Pu_R = \frac{\int_0^{\tau_{Production}} c_A^R(\tau)\,d\tau}{\int_0^{\tau_{Production}} (c_A^R(\tau)+c_B^R(\tau))\,d\tau} \geq Pu_{R,min}$$

Extract fractionation:
$$Pu_E = \frac{\int_{1-\tau_{Production}}^1 c_B^E(\tau)\,d\tau}{\int_{1-\tau_{Production}}^1 (c_A^E(\tau)+c_B^E(\tau))\,d\tau} \geq Pu_{E,min}$$
$$Pu_R = \frac{\int_0^1 c_A^R(\tau)\,d\tau}{\int_0^1 (c_A^R(\tau)+c_B^R(\tau))\,d\tau} \geq Pu_{R,min}$$

Maximum flow-rate constraint:

$Q_I \leq Q_{max}$

Feasibility constraint on $\tau_{Feedback}$:

$0 \leq \tau_{Feedback} \leq 1$

Feasibility constraints on m-values:

$m_I - m_{II} > 0,\ m_I - m_{IV} > 0,\ m_{III} - m_{II} > 0,\ m_{III} - m_{IV} > 0$

used for the optimization of a broad variety of different operating regimes, such as classical SMB [53], reactive SMB [54] and VariCol system [55, 56]. However, since the model equations are integrated in time for many periods, the efficiency of this method significantly depends on the performance of the integrator. In addition, it can only deal with open-loop stable systems, and no a priori estimation on its convergence behavior exists.

In order to reduce the computational effort associated with the temporal integration required in the sequential method, tailored simultaneous al-

gorithms were proposed, where the CSS condition is formulated as an additional constraint of the optimization problem. Essentially, two types of simultaneous methods have been examined in the literature. In the single discretization approach, the optimizer searches for both the optimal operating parameters and concentration profiles simultaneously. For the evaluation of the derivatives with respect to the decision variables, the sensitivity equations are integrated along with the original system of differential equations. This scheme was suggested for the optimization of pressure swing adsorption (PSA) processes [70], as well as SMB, PowerFeed and VariCol in the framework of the direct multiple shooting [71]. On the other hand, for the full discretization method, the process model is discretized in both spatial and temporal coordinates, and the original PDE constrained optimization problem can then be transcribed into a large-scale problem constrained by nonlinear algebraic equations. Thus, the time-consuming integration can be eliminated. Kloppenburg and Gilles [73] first applied this full discretization method to the optimization of SMB and PowerFeed processes. But the authors complained that the efficiency and speed of the solver do not completely meet the expectations. Recently, Kawajiri and Biegler revisited the approach systematically by using a different discretization scheme and a more efficient optimizer. Successful applications of this large-scale nonlinear optimization strategy have been reported in their publications [62, 63, 64, 66]. Meanwhile, the same method has been also adopted by Mota and coworkers [68] to optimize their single-column model [67], which was developed to reproduce the CSS behavior of a set of physically realizable asynchronous SMB processes.

For the FF-SMB process, it is not straightforward for the simultaneous approach to deal with the discontinuous on-off characteristics exhibited at both the feed inlet and the fractionated outlet. Instead, the sequential method

discussed above was employed in the present work. In particular, the PDE model described in Section 4.2 was discretized by the OCFE method, and the resulting system of DAEs was integrated using the package DASPK3.1 [33]. In recent years, some derivative-free stochastic optimization techniques, such as simulated annealing and genetic algorithms, have also received great popularity [57, 58, 59, 60, 61, 69, 72]. However, these techniques cannot check the optimality conditions, and often require more computational effort. Alternatively, Newton-based approaches make use of gradient information and have greater potential to solve optimization problems efficiently. In this work, subroutine E04UCF from the NAG Fortran Library [74], a solver based on sequential quadratic programming (SQP) technique, was chosen as the optimizer. In each iteration, the direct dynamic simulation was used to determine the CSS solution. A tolerance was enforced on the difference between the concentration profiles at the end of two successive periods. Once the tolerance was fulfilled for both components simultaneously, the CSS was considered to be attained. For the case studies in the following section, the tolerance was specified to be 1×10^{-4} with the concentration profile of each component normalized with respect to its feed concentration.

In a Newton-based approach, the gradients of the objective function and constraints are required by the solver. They can be obtained analytically except for those of the purity constraints in Eqs. (4.21)–(4.22). In this work, these gradients are evaluated by finite difference approximation. Care must be taken in choosing appropriate intervals of finite differences; poor approximation may lead to a large number of iterations in optimization. Nevertheless, finding appropriate difference intervals is not a difficult task for our problem, since the number of decision variables is small (up to seven) and a small-scale nonlinear optimization problem results. We also investigated

the sensitivity equation approach to evaluate the gradients exactly, utilizing the automatic differentiation (AD) technique. This was implemented by combining DASPK3.1 and an AD tool TAPENADE [75]. It was noticed that although the number of iterations decreases significantly in this approach, the total computational time exceeds that required by the finite difference approximation. This is mainly due to the large number of sensitivity equations which need to be integrated simultaneously with the model equations.

4.4 Results and discussion

4.4.1 Example process

A binary separation problem characterized by a nonlinear adsorption behavior was considered to investigate the FF-SMB process in [26]. The same example was also used here to demonstrate the effectiveness of our optimization approach and to evaluate the optimal performance of this regime. The separation was carried out on a laboratory-scale four-zone SMB unit. The system consists of four identical chromatographic columns, each of which is characterized by a low efficiency indicated by an N_p value of 40 (Eq. (2.4)). For FF-SMB, the raffinate outlet was used for fractionation. Furthermore, it was assumed that initially the buffer vessel contains only fresh solvent. The model parameters and operating conditions are summarized in Table 4.2. The adsorption behavior was assumed to be governed by the competitive Langmuir isotherm model described by Eq. (2.6). The corresponding coefficients are listed in Table 4.3, which were adapted from experimental data given in [76] and characterize the separation of cycloheptanone and cyclohexanone on silica using n-hexane:ethylacetate (85:15) as mobile phase. Note that the linear adsorption behavior was derived from the nonlinear case by

setting the coefficients $K_i\,(i = A, B)$ to zero. The feed concentration of each component in the feed tank was fixed at 1 g/l. For the small-scale unit, the maximum allowable internal flow-rate Q_{max} was specified as 10 ml/min. Here the selection of low column efficiency ($N_p = 40$) and small adsorption selectivity ($\alpha = 1.126$) was motivated by our primary interest of evaluating the potential of the new concept for difficult separations.

Table 4.2: Model parameters and operating conditions for the example process.

SMB configuration [-]	1-1-1-1
Column dimensions [cm]	1×10
Fractionated outlet [-]	Raffinate
ϵ [-]	0.667
N_p per column [-]	40
c_i^{Feed}, $i = A$, B [g/l]	1
Q_{max} [ml/min]	10
$c_{i,0}^{Buffer}$, $i = A$, B [g/l]	0
$V_{Buffer,0}$ [ml]	4

Table 4.3: Summary of adsorption isotherm parameters.

Component	H [-]	K [l/g]
A	5.078	0.089
B	5.718	0.105

4.4.2 Case Study 1: Maximization of feed throughput

In this case, the desired extract product purity was fixed at 90%, while a set of purity specifications ranging from 80% to 95% was imposed on the raffinate product. In order to identify the optimum feeding regime for the FF-SMB process, the performance was optimized for each of the two feeding sequences (raffinate recyclate followed by fresh feed or fresh feed followed by raffinate recyclate). For simplicity, these feeding options are abbreviated as "RF" and "FR", respectively.

Linear isotherm

For the specified raffinate purity requirements, the maximum feed throughputs delivered by the classical SMB and the FF-SMB with two feeding sequences are shown in Fig. 4.6. The new process with the feeding sequence "RF" is capable of fulfilling all the purity specifications examined here. The same process using the opposite feeding sequence "FR", can provide raffinate purities up to 93%. However, with conventional SMB the highest attainable purity is only 92%. The results demonstrate that the fractionation and feedback concept has potential for improving product purities.

On the other hand, it can be readily observed that for the same purity, the optimal $\overline{Q}_F$ obtained with either feeding sequence is higher than Q_F for SMB. Furthermore, this degree of improvement depends on the purity requirement. The stricter the purity expectations, the larger the advantages gained by the new concept over the classical mode. For example, when the feeding sequence "RF" is applied, the processable feed can be improved by 94%, 152% and 365% for the desired purity of 90%, 91% and 92%, respectively. In contrast, for the same set of purity specifications, an improvement of 36%, 62% and 159% can be achieved with the reversed feeding sequence. Both

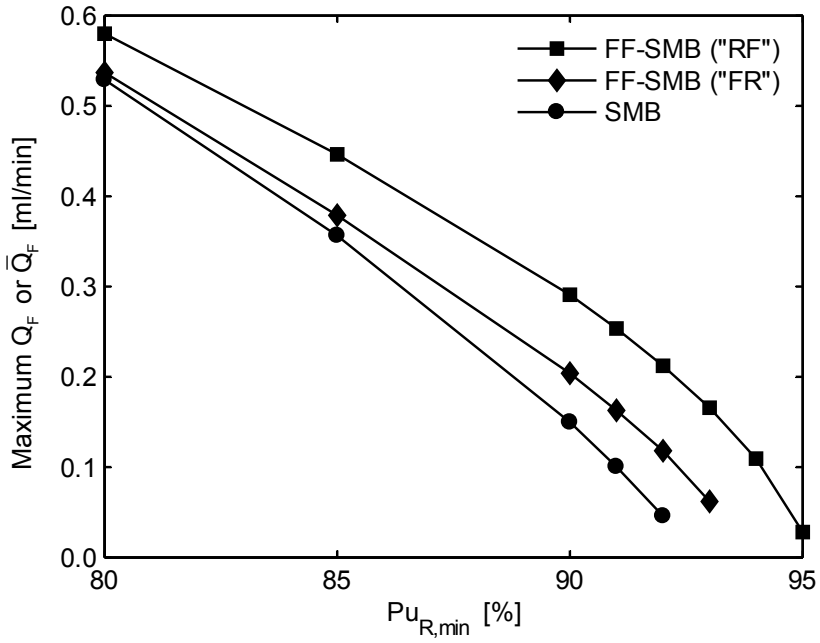

Figure 4.6: Comparison of maximum feed throughput for conventional SMB (circles) and FF-SMB with feeding sequence "FR" (diamonds) and "RF" (squares) (linear isotherms).

cases indicate that more fresh feed can be treated by the FF-SMB process during the feeding period (i.e., $\tau_{Feeding}$) than that by the conventional SMB over the complete period.

The optimal feeding sequence "RF", which was identified here to be more attractive, coincides well with the prediction made previously (see Fig. 4.5). In the following, we restrict the further discussion to only this sequence and ignore the results for the other one.

In order to provide more rational explanations for the performance improvement achieved by FF-SMB, the optimization results were also analyzed in the context of equilibrium theory discussed in Section 2.3. Within this framework, a modified formulation of the original dimensionless factor m_{III}

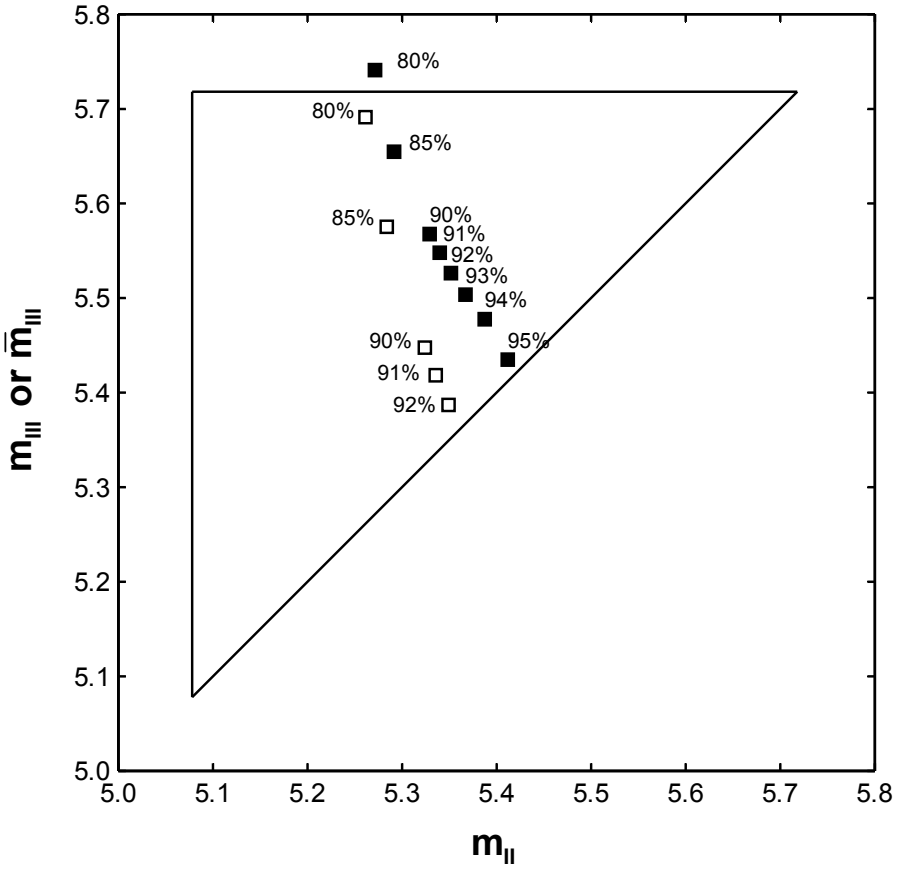

Figure 4.7: Comparison of classical SMB (open squares) and FF-SMB (solid squares) in the combined (m_{II}, m_{III}) and $(m_{II}, \overline{m}_{III})$ planes for linear adsorption isotherms. For each process, the raffinate purity requirements examined are also marked near the optimal operating points.

is introduced for the FF-SMB concept to reflect the reduced feeding time [26]:

$$\overline{m}_{III} = m_{II} + \frac{\overline{Q}_F \, t_s}{V_{Col} \, (1 - \epsilon)} \tag{4.25}$$

The optimal values of m_{II} and $\overline{m}_{III}$ for FF-SMB with the feeding sequence "RF" are shown in the $(m_{II}, \overline{m}_{III})$ plane in Fig. 4.7. The optimal (m_{II}, m_{III}) pairs obtained from the conventional concept are plotted in the (m_{II}, m_{III}) plane in the same figure. In addition, the raffinate purity requirements are also shown together with the corresponding optimal operating points. The following observations can be made. First, as the purity demand increases, the operating points for both processes move towards the diagonal of the respective operating plane, leading to a gradual reduction of the size of the feasible region. For stricter purity requirements, the optimization scheme failed to find a solution, which indicates that such high purities cannot be fulfilled and are infeasible. For FF-SMB, the highest achievable purity observed in the case study is 95%, while it is only 92% for the classical SMB. Second, the optimal value of m_{II} for FF-SMB is very similar to that of the conventional mode. This accordance is due to the fact that the extract purity is mainly influenced by the flow-rate in zone II, and for both processes the extract outlet stream, which is continuously withdrawn over the complete period, needs to satisfy the same purity of 90%. Compared to m_{III} for the SMB concept, a higher value of $\overline{m}_{III}$ can be delivered by the FF-SMB approach for the same raffinate purity. The difference between $\overline{m}_{III}$ and m_{III} tends to be more pronounced when the purity becomes more stringent. This indicates that using raffinate fractionation has a significant effect on $\overline{m}_{III}$, allowing the new process to exploit more productive operation points.

The additional dimensionless parameters of the FF-SMB process, $\tau_{Production}$ and $\tau_{Feedback}$, are shown in Fig. 4.8a and b, respectively. In order to better illustrate the development of these two variables, the optimization results

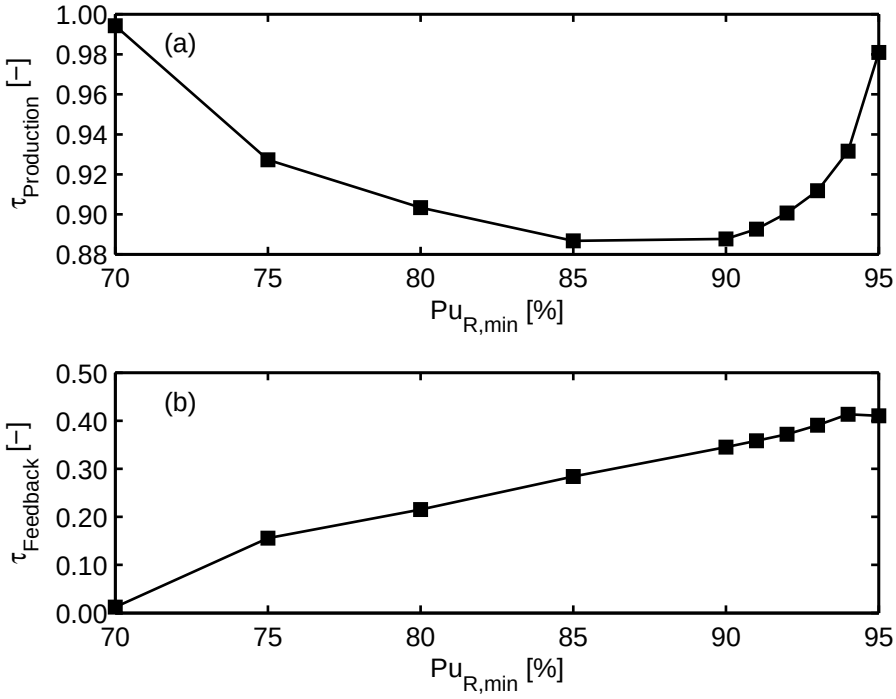

Figure 4.8: Development of (a) optimal production period $\tau_{Production}$ and (b) feedback period $\tau_{Feedback}$ for FF-SMB (linear isotherms).

for two lower purity requirements for the raffinate (i.e., 70% and 75%) are also given there. For the purity of 70%, the optimal $\tau_{Production}$ approaches 1, and the resulting $\tau_{Feedback}$, calculated with Eq. (4.20) for the case of raffinate fractionation, is close to 0. This fact implies that both outlet fractionation and feedback become negligible. In this case, the FF-SMB has almost degenerated into one of its special cases, the conventional SMB, discussed in Section 4.2.3. Thereafter, $\tau_{Production}$ decreases rapidly in order to fulfill the increasing purity requirements. For the purity of 90%, for example, the optimal value is nearly 0.89. For stricter purity specifications (e.g., from 91% to 95%), $\tau_{Production}$ begins to increase towards 1. For example, $\tau_{Production}$ is more than 0.98 for the raffinate purity of 95%. This observation reveals that

for the separation under examination, the function of recycling the off-spec fraction tends to be most pronounced for the purity requirements around 90%. In contrast, a monotonic increase up to about 0.41 can be observed for $\tau_{Feedback}$, which indicates that within each switching period longer time is spent to feed back recyclate.

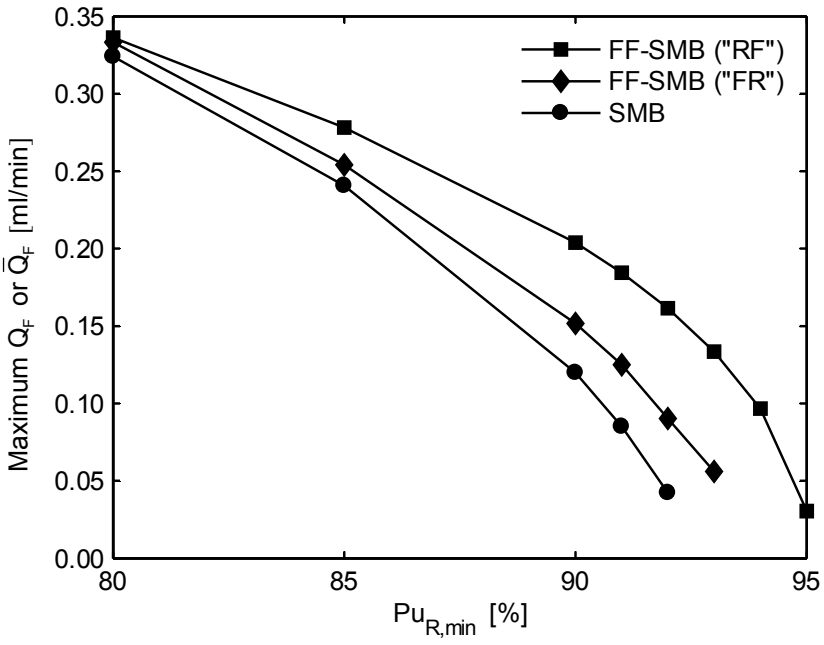

Figure 4.9: Comparison of maximum feed throughput for conventional SMB (circles) and FF-SMB with feeding sequence "FR" (diamonds) and "RF" (squares) (nonlinear isotherms).

Nonlinear isotherm

In the case of nonlinear isotherms, the maximum feed throughput for different purity specifications is illustrated in Fig. 4.9. It is found again that FF-SMB with either feeding sequence achieves higher purities. Furthermore, as in the linear case, the optimized value of $\overline{Q}_F$ is higher than that of Q_F. For example,

with the feeding sequence "RF", $\overline{Q}_F$ is 1.70, 2.17 and 3.82 times higher for the raffinate purity of 90%, 91% and 92%, respectively. The improvement tends to decrease when using the opposite feeding sequence. These results show again that the FF-SMB process not only allows to provide higher raffinate purities compared to the conventional concept, but also improves productivities for the same purity requirement. Similarly, the feeding sequence "RF" proves to be better. Thus, only this sequence was considered further.

The optimum operating conditions for different purities are shown in the combined (m_{II}, m_{III}) and $(m_{II}, \overline{m}_{III})$ planes in Fig. 4.10 for both processes. It can be seen that in order to satisfy more stringent purity requirements, the optimal operating point of each mode enters the complete separation region, and moves towards the diagonal of the corresponding operating plane. This is similar to the behavior observed in the linear case. Moreover, for the same purity requirement, $\overline{m}_{III}$ is similar to or smaller than m_{III} in the conventional process, and m_{II} always shows lower values compared to that of SMB. Thus, the larger value of $\overline{m}_{III} - m_{II}$ achieved by FF-SMB is due to a smaller m_{II}, rather than a higher $\overline{m}_{III}$, which obviously differs from the observation made for the linear case.

The dimensionless parameters $\tau_{Production}$ and $\tau_{Feedback}$ are illustrated in Fig. 4.11a and b, respectively. Compared to the linear case (see Fig. 4.8), similar tendencies can be observed for these two parameters. Note that in this case, the optimal value of $\tau_{Production}$ does not begin to increase towards 1 until purities higher than 91% are requested.

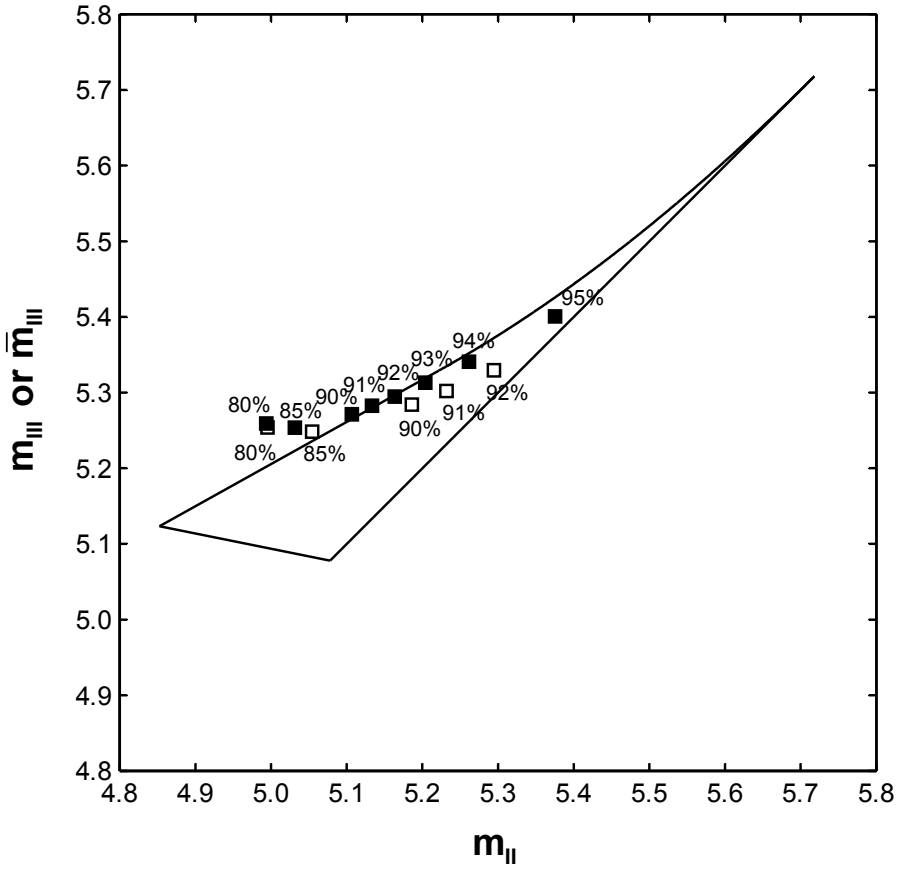

Figure 4.10: Comparison of classical SMB (open squares) and FF-SMB (solid squares) in the combined (m_{II}, m_{III}) and $(m_{II}, \overline{m}_{III})$ planes for nonlinear adsorption isotherms. For each process, the raffinate purity requirements examined are also marked near the optimal operating points.

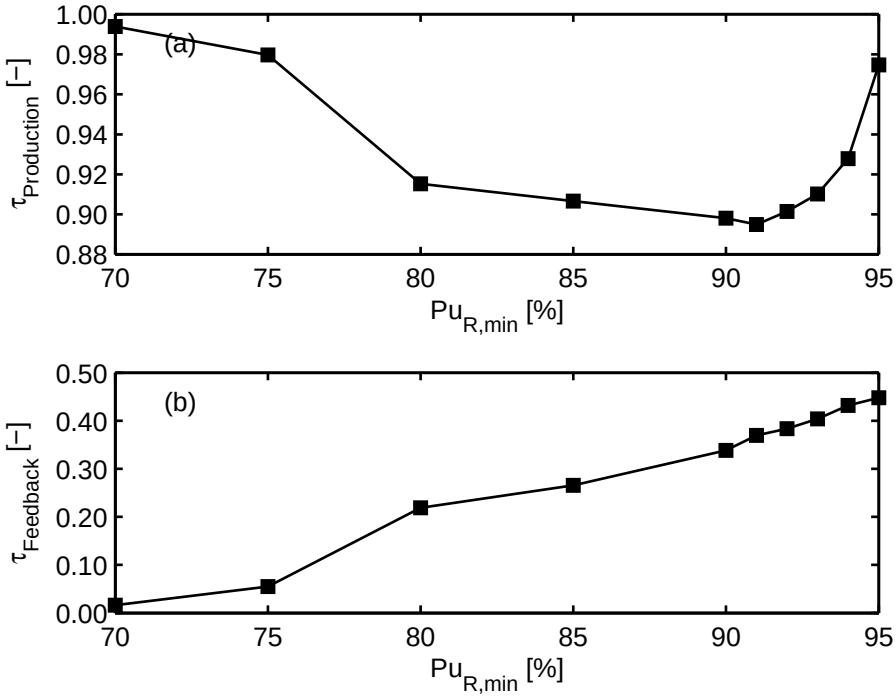

Figure 4.11: Development of (a) optimal production period $\tau_{Production}$ and (b) feedback period $\tau_{Feedback}$ for FF-SMB (nonlinear isotherms).

4.4.3 Case Study 2: Minimization of desorbent consumption

In many SMB applications, the desorbent consumption is one of the dominant factors that contribute to overall separation costs. Reducing desorbent consumption can therefore considerably improve the process economics. In the second case study, conditions allowing the minimization of desorbent consumption were optimized for a given feed throughput. The primary purpose was to evaluate the potential of the fractionation and feedback approach in terms of desorbent savings.

In our optimization study, the feed flow-rate Q_F was assumed to be 0.12

ml/min, considering the small dimensions of the laboratory-scale unit. The same value was specified for the modified feed throughput $\overline{Q}_F$ in the case of FF-SMB. In order to determine which feeding sequence enables a more economic desorbent usage, both sequences ("RF" and "FR") were optimized. The results obtained for both linear and nonlinear isotherms are summarized in Table 4.4a and b, respectively. Again, a minimum extract purity of 90% was required for all optimization runs, and different purity constraints were enforced on the raffinate product (see Table 4.4).

For the classical SMB mode, the minimum desorbent flow-rate increases dramatically as the raffinate purity becomes higher. For example, in the case of linear isotherms (see Table 4.4a, SMB process), the desorbent consumed for delivering a purity of 90%, is up to 2.5 times higher than that for a lower purity of 85%. For the nonlinear case, a more than twofold increase in Q_D can be observed. Such a high sensitivity of desorbent consumption with respect to the purity requirement is mainly caused by the difficulty of the separation under study. When a purity of 91% or higher was specified, the optimizer failed for both types of isotherms.

For the fractionation and feedback approach with either feeding sequence, the potential desorbent savings (shown in brackets in Table 4.4a and b) can be clearly identified for the same set of purity specifications (i.e., 80%, 85%, 90%). For increased purity expectations, the advantage over the conventional process tends to be more significant. For example, in the linear case, a desorbent flow-rate reduced by about 50% can be achieved by FF-SMB with the sequence "RF" for the purity of 90%. For the nonlinear case, the consumption can be reduced by nearly 45%. The same concept using the sequence "FR" allows a reduction of 27.9% and 23.9% for the linear and nonlinear conditions, respectively. In contrast, the benefits become small for lower purity

Table 4.4: Results of minimization of desorbent consumption for SMB and FF-SMB with two feeding sequences.

(a) Linear isotherm

	minimum Q_D [ml/min]		
$Pu_{R,min}$ [%]	SMB	"FR"	"RF"
80	0.384	0.375 (-2.2%)	0.347 (-9.5%)
85	0.593	0.549 (-7.4%)	0.470 (-20.7%)
90	1.482	1.070 (-27.9%)	0.760 (-48.8%)
91	–	1.351	0.882
92	–	–	1.066
93	–	–	1.390

(b) Nonlinear isotherm

	minimum Q_D [ml/min]		
$Pu_{R,min}$ [%]	SMB	"FR"	"RF"
80	0.609	0.592 (-2.8%)	0.571 (-6.3%)
85	0.863	0.813 (-5.8%)	0.724 (-16.1%)
90	1.899	1.444 (-23.9%)	1.053 (-44.5%)
91	–	1.779	1.183
92	–	–	1.374
93	–	–	1.695

demands (e.g., 80%). Furthermore, it is interesting to note that for stricter purity requirements (e.g., 91% or higher), only the fractionation and feedback regime allows to deliver both products while maintaining relatively low desorbent consumptions. From Table 4.4, it can be observed that for both isotherms, the highest achievable purity is 93% for the sequence "RF", and 91% for the opposite sequence. Thus, the feeding sequence "RF" (raffinate recyclate followed by fresh feed) again provides the best performance and was found to be optimal in this case study.

4.5 Conclusions

In this chapter, the FF-SMB concept with one outlet fractionation was investigated by a systematic optimization strategy. A rigorous model-based optimization framework was presented which allows dealing with the flexibility and exploiting the full potential of the fractionation and feedback approach. Two typical optimization problems using single objective functions and addressed by the sequential method were examined. On the basis of the extensive optimization studies performed for a difficult separation task, the optimum performance of FF-SMB featuring raffinate outlet fractionation was evaluated with respect to that of the conventional concept. The quantitative results clearly demonstrated that the more flexible FF-SMB consistently outperforms SMB in terms of the maximum feed throughput and minimum desorbent consumption for both linear and nonlinear isotherms. For high purity requirements, the advantages become particularly pronounced. Moreover, the influence of the feeding sequence on the optimal performance of FF-SMB was also examined. For the example considered in this chapter, the sequence of raffinate recyclate followed by original fresh feed achieves

superior performance in the case studies.

In the following chapter, we will extend the concept of single fractionation to the general scenario realizing simultaneous double fractionation of both outlets. In particular, our emphasis will be concentrated on addressing problems related to the practical applicability of FF-SMB.

4.6 Nomenclature

c	liquid phase concentration [g/l]
H	Henry coefficient [-]
K	adsorption equilibrium constant [l/g]
m	flow-rate ratio [-]
N_p	number of theoretical plates [-]
Pu	purity [%]
Q	liquid phase flow-rate [ml/min]
t	time [min]
t_s	switching period [min]
V	liquid phase volume [ml]
V_{Col}	column volume [ml]

Greek letters

α	selectivity [-]
ϵ	column porosity [-]
ρ	liquid level factor [-]
τ	normalized time [-]

Roman letters

I, II, III, IV	zone index

Subscripts and superscripts

$-$	adapted parameters for FF-SMB
0	initial conditions

A	less retained component
B	more retained component
$Buffer$	buffer vessel
D	desorbent
E	extract
F	feed
$Feed$	original feed tank
$Feedback$	feedback from buffer vessel
$Feeding$	feed from original feed tank
i	component index, $i = A$, B
in	inlet effluent of buffer vessel
k	outlet used for fractionation, $k = E$ or R
out	outlet effluent of buffer vessel
$Production$	outlet stream is withdrawn as product
R	raffinate
$Recycle$	outlet stream is recycled to buffer vessel

5

Fractionation of both outlets

By considering raffinate fractionation as an example, significant advantages of FF-SMB over classical SMB chromatography have been clearly demonstrated in the previous chapter. The promising results obtained motivate us to explore the optimal potential of the more flexible but challenging regime which realizes double fractionation of both outlets in this chapter. We begin with a short schematic description of the generalized concept of double fractionation. The process model and the mathematical optimization framework, previously adopted to investigate the single fractionation mode, are then extended to deal with this more flexible operating scheme. In order to illustrate its superiority, a systematic comparison of the optimal performance among the existing fractionation policies and conventional SMB is carried out based on a specific separation problem. A further evaluation of the extension of double fractionation in terms of a set of commonly used performance parameters is also provided. Moreover, the effect of product purity, adsorption selectivity, column efficiency, etc., on the relative advantage of the new concept over SMB is examined in detail, mainly aiming to reveal its applicability.

5.1 FF-SMB with double fractionation

As shown in Chapter 4, outlet fractionation and feedback are two key characteristics of an FF-SMB process. They can be applied to both extract and raffinate streams, resulting in an extension from the single fractionation to the general case. Since such extension is straightforward, only a brief introduction to the principle of FF-SMB with double fractionation is given below. A more detailed description of SMB and the fractionation and feedback approach can be found in Chapters 2 and 4, respectively.

During the operation of FF-SMB, each outlet stream is fractionated into two portions—product and recycle fractions, accordingly splitting one switching period into a production period of length $\tau^k_{Production}$ and a recycle period of length $\tau^k_{Recycle}$, $k = E, R$. This outlet fractionation strategy is shown in Fig. 5.1a and b for the extract and raffinate outlets, respectively. Over the production period of each outlet, the outlet stream fulfills a given integral purity requirement and thus is withdrawn as product. Within the recycle period, the stream is directed to an additional buffer vessel as off-spec product. The off-spec fraction collected in each buffer vessel is fed back into the unit alternatingly with the fresh feed within each period. Due to the alternating supply of three different sources, FF-SMB is characterized by a non-constant feeding regime, which obviously differs from the classical constant feeding of SMB. The novel feeding mode is illustrated in Fig. 5.2, where a specific feeding sequence of using the raffinate buffer vessel first, followed by the original feed tank, and finally the extract buffer vessel (abbreviated to "RFE" hereafter) is chosen for illustration purposes. The feeding scheme described above divides one complete switching interval into three sub-periods, i.e., the raffinate feedback period $\tau^R_{Feedback}$, feeding period $\tau_{Feeding}$ and extract feedback period $\tau^E_{Feedback}$, during which the corresponding sources are

continuously supplied to the unit.

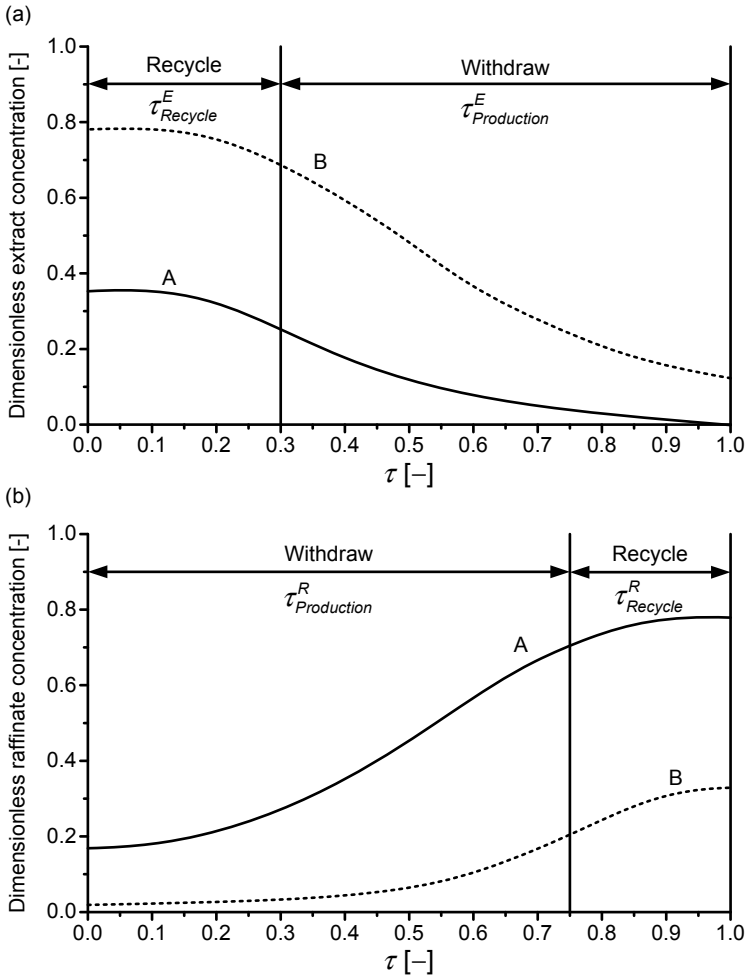

Figure 5.1: Principle of outlet fractionation of both extract and raffinate streams. (a) Extract outlet fractionation. (b) Raffinate outlet fractionation.

The FF-SMB process shown above can be conveniently implemented by adding only two buffer vessels and three valves to a standard SMB setup. A schematic representation of an SMB unit realizing simultaneous double fractionation and feedback is illustrated in Fig. 5.3. Two three-way valves installed at the outlets are used to fractionate the streams and one four-way feed valve enables an alternating feed supply. It should be pointed out

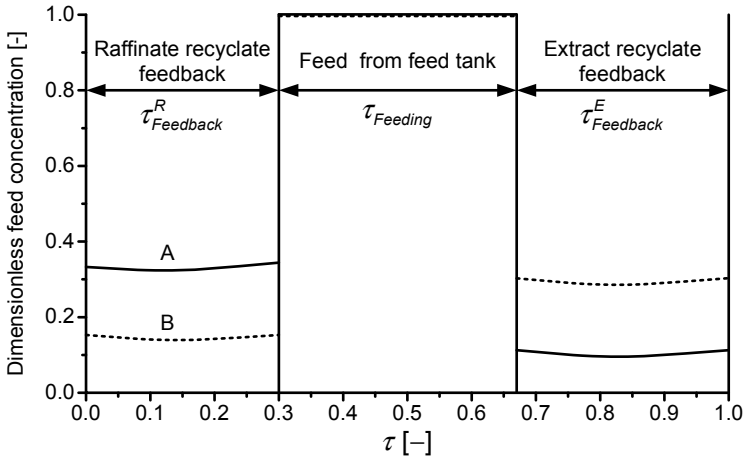

Figure 5.2: Feeding sequence "RFE" and resulting distinct feeding scheme. Solid line: feed concentration for A; dotted line: feed concentration for B. The feed concentration of each component is normalized with respect to that of the fresh feed.

that the off-spec fraction recycled from each outlet differs from one another in composition. For example, the less retained component A is enriched in the raffinate recyclate, while B is concentrated in the extract recyclate (see Fig. 5.2). As a result, collecting these two sorts of recyclates into one buffer vessel and remixing them with the fresh feed destroy the achieved resolution and thus are less desirable. This motivates the introduction of one separate buffer vessel for each outlet.

5.2 Modeling and optimization

For the single fractionation scenario discussed in Chapter 4, additional mass balance equations were derived to characterize the discontinuous product draw-off and alternating feed supply. A simplified model assuming well-mixed conditions was used to predict the dynamic behavior of the buffer

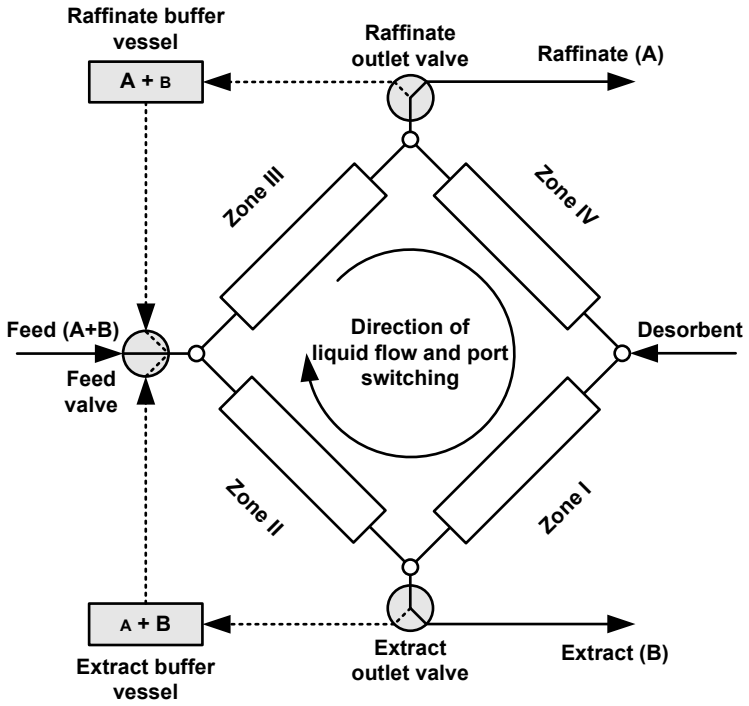

Figure 5.3: Schematic illustration of a modified SMB unit realizing double fractionation and feedback. Additional hardware investment includes two buffer vessels and three valves.

vessel. In the case of double fractionation, the relevant modeling equations and the dynamics of buffer vessels can be easily obtained and thus are summarized in Table 5.1 for brevity. Compared to the classical SMB concept, the generalized case introduces four additional degrees of freedom, i.e., $\tau^k_{Production}$ and $\tau^k_{Feedback}$, $k = E, R$. In addition, the feeding sequence can be also regarded as one degree of freedom, which offers six candidate sequences. This diversity is due to the existence of three different inlet sources.

The detailed optimization problem for the maximization of feed throughput is outlined in Table 5.2. Note that the objective function $\overline{Q}_F$, representing the average rate of processing fresh feed, was adapted from the version used

Table 5.1: Summary of balance equations and buffer vessel dynamics used to characterize double fractionation and feedback approach.

Balance equations for production and recycle periods:

$\tau^k_{Production} + \tau^k_{Recycle} = 1, \quad k = E,\, R$

Volumes collected in product tank and buffer vessel:

$V^k_{Production} = \tau^k_{Production}\, t_s\, Q_k$

$V^k_{Recycle} = \tau^k_{Recycle}\, t_s\, Q_k, \quad k = E,\, R$

Balance equation for feedback and feeding periods:

$\tau^E_{Feedback} + \tau^R_{Feedback} + \tau_{Feeding} = 1$

Volumes supplied from feed tank and buffer vessel:

$V_{Feeding} = \tau_{Feeding}\, t_s\, Q_F$

$V^k_{Feedback} = \tau^k_{Feedback}\, t_s\, Q_F, \quad k = E,\, R$

Feed concentration is dependent on feeding sequence. For sequence "RFE":

$$c^F_i(t) = \begin{cases} c_i^{Buffer,R}(t), & \frac{t}{t_s} \in [0, \tau^R_{Feedback}] \\ c_i^{Feed}, & \frac{t}{t_s} \in (\tau^R_{Feedback}, 1 - \tau^E_{Feedback}] \\ c_i^{Buffer,E}(t), & \frac{t}{t_s} \in (1 - \tau^E_{Feedback}, 1] \end{cases}, \qquad i = A,\, B$$

Buffer vessel dynamics:

$\frac{dV^k_{Buffer}}{dt} = Q^k_{in}(t) - Q^k_{out}(t)$

$\frac{d(V^k_{Buffer}\, c_i^{Buffer,k})}{dt} = Q^k_{in}(t)\, c^k_i(t) - Q^k_{out}(t)\, c_i^{Buffer,k}(t),\ i = A,\, B,\ k = E,\, R$

where $Q^k_{in}\,(k = E,\, R)$ are defined as below:

$$Q^E_{in} = \begin{cases} Q_E, & \frac{t}{t_s} \in [0, 1 - \tau^E_{Production}] \\ 0, & \frac{t}{t_s} \in (1 - \tau^E_{Production}, 1] \end{cases}, \; Q^R_{in} = \begin{cases} 0, & \frac{t}{t_s} \in [0, \tau^R_{Production}] \\ Q_R, & \frac{t}{t_s} \in (\tau^R_{Production}, 1] \end{cases}$$

$Q^k_{out}\,(k = E,\, R)$ depend on feeding sequence. For sequence "RFE":

$$Q^E_{out} = \begin{cases} 0, & \frac{t}{t_s} \in [0, 1 - \tau^E_{Feedback}] \\ Q_F, & \frac{t}{t_s} \in (1 - \tau^E_{Feedback}, 1] \end{cases}, \; Q^R_{out} = \begin{cases} Q_F, & \frac{t}{t_s} \in [0, \tau^R_{Feedback}] \\ 0, & \frac{t}{t_s} \in (\tau^R_{Feedback}, 1] \end{cases}$$

Initial conditions: $V^k_{Buffer}|_{t=0} = V^k_{Buffer,0}, \quad c_i^{Buffer,k}|_{t=0} = c^{Buffer,k}_{i,0}$

in Chapter 4:

$$\overline{Q}_F = (1 - \tau^E_{Feedback} - \tau^R_{Feedback})\, Q_F \tag{5.1}$$

The optimization variables include the dimensionless flow-rate ratios, i.e., the so-called m-factors, the feed flow-rate Q_F and the two dimensionless production periods $\tau^E_{Production}$, $\tau^R_{Production}$. We also restrict the present study to one special case where $V^k_{Recycle}$ matches $V^k_{Feedback}$, $k = E$, R. This case can ensure that each buffer vessel neither overflows nor "runs dry", and an overall constant liquid volume over one switching period can be maintained. As a result, the two dimensionless feedback periods can be determined through the relations

$$\tau^E_{Feedback} = \frac{(m_I - m_{II})(1 - \tau^E_{Production})}{m_{III} - m_{II}} \tag{5.2}$$

$$\tau^R_{Feedback} = \frac{(m_{III} - m_{IV})(1 - \tau^R_{Production})}{m_{III} - m_{II}} \tag{5.3}$$

and are thus excluded from the independent variables.

In addition to the inequality constraints imposed on both product purities and the highest internal flow-rate Q_I, the following set of constraints must be respected for the feedback periods

$$0 \leq \tau^E_{Feedback} \leq 1,\ 0 \leq \tau^R_{Feedback} \leq 1,\ 0 \leq \tau^E_{Feedback} + \tau^R_{Feedback} \leq 1 \tag{5.4}$$

in order to guarantee a feasible feedback operation for each buffer vessel.

The nonlinear programming (NLP) problem was addressed by the sequential approach. This solution strategy is detailed in Chapter 4 and only sketched here for brevity. The FF-SMB model described above is discretized only in space and the resulting system of differential equations is integrated repeatedly until the CSS is attained. The constraints and objective function are then evaluated and provided to an external optimizer. The procedure is repeated until the optimal operating condition is found. In this work,

Table 5.2: Outline of nonlinear optimization problem for FF-SMB with double fractionation and feedback.

Objective function:

$$\max\ \overline{Q}_F = \max\ (1 - \tau^E_{Feedback} - \tau^R_{Feedback})\, Q_F$$

Optimization variables:

$$m_I, m_{II}, m_{III}, m_{IV}, Q_F, \tau^E_{Production}, \tau^R_{Production}$$

Product purity requirements:

$$Pu_E = \frac{\int_{1-\tau^E_{Production}}^{1} c^E_B(\tau)\, d\tau}{\int_{1-\tau^E_{Production}}^{1} (c^E_A(\tau)+c^E_B(\tau))\, d\tau} \geq Pu_{E,min}$$

$$Pu_R = \frac{\int_{0}^{\tau^R_{Production}} c^R_A(\tau)\, d\tau}{\int_{0}^{\tau^R_{Production}} (c^R_A(\tau)+c^R_B(\tau))\, d\tau} \geq Pu_{R,min}$$

Maximum flow-rate restriction:

$$Q_I \leq Q_{max}$$

Feasibility constraints on feedback periods:

$$0 \leq \tau^E_{Feedback} \leq 1,\ 0 \leq \tau^R_{Feedback} \leq 1,\ 0 \leq \tau^E_{Feedback} + \tau^R_{Feedback} \leq 1$$

Feasibility constraints on m-values:

$$m_I - m_{II} > 0,\ m_I - m_{IV} > 0,\ m_{III} - m_{II} > 0,\ m_{III} - m_{IV} > 0$$

the DAE model obtained from the orthogonal collocation on finite elements discretization was solved by the package DASPK3.1 [33], and the NAG Library routine E04UCF [74], which implements an SQP algorithm, was used as the optimizer. The CSS was considered to be established once the difference between the dimensionless concentration profiles at the end of two successive periods became lower than a specified tolerance 1×10^{-4}. The gradients required by the SQP solver were determined explicitly except for those of the purity constraints, which were numerically approximated by a finite-difference scheme.

It is worth noting that in Chapter 4 the best feeding sequence for the

case of single fractionation was determined by optimizing each scenario and comparing their performances. However, for this general case, we consider only one feeding sequence "RFE", although it is feasible to identify the optimum sequence among the six possibilities ("EFR", "RFE", etc.) by following the same procedure. Our selection was not made arbitrarily but rather is supported by the previous work. For the raffinate fractionation, the optimization results reveal that the sequence of raffinate recyclate followed by fresh feed ("RF") significantly outperforms the opposite one for the process under examination. We also predicted that the sequence of original feed prior to extract recyclate ("FE") could be preferable when fractionating the extract outlet. These aspects motivate us to explore the sequence "RFE" exclusively for this double fractionation scheme.

5.3 Results and discussion

A laboratory-scale binary separation was used as an illustrating example in Chapter 4 to evaluate the potential of FF-SMB with one outlet fractionation. We also chose this model process here to examine the double fractionation scenario. This reference system represents a difficult separation due to a low column efficiency ($N_p = 40$) and a small selectivity ($\alpha = 1.126$). The detailed parameters used to quantify the process are listed in Table 4.2. Note that in order to enable the simultaneous fractionation of both outlets and feedback, two separate buffer vessels were introduced, each of which was assumed to contain only fresh solvent of volume of 4 ml initially. The nonlinear isotherm parameters characterizing the separation are summarized in Table 4.3. To investigate the linear adsorption behavior, the nonlinearity coefficients $K_i\,(i = A,\, B)$ were set to zero.

5.3.1 Comparison of different operating schemes

We examined four different operating regimes, i.e., conventional SMB, FF-SMB fractionating either raffinate or extract alone, and FF-SMB fractionating both outlet streams simultaneously. For the raffinate fractionation, the process was operated with the feeding sequence "RF", which was found to be optimal in Chapter 4. When fractionating the other outlet, both sequence "FE" and "EF" were considered. As mentioned before, for the double fractionation we restricted to only one sequence "RFE". For each scheme, the same set of purity requirements ranging from 85% to 95% was specified to both extract and raffinate products. The proposed optimization approach was used to search the optimal operating parameters that enable the maximum feed throughput and fulfill the imposed constraints listed in Table 5.2.

The optimization results for both linear and nonlinear isotherms are shown in Figs. 5.4 and 5.5, respectively. Note that for the extract fractionation, which was not examined in Chapter 4 in detail, it is found that following the sequence "FE" allows processing more fresh feed. Only results for this sequence are shown here for comparison.

From the results illustrated in Figs. 5.4 and 5.5 the following conclusions can be drawn. For the separation under study, FF-SMB realizing any kind of single fractionation provides better performance than the conventional SMB concept. For the purity of 90%, for example, when fractionating the raffinate, the feed throughput can be enhanced by more than 94% and 70% for the linear and nonlinear isotherms, respectively. Alternatively, as the other outlet is used for fractionation, the improvement is nearly 72% and 56%. Furthermore, the maximum attainable purity is 91% and 92% for the extract and raffinate fractionation, respectively. Both are higher than that of SMB (only 90%). It can be also observed that the raffinate fractionation outper-

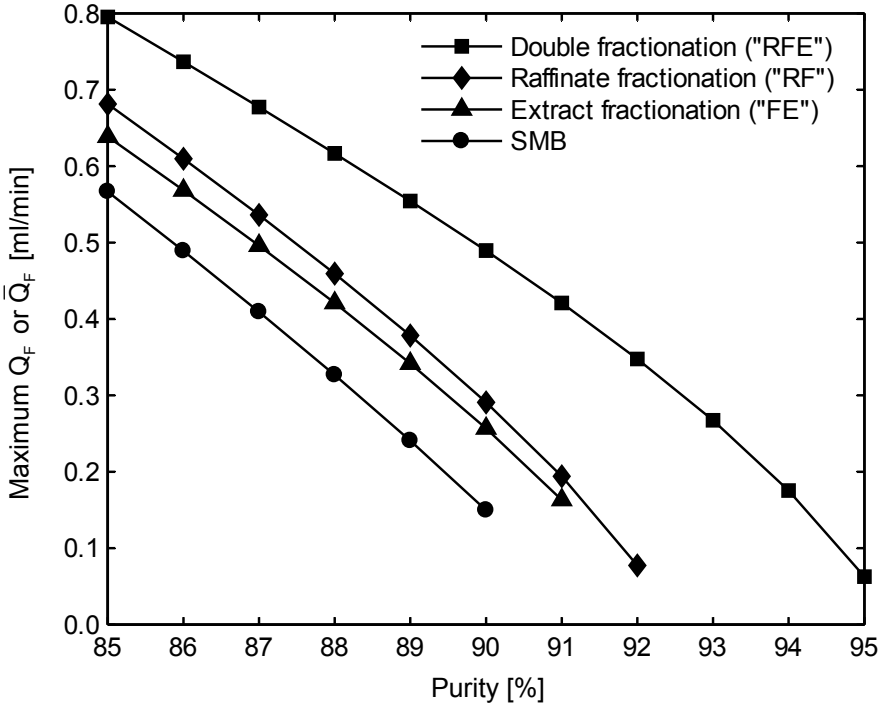

Figure 5.4: Comparison of maximum feed throughput for conventional SMB (circles), FF-SMB fractionating one outlet (extract: triangles, raffinate: diamonds) and both outlets (squares) (linear isotherms). The feeding sequence used for FF-SMB with extract, raffinate and double fractionation is "FE", "RF" and "RFE", respectively.

forms the extract fractionation for the linear isotherm. For the nonlinear case, however, such difference appears not to be obvious. It should be emphasized that for a given separation the selection of the most favorable type of single fractionation is not trivial. Our optimization approach can help to make such selection.

When combining both extract and raffinate outlets for fractionation, further performance potential can be exploited. For example, for the same purity of 90%, the feed throughput now can be increased by 227% and 183%

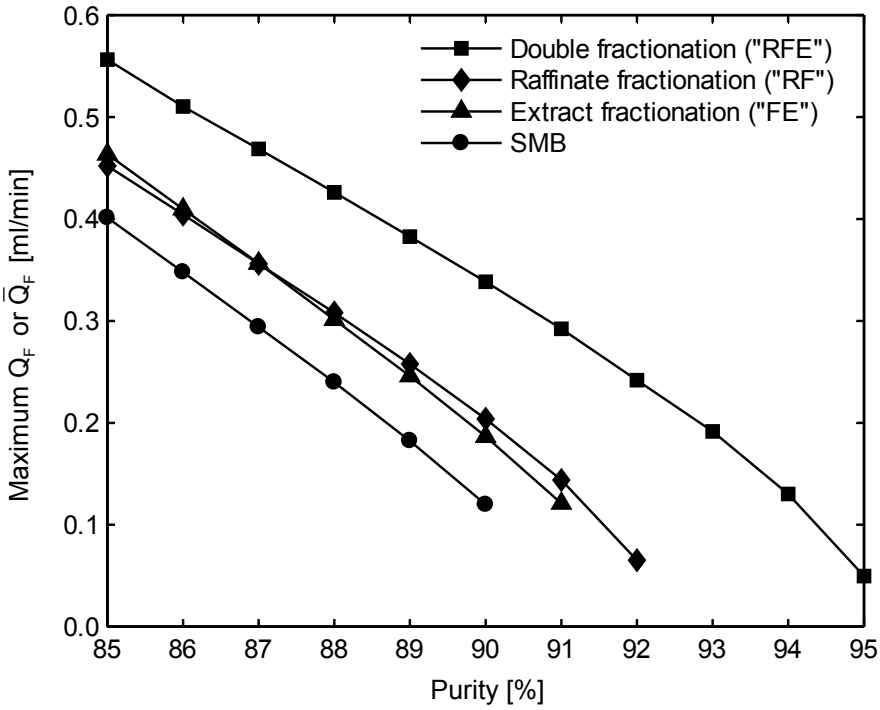

Figure 5.5: Comparison of maximum feed throughput for conventional SMB (circles), FF-SMB fractionating one outlet (extract: triangles, raffinate: diamonds) and both outlets (squares) (nonlinear isotherms). The feeding sequence used for FF-SMB with extract, raffinate and double fractionation is "FE", "RF" and "RFE", respectively.

for the linear and nonlinear isotherms, respectively. The high flexibility of the double fractionation also enables the process to deliver a purity of up to 95% for both products. It is also seen that the improvement of this scheme with respect to the single fractionation is larger than that achieved by the single fractionation over the classical SMB mode. The above results reveal that although the extension to the general case is simple, the benefit can be significant.

Finally, for the FF-SMB concept realizing either single or double frac-

tionation, the degree of improvement depends on the desired target purity: the higher the purity demand, the more pronounced the improvement tends to be.

The optimal values of $\tau^E_{Production}$ and $\tau^R_{Production}$ are illustrated in Fig. 5.6a and b for the linear and nonlinear isotherms, respectively. The other two feedback periods $\tau^E_{Feedback}$ and $\tau^R_{Feedback}$, which were obtained using Eqs. (5.2) and (5.3) respectively, are shown in Fig. 5.6c and d for the same two types of isotherms. For the linear isotherm, as the purity increases, $\tau^E_{Production}$ first undergoes a drop from about 0.82 to 0.8 and then goes up slowly; $\tau^R_{Production}$ steadily increases from nearly 0.76 to 0.78. In contrast, the tendency is not much clear in the nonlinear case. However, both operating parameters evolve within a certain range: $\tau^E_{Production}$ varies over the range from about 0.81 to 0.87 and $\tau^R_{Production}$ from about 0.72 to 0.77. For both isotherms, the two feedback periods gradually increase up to around 0.45 (see Fig. 5.6c and d). Such an increase leads to a reduction of the feeding period $\tau_{Feeding}$ (i.e., $1 - \tau^E_{Feedback} - \tau^R_{Feedback}$) from about 0.5 to 0.1.

The performance comparison performed in this section shows that the double fractionation mode is the most productive alternative among various fractionation schemes and the standard SMB process. It should be pointed out that the feeding sequence studied for this operation policy is based on the heuristic approach discussed in Section 5.2. Exploring all the other sequences may even lead to further improvement.

5.3.2 Comparison of performance parameters

We also quantitatively evaluated the relative potential of FF-SMB with respect to the conventional SMB operation in terms of one set of specific performance parameters. These parameters include the productivity, elu-

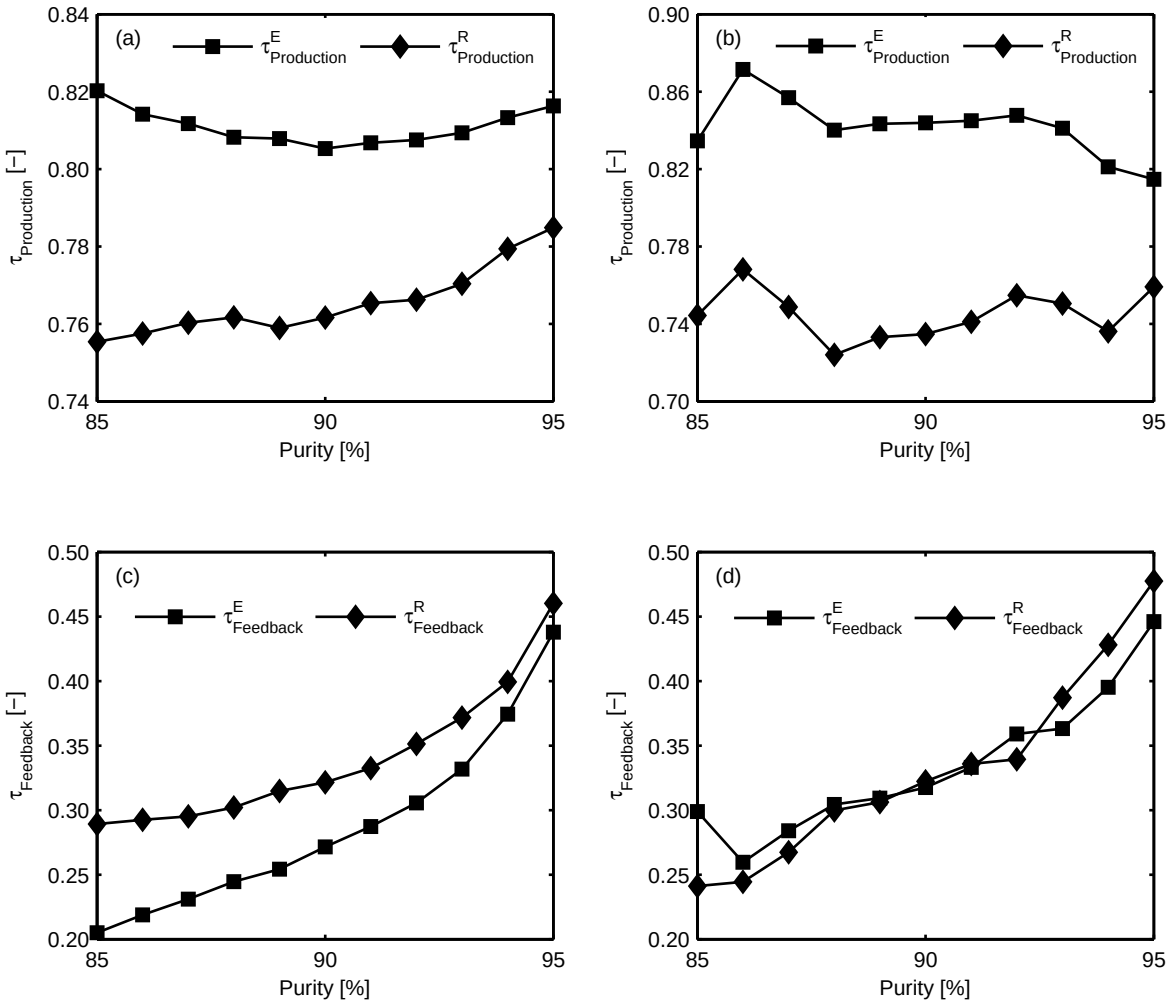

Figure 5.6: Optimal production and feedback periods for FF-SMB with double fractionation. Optimal production periods $\tau^E_{Production}$ (squares) and $\tau^R_{Production}$ (diamonds) are plotted in (a) for linear and in (b) for nonlinear isotherms. Feedback periods $\tau^E_{Feedback}$ (squares) and $\tau^R_{Feedback}$ (diamonds) are plotted in (c) for linear and in (d) for nonlinear isotherms.

ent consumption, average product concentration, and recovery yield for both products. Note that in the context of FF-SMB, these parameters must be properly adapted to allow a fair comparison with SMB. The revised versions for these criteria were detailed in [26] for one outlet fractionation and can be easily extended to the general case. The parameters were calculated at the optimum operating conditions determined in Section 5.3.1 for each operating mode. The results are demonstrated in Fig. 5.7 for the extract product under linear conditions. For the nonlinear case and the raffinate product, the results are qualitatively similar to those shown in Fig. 5.7 and omitted here for the sake of brevity.

From Fig. 5.7a, b and c, the potential benefits can be clearly identified for the productivity, eluent consumption and product concentration. For a minimum purity of 90%, the double fractionation operation allows the process to increase the extract productivity by 227% and simultaneously reduce the eluent consumption by 62%. The extract product concentration can be enhanced by 168%. Furthermore, as pointed out in Section 5.3.1 for the optimized feed throughput, the extent of improvement for these parameters also shows an obvious dependence on the purity demand for both products. Both observations show that the concept is extremely appealing for applications requiring high product purity. Concerning the product recovery (see Fig. 5.7d), the results indicate that the FF-SMB concept performs comparable to the classical process and is clearly superior to that of the "Partial Discard" strategy.

5.3.3 Effect of selectivity

In order to examine the effect of selectivity on the performance of FF-SMB, the Henry constant for the more retained component H_B was altered from

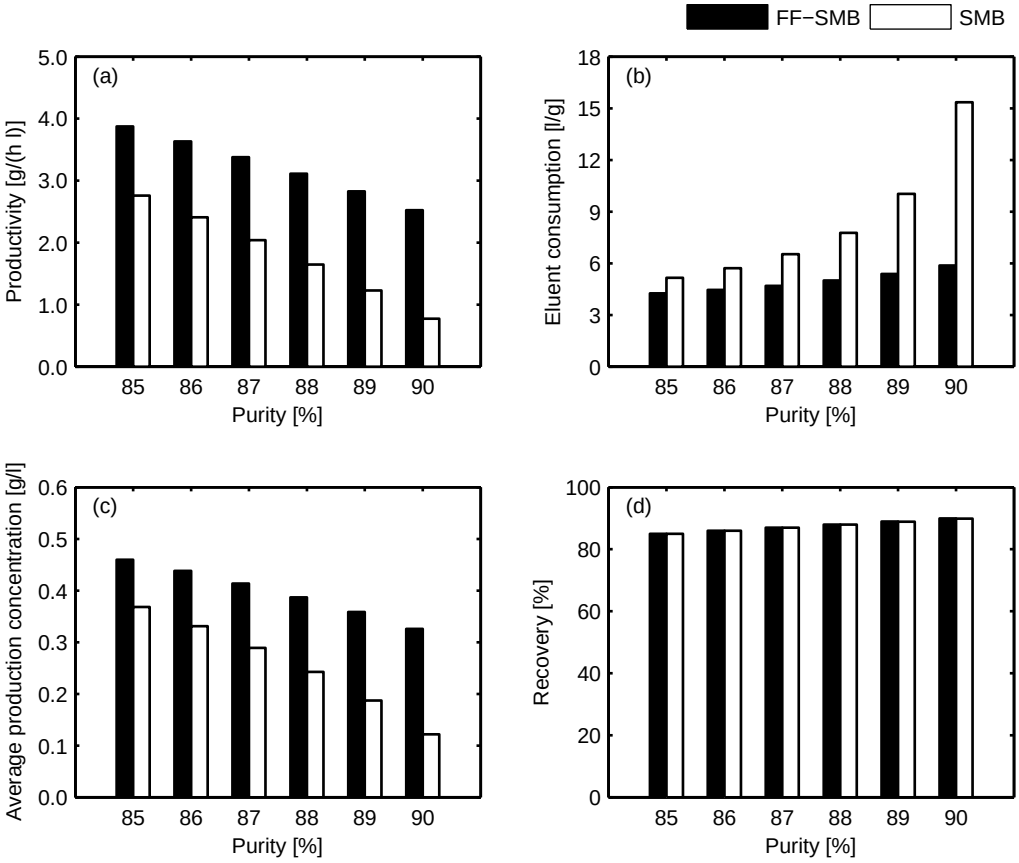

Figure 5.7: Comparison of the performance parameters of the optimized FF-SMB with double fractionation and the optimized SMB. (a) Productivity, (b) eluent consumption, (c) average product concentration and (d) recovery. The performance criteria are calculated for the extract product under linear conditions.

that of the reference system. The adjusted values and the resulting separation factors are summarized in Table 5.3. H_A and all the other parameters were fixed at their reference values listed in Table 4.3. For each modified system of different adsorption selectivity, the optimization was performed to maximize the feed throughput of FF-SMB ($\overline{Q}_F$) and standard SMB (Q_F). Note that the minimum purity was fixed at 90% for both products during the optimization. The optimal values for both operating schemes are reported in Table 5.4a and b for the linear and nonlinear isotherms, respectively. For the sake of comparison, the solutions previously obtained for the reference system ($\alpha = 1.126$) along with the achievable improvements of FF-SMB over the conventional concept are also shown there.

Table 5.3: Henry constants and separation factors used in Section 5.3.3.

H_B [-]	7.617	7.109	6.601	6.094	5.718	5.535
α [-]	1.500	1.400	1.300	1.200	1.126	1.090

It can be seen that for each separation, the performance of FF-SMB is always superior to that of SMB. As the separation factor approaches unity, the attainable advantage becomes more and more pronounced. Specifically, when $\alpha = 1.5$, the improvement is only 10% and 9% for the case of linear and nonlinear isotherms, respectively. As α decreases to the reference value of 1.126, as already reported in Section 5.3.1, the ability to treat fresh feed can be enhanced by 227% and 183%. For a lower α-value of 1.090, the optimizer failed to find solution for SMB, and only the FF-SMB process is proven feasible using a relatively low value of $\overline{Q}_F$. The results presented in this case study imply that the newly proposed process is attractive in particular for low selectivity separations, for which classical SMB chromatography is less efficient or even infeasible.

Table 5.4: Maximum feed throughput of FF-SMB and SMB with different separation factors.

α [-]	1.500	1.400	1.300	1.200	1.126	1.090
(a) Linear isotherm						
$\overline{Q}_F$ [ml/min]	2.7900	2.3040	1.7438	1.0891	0.4894	0.0886
Q_F [ml/min]	2.5355	2.0364	1.4626	0.7850	0.1497	–
Improvement [%]	10	13	19	39	227	–
(b) Nonlinear isotherm						
$\overline{Q}_F$ [ml/min]	2.4089	1.9519	1.4371	0.8411	0.3385	0.0637
Q_F [ml/min]	2.2183	1.7564	1.2302	0.6269	0.1198	–
Improvement [%]	9	11	17	34	183	–

5.3.4 Effect of column efficiency

Another interesting aspect in evaluating the practical applicability of FF-SMB is to investigate the influence of column efficiency on its potential. This is achieved next by examining different separation processes that are identical to the reference system but with varied column efficiencies. For each efficiency value assumed, the feed throughput maximization problem subject to the minimal extract and raffinate purities of 90% was solved again. The optimization results and various N_p values used are summarized in Table 5.5 for both types of isotherms.

It can be observed that with a decrease of column efficiency (i.e., N_p varying from 100 to 30), the capability of processing feed is reduced for both FF-SMB and SMB. For the same efficiency, adopting the fractionation and feedback approach allows the system to deliver a higher feed throughput. The extent of such improvement dramatically increases at the lower values

Table 5.5: Maximum feed throughput of FF-SMB and SMB with different column efficiencies.

N_p [-]	30	40	60	80	100
(a) Linear isotherm					
$\overline{Q}_F$ [ml/min]	0.1873	0.4894	0.7244	0.8240	0.8782
Q_F [ml/min]	–	0.1497	0.5076	0.6661	0.7456
Improvement [%]	–	227	43	24	18
(b) Nonlinear isotherm					
$\overline{Q}_F$ [ml/min]	0.1395	0.3385	0.4856	0.5416	0.5733
Q_F [ml/min]	–	0.1198	0.3575	0.4531	0.4953
Improvement [%]	–	183	36	20	16

of column efficiency. For an N_p value of 30, only the FF-SMB process can be operated at the maximum rate of supplying feed while respecting the given purity requirements. The conventional SMB is found to be infeasible. The quantitative evaluation carried out indicates that for difficult separations using columns of low efficiency, FF-SMB shows its significant superiority. This fact also means that FF-SMB allows the use of cheaper low-efficient stationary phases, thus considerably reducing the overall separation costs.

5.3.5 Effect of column number

We have examined the impact of different numbers of columns upon the optimal performance of FF-SMB relative to that of SMB. The highest feed throughput obtained for each operating mode is summarized in Table 5.6. Note that for 5 and 6 columns, only the 1-1-2-1 and 1-2-2-1 configurations were optimized, respectively.

Table 5.6: Maximum feed throughput of FF-SMB and SMB with different numbers of columns.

N_{Col} [-]	4 (1-1-1-1)	5 (1-1-2-1)		6 (1-2-2-1)		
$Pu_{k,min}, k = E, R$ [%]	90	90	95	95	99.5	99.6
(a) Linear isotherm						
$\overline{Q}_F$ [ml/min]	0.4894	0.7196	0.4321	0.6079	0.0958	0.0635
Q_F [ml/min]	0.1497	0.5783	0.1864	0.6066	0.0838	0.0407
Improvement [%]	227	24	132	0.2	14	56
(b) Nonlinear isotherm						
$\overline{Q}_F$ [ml/min]	0.3385	0.4677	0.2870	0.3894	0.0865	0.0558
Q_F [ml/min]	0.1198	0.3478	0.1339	0.3894	0.0742	0.0403
Improvement [%]	183	34	114	0	17	38

Let us first take a look at the results for the linear case. It can be noted that as the column number increases from 4 to 5, the improvement achieved by using the new concept drops from 227% to only 24% for the purity of 90%. However, when a higher value of 95% is requested for both products, a significant advantage over SMB can still be identified with the same 5-column FF-SMB. Furthermore, for a 6-column unit, the benefit previously attained in the 5-column case for the purity of 95% almost disappears. In fact, FF-SMB behaves like SMB in this case, since the fractionation and feedback for both outlets is found not to be needed. As expected, the potential of FF-SMB becomes more pronounced only as a higher purity level is required in the 6-column configuration. The room for improvement, in contrast to that of the preceding 4- and 5-columns cases, tends to be reduced. For the nonlinear isotherm, qualitatively similar results can be clearly observed from Table 5.6b. Based on these observations, it is concluded that for difficult

separations with a small number of columns (e.g., 4 or 5), the superiority due to the fractionation and feedback modification is particularly significant.

5.3.6 Effect of column configuration

In this section, our aim is to evaluate the effect of column configuration on the potential of FF-SMB. In particular, we are interested in how the column arrangement influences the fractionation and feedback operation of FF-SMB. For these purposes, we have optimized the feed throughput of the 5-column SMB and FF-SMB processes with four different column configurations. For each configuration, a minimum purity of 95% was specified to the extract and raffinate products. The optimization results are presented in Table 5.7 for both linear and nonlinear isotherms.

Table 5.7: Maximum feed throughput of FF-SMB and SMB with different column configurations (5 columns).

Configuration [-]	2-1-1-1	1-2-1-1	1-1-2-1	1-1-1-2
(a) Linear isotherm				
$\overline{Q}_F$ [ml/min]	0.1728	0.4284	0.4321	0.1622
Q_F [ml/min]	–	0.1578	0.1864	–
Improvement [%]	–	171	132	–
(b) Nonlinear isotherm				
$\overline{Q}_F$ [ml/min]	0.1238	0.2932	0.2870	0.1304
Q_F [ml/min]	–	0.1169	0.1339	–
Improvement [%]	–	151	114	–

It is observed that when the additional column is arranged in each of the two central zones (i.e., 1-2-1-1 and 1-1-2-1), both SMB and FF-SMB

are able to deliver the on-spec products with the highest feed throughput. Furthermore, the more flexible fractionation and feedback regime consistently outperforms the conventional mode for these configurations. In particular, for the configuration of 1-2-1-1 the optimal value can be enhanced by more than 1.5 times for both isotherms. Once the column is moved from the central zones to zone I or IV, however, no feasible operating conditions were found for SMB to fulfill the required purity specifications. The results reflect that using the column arrangements of 2-1-1-1 and 1-1-1-2, the classical SMB mode is no longer infeasible for such high purity level. By contrast, with the same arrangements the new process still allows to offer the optimal feed throughput, while respecting the specified product purities. In addition, for FF-SMB a rather similar performance is achieved by the configurations of 1-2-1-1 and 1-1-2-1. However, the configuration 1-1-2-1 is clearly better than the configuration 1-2-1-1 in the case of SMB. For both operating regimes, the above configurations are significantly superior to the other two cases.

For the 5-column FF-SMB, the development of the optimal production periods and resulting feedback periods with respect to the column distribution in the case of nonlinear isotherms are demonstrated in Fig. 5.8a and b, respectively. The results obtained for the linear case exhibit a qualitatively similar tendency and thus are not shown here. It is interesting to note that once one arranges the additional column to zone II (i.e., 1-2-1-1), the optimal $\tau^E_{Production} = 1$ and $\tau^E_{Feedback} = 0$, indicating that the fractionation and feedback regime for the extract outlet becomes inactive. In this case, however, the operation on the raffinate outlet remains active, which is based on the observation that the optimal value of $\tau^R_{Production}$ is near 0.75 and $\tau^R_{Feedback}$ slightly greater than 0.5. On the other hand, if zone III includes two columns, the raffinate fractionation and feedback is found to be inactive. Furthermore,

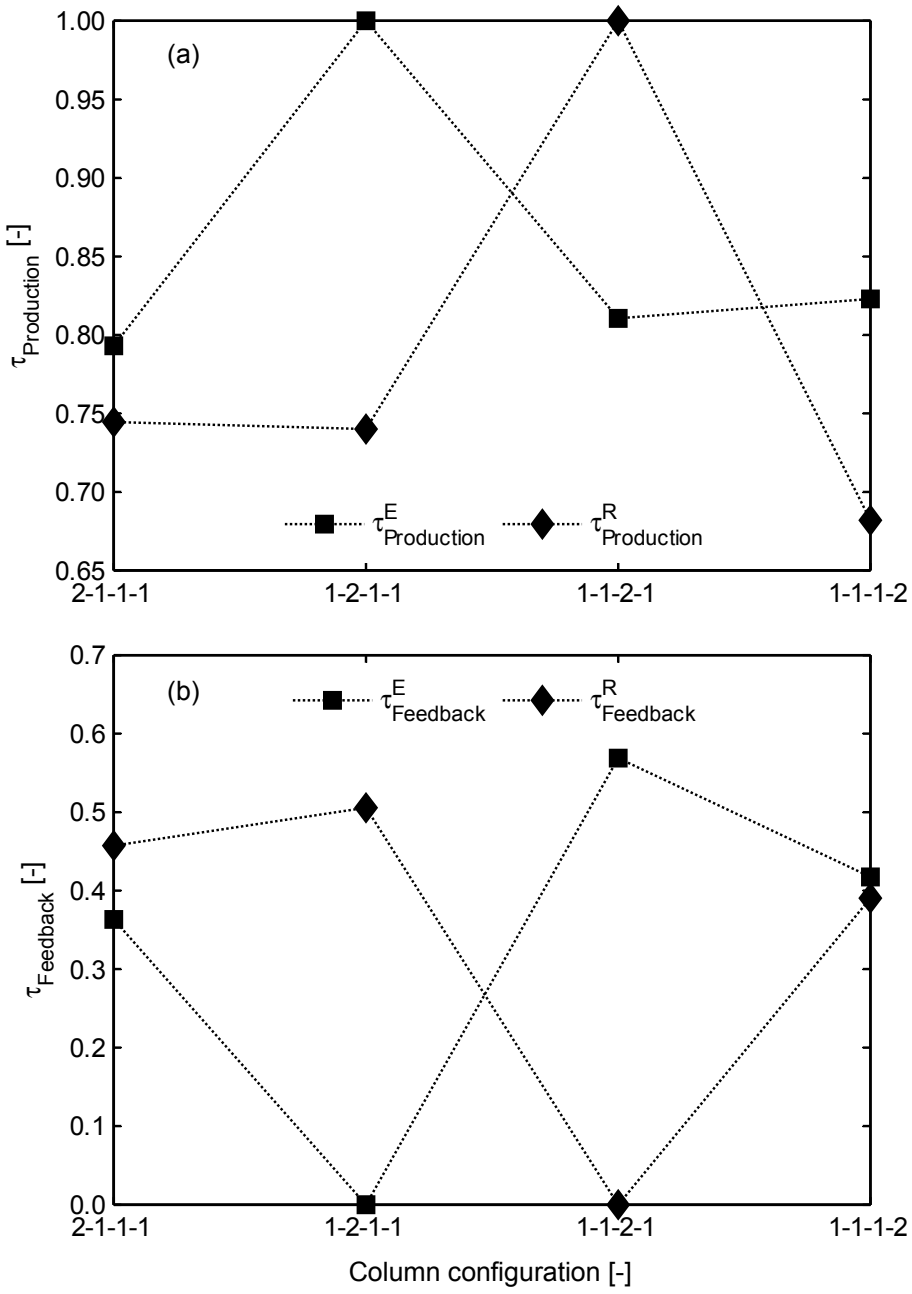

Figure 5.8: Effect of column configuration on the optimal production and feedback periods of the 5-column FF-SMB process. (a) Optimal production periods, and (b) feedback periods calculated by Eqs. (5.2) and (5.3).

for the other configurations where both central zones have only one column, the fractionation and feedback for both outlets is activated again. The interesting results indicate that for the 5-column system under consideration, how to arrange the columns in different zones has a significant impact on the fractionation and feedback behavior. In particular, arranging more columns in zone II (III) helps improve the resolution of the extract (raffinate) stream, and thus allows it to be fully withdrawn as the on-spec product without activating the fractionation and feedback operation.

5.4 Concluding remarks

In this chapter, we extended the FF-SMB concept to the general case that realizes a simultaneous fractionation of both extract and raffinate streams. The model-based optimization strategy proposed previously for one outlet fractionation was also extended to deal with this generalized operating alternative. To assess its potential over two existing single fractionation policies and standard SMB, extensive optimization studies were performed on the basis of a specific case study. The quantitative results demonstrated that the double fractionation is the most productive operating regime for both linear and nonlinear isotherms, although each single fractionation approach also obviously outperforms conventional SMB chromatography. The effectiveness of the extension was evaluated in terms of a number of commonly used performance parameters. It was shown that FF-SMB provides significant enhancements in productivity, product concentration and substantial savings in eluent consumption, while retaining a level of recovery comparable to that of SMB.

Further evaluation of the practical applicability of FF-SMB was carried

out with the aid of the optimization tool developed. In particular, the influence of product purity, adsorption selectivity, column efficiency etc., on the relative potential of FF-SMB was quantitatively analyzed. It was found that FF-SMB has significant advantages for difficult separations characterized by high product purity requirements, low column efficiency, small selectivity and a small number of columns. For this type of applications, FF-SMB has the potential to be a highly competitive alternative to SMB and its other derivatives. Moreover, the optimization results further revealed that for the same number of columns, the column distribution in different zones has a strong impact on the fractionation and feedback operation of FF-SMB.

5.5 Nomenclature

c	liquid phase concentration [g/l]
H	Henry coefficient [-]
K	adsorption equilibrium constant [l/g]
m	flow-rate ratio [-]
N_{Col}	number of columns [-]
N_p	number of theoretical plates [-]
Pu	purity [%]
Q	liquid phase flow-rate [ml/min]
t	time [min]
t_s	switching period [min]
V	liquid phase volume [ml]

Greek letters

α	selectivity [-]
τ	normalized time [-]

Roman letters

I, II, III, IV	zone index

Subscripts and superscripts

$-$	adapted parameters for FF-SMB
0	initial conditions
A	less retained component
B	more retained component

$Buffer$	buffer vessel
D	desorbent
E	extract
F	feed
$Feed$	original feed tank
$Feedback$	feedback from buffer vessel
$Feeding$	feed from original feed tank
i	component index, $i = A$, B
in	inlet effluent of buffer vessel
k	SMB outlet or buffer vessel index, $k = E$, R
out	outlet effluent of buffer vessel
$Production$	outlet stream is withdrawn as product
R	raffinate
$Recycle$	outlet stream is recycled to buffer vessel

6

Enhancing performance of FF-SMB by incorporating an enrichment step

In this chapter, a new idea that introduces an enrichment step to the recycled fractions is proposed for FF-SMB to improve its performance. We first present the motivation for suggesting the concept. By taking the solvent evaporation as an illustrative example, we then provide a mathematical model capable of characterizing the dynamic behavior of the buffer vessels realizing the enrichment operation, followed by a brief optimization problem formulation. The effectiveness of this scheme is evaluated with the optimization tool developed for standard FF-SMB. The optimal performance of the new evaporative FF-SMB is compared to that of the normal non-enriched scenario and conventional SMB. The effect of the evaporating rate on the benefit gained by exploiting enrichment is analyzed. Some limitations of this operation are also discussed.

6.1 Motivation

Before providing the motivation for the enrichment operation, let us first gain a quantitative insight into the behavior of the buffer vessels by examining the reference system considered in Chapters 4 and 5. The detailed description of this separation example is given in Section 4.4.1. The operating parameters used for the simulation of the model system are summarized in Table 6.1. Note that the set of operating conditions was obtained by solving the feed throughput maximization problem of FF-SMB subject to a minimum purity requirement of 90% for both extract and raffinate products.

Table 6.1: Summary of operating conditions used to simulate the reference system given in Section 4.4.1.

Mode	FF-SMB with double fractionation		
m_I [-]	6.1762	Feeding sequence [-]	"RFE"
m_{II} [-]	4.6124	$\tau^E_{Production}$ [-]	0.8439
m_{III} [-]	5.3810	$\tau^R_{Production}$ [-]	0.7348
m_{IV} [-]	4.4471	$\tau^E_{Feedback}$ [-]	0.3175
Q_F [ml/min]	0.9397	$\tau^R_{Feedback}$ [-]	0.3223

The obtained transient concentration profiles for the extract and raffinate buffer vessels during the startup period are illustrated in Fig. 6.1a and b, respectively. Note that for each buffer vessel, the corresponding concentrations of the two components are normalized with respect to those of the fresh feed. As already mentioned in Chapters 4 and 5, since the recycled fractions present in the buffer vessels have been partially separated, they have substantially different compositions from the fresh feed. More specifically, the compositions of the extract and raffinate recyclates are shifted favorably

towards component B and A, respectively, which can be seen from Fig. 6.1.

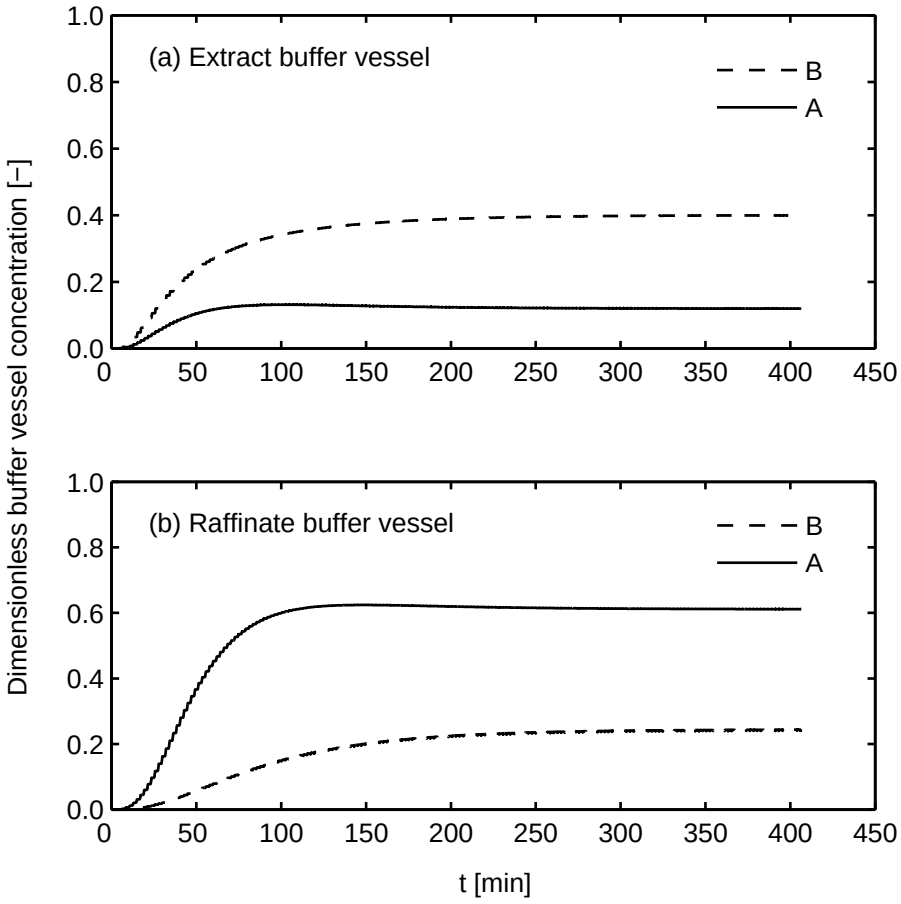

Figure 6.1: Transient concentration profiles for (a) extract buffer vessel, and (b) raffinate buffer vessel. The profiles were obtained by simulating the reference system with operating parameters listed in Table 6.1.

This advantage is satisfactorily exploited in the FF-SMB concept. However, it is also noted from Fig. 6.1 that the off-spec fractions are significantly diluted compared to the original feed. This is particularly serious for the extract recyclate. This observation motivates us to concentrate the recycled fractions before they are fed back into the unit. It is worth pointing out that

this idea of taking advantage of enrichment is not unique to our work. It has been successfully used in several multi-component chromatographic separation systems. In the case of enriched extract SMB (EE-SMB) [77], a portion of the extract stream is concentrated and the resulting enriched version is re-injected at the same point of the unit. For SSR chromatography reviewed in Section 3.1.2, Siitonen et al. [78] recently have explored the possibility to improve the mixed-recycle SSR performance by concentrating the recycle fraction through solvent removal.

6.2 Modeling and optimization

In order to achieve higher feedback concentrations, different methods such as solvent removal and membrane filtration can be applied to the recyclates. Throughout this chapter, the approach of solvent removal by continuous evaporation was selected for illustration and evaluation purposes.

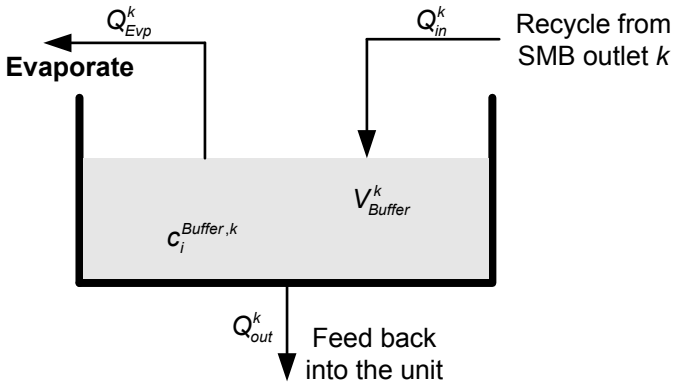

Figure 6.2: Illustration of recyclate enrichment by solvent evaporation for each buffer vessel.

The enrichment operation for each buffer vessel is schematically illustrated in Fig. 6.2. Here a new operating variable Q^k_{Evp} is introduced for

buffer vessel k, which represents the flow-rate of solvent evaporated from the vessel, $k = E, R$. In this work, Q^k_{Evp} is assumed to be constant. The removed solvent can be recovered as eluent and reused, thus reducing the consumption of fresh eluent.

For each buffer vessel, the following mass balance equations can be easily derived:

$$\frac{d\,V^k_{Buffer}}{dt} = Q^k_{in}(t) - Q^k_{out}(t) - Q^k_{Evp} \tag{6.1}$$

$$\frac{d(V^k_{Buffer}\,c_i^{Buffer,k})}{dt} = Q^k_{in}(t)\,c^k_i(t) - Q^k_{out}(t)\,c_i^{Buffer,k}(t) \tag{6.2}$$

with the initial conditions

$$V^k_{Buffer}|_{t=0} = V^k_{Buffer,0}, \quad c_i^{Buffer,k}|_{t=0} = c^{Buffer,k}_{i,0} \tag{6.3}$$

where $i = A, B$ and $k = E, R$. Within each switching period, in addition to the liquid volume recycled from the corresponding outlet

$$V^k_{Recycle} = (1 - \tau^k_{Production})\,t_s\,Q_k \tag{6.4}$$

and the volume fed back from the buffer vessel to the unit

$$V^k_{Feedback} = \tau^k_{Feedback}\,t_s\,Q_F \tag{6.5}$$

one should also consider the solvent volume evaporated

$$V^k_{Evp} = Q^k_{Evp}\,t_s \tag{6.6}$$

Depending on whether $V^k_{Recycle}$ matches the sum of $V^k_{Feedback}$ and V^k_{Evp}, each buffer tank is characterized by three qualitatively different scenarios. For simplicity, we concentrate on the case where $V^k_{Recycle} = V^k_{Feedback} + V^k_{Evp}$. This guarantees that neither overflow nor "running dry" will occur in the vessel.

The other modeling details are the same as those of normal FF-SMB. They can be found in the relevant sections of Chapters 4 and 5 and are not presented here.

For the optimization of the evaporative FF-SMB, we maximize the averaged feed throughput

$$\max \quad \overline{Q}_F = (1 - \tau^E_{Feedback} - \tau^R_{Feedback})\, Q_F \tag{6.7}$$

subject to the product purity specifications and maximum flow-rate restriction. The problem formulation is the same as that given in Table 5.2 and thus omitted in this section. Note that the evaporating rate Q^k_{Evp} was not treated as a free decision variable but as a parameter, whose influence on the optimal performance of the enrichment operation will be examined below. Furthermore, the concentrated fractions were assumed to be fed back into the system by following the feeding sequence "RFE". The sequential approach described in Section 4.3 was used again to solve the NLP problem.

6.3 Results and discussion

The reference system used to investigate FF-SMB in Chapters 4 and 5 was examined here to evaluate the new enrichment regime. In the first case study, the evaporating rates $Q^k_{Evp}\,(k = E,\, R)$ were maintained at 0.06 ml/min. Selection of such a relatively low value is due to the small dimensions of the unit under consideration. For the sake of comparison, in addition to the 4-column systems, a 5-column standard SMB with configuration 1-1-2-1 was also optimized. Note that this configuration has been proven to be optimal (see the discussion in Section 5.3.6). The optimization results for different purity requirements are shown in Fig. 6.3a and b for the case of linear and nonlinear Langmuir isotherms, respectively. It is found that the 4-column standard SMB is feasible only for the purity level of 90%. The proposed enrichment strategy is effective and allows the 4-column FF-SMB to achieve a feed throughput comparable to or even better than that of the 5-column

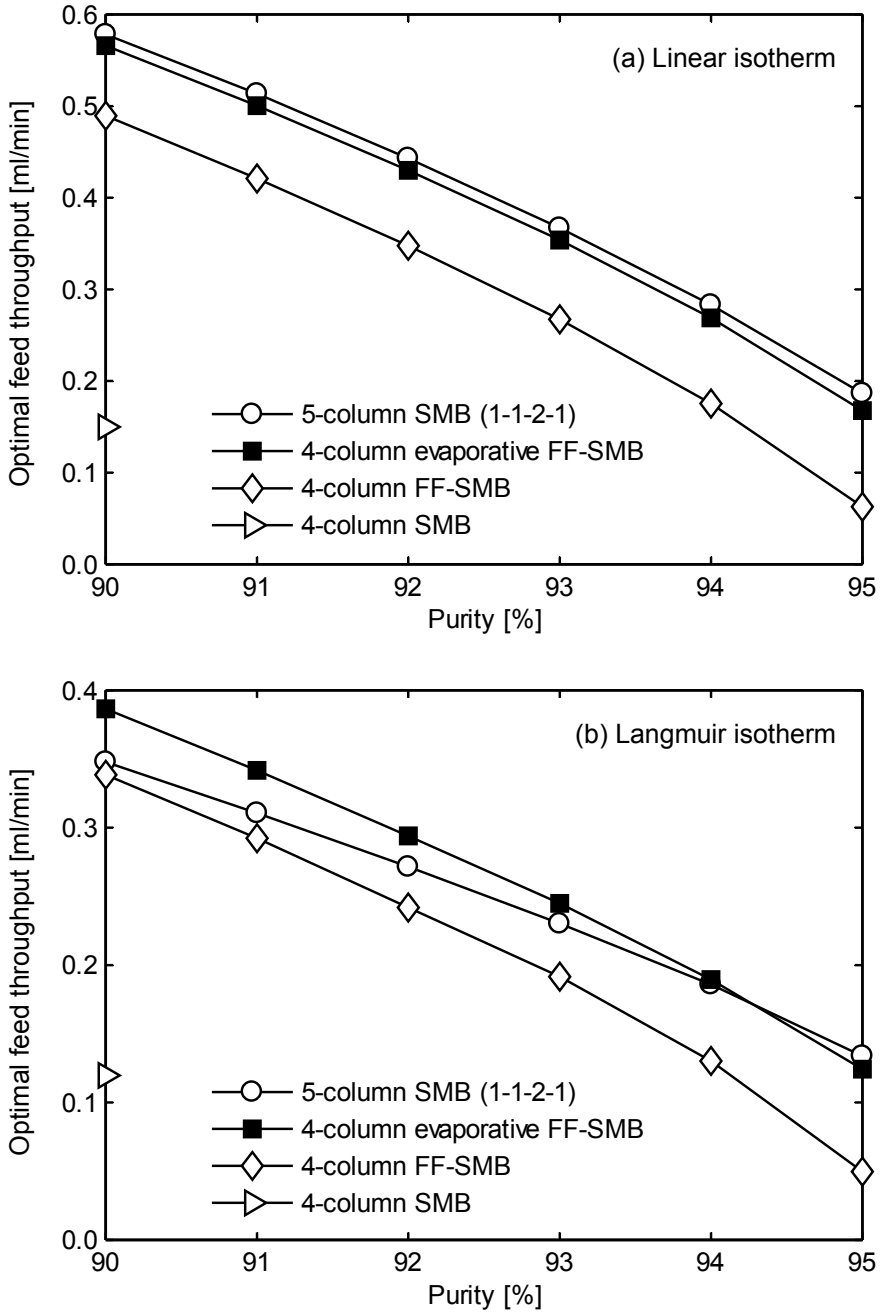

Figure 6.3: Comparison of optimal feed throughput for different operating regimes.

standard SMB process. Furthermore, for the same 4-column FF-SMB, the enrichment regime clearly outperforms the non-enriched scenario. The obtained improvement shows a strong dependence on the purity requirements: the higher the product purities, the more significant the improvement becomes. For example, in the case of Langmuir isotherm the ability to process fresh feed can be enhanced by 150% for the purity of 95%, while the improvement is reduced to only 14% as the purity of 90% is imposed.

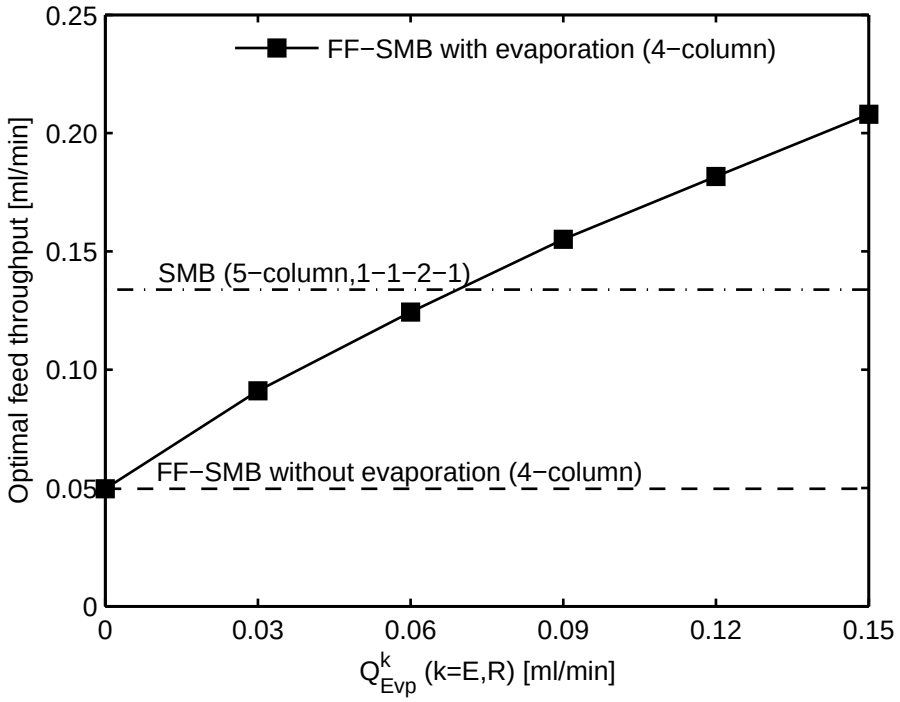

Figure 6.4: Optimal feed throughout of evaporative FF-SMB with different solvent removal rates. The dashed and dash-dotted lines mark the optimal values of the 4-column FF-SMB without enrichment and 5-column SMB, respectively.

In the second case study, we examined the effect of the evaporating rate on the potential of the evaporative FF-SMB process. The minimum purity

specification was fixed at 95% for both products. The optimal performance of the 4-column FF-SMB with different solvent evaporation rates is shown in Fig. 6.4 for the Langmuir isotherm. It is noted that the improved feed throughput over that of the non-enriched case increases quickly with increasing the evaporating rate. In particular, at a rate of 0.09 ml/min or higher, the optimal value exceeds that of the 5-column SMB. Furthermore, for the rate of 0.15 ml/min, we also evaluated the averaged concentrations of both recyclates at CSS. A detailed comparison with the concentrations obtained without enrichment step is summarized in Table 6.2. As expected, by removing the solvent from the buffer vessels the recycled fractions are significantly concentrated.

Table 6.2: Comparison of concentrations of recycled fractions with and without enrichment operation.

Component	Enriched case [g/l]	Non-enriched case [g/l]
Extract buffer vessel:		
A	0.0956	0.0158
B	0.5832	0.0923
Raffinate buffer vessel:		
A	0.9848	0.1083
B	0.2381	0.0204

Although the method of enriching recyclates by solvent evaporation opens up the possibility of improving the performance of FF-SMB, it has some limitations worth noting. First of all, the additional evaporation cost must be consumed to realize this concept. Furthermore, the extent of solvent removal is restricted typically by the solubility of the two components. The components in the fresh feed often reach their solubility limits. Thus, excessive

solvent evaporation should be avoided to prevent the recyclates exceeding the limits. For both case studies examined above, it is found that the concentrations of the fractions after evaporation remain lower than the original feed concentrations.

6.4 Conclusions

The novel concept of continuously enriching recyclates was suggested to enhance the potential of FF-SMB. The effectiveness of the proposed regime was demonstrated by systematic optimization studies. It resulted that the enrichment operation is advantageous for FF-SMB and provides considerable performance improvement over the non-enriched case. The benefit attainable turns out to be more pronounced as the extent of enrichment increases. It can be expected that the idea is particularly attractive for those cases where the process is not operated close to the solubility limits of the components.

6.5 Nomenclature

c	liquid phase concentration [g/l]
m	flow-rate ratio [-]
Q	liquid phase flow-rate [ml/min]
t	time [min]
t_s	switching period [min]
V	liquid phase volume [ml]

Greek letters

τ	normalized time [-]

Roman letters

I, II, III, IV	zone index

Subscripts and superscripts

$-$	adapted parameters for FF-SMB
0	initial conditions
A	less retained component
B	more retained component
$Buffer$	buffer vessel
E	extract
Evp	evaporation
F	feed
$Feed$	original feed tank
$Feedback$	feedback from buffer vessel

i	component index, $i = A$, B
in	inlet effluent of buffer vessel
k	SMB outlet or buffer vessel index, $k = E$, R
out	outlet effluent of buffer vessel
$Production$	outlet stream is withdrawn as product
R	raffinate
$Recycle$	outlet stream is recycled to buffer vessel

7

Transient operation of SMB chromatography

SMB represents one of the widely established adsorption processes. Its periodic port switching mechanism and complex hybrid dynamics significantly complicate research of the transient startup and shutdown behavior. This introductory chapter gives a short overview of the transient operation of SMB chromatography, laying particular emphasis on the relevance and benefits of exploring the challenging subject. Previous related contributions to this topic are reviewed briefly.

7.1 Introduction

The production cycle of many chemical processes is typically characterized by two distinct operating modes:

- The steady state operation, which is productive and generally dominates most of the operating duration.
- The transient stages, such as startup, shutdown as well as product changeover. Although such procedures may occur infrequently, they often last a long time, consume many resources (raw materials, energy, etc.), and produce a large amount of off-spec products. These disadvantages motivate researchers to optimize the transient operations and to improve their performance.

Operating an SMB unit for a given separation task in general also undergoes these modes. Throughout this work we restrict our attention to only the startup and shutdown. Other types of transients, such as transitions between different cyclic steady states, are also interesting but beyond the scope of this work. In the following, we refer to the startup and shutdown also as the transient processes for convenience.

For industrial SMB applications, typically dilute products are produced over startup and shutdown stages. These transient products do not necessarily meet purity requirements specified for the normal products and thus only CSS is used for production purposes. On the other hand, significant research efforts also exclusively focus on CSS in the academic community. Nevertheless, investigating the transient periods with the aim to improve their performance is always advantageous for SMBs at all scales from laboratory to industrial production. For large-volume purifications, emergency situations might occur and regular maintenance of columns is indispensable (see

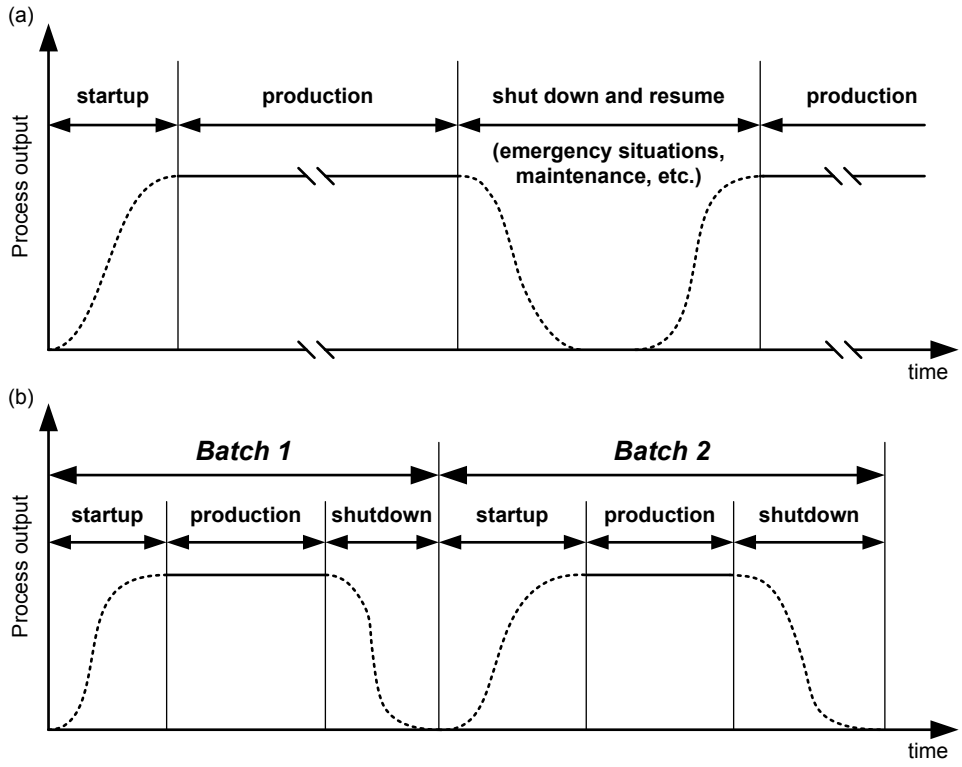

Figure 7.1: Illustration of different stages experienced during operating an SMB unit. (a) Large-volume industrial applications, where the production stage occupies most of the overall operating time, and (b) small-scale short campaigns, where the same unit is used to process different feed batches and the transient duration can be comparable to the production time.

Fig. 7.1a). Fast startup and shutdown procedures allow to resume normal production quickly and to reduce non-productive duration. They also enable more flexible system maintenance. In the case of small-scale separation campaigns, very often the same SMB unit is operated repeatedly to process small batches of well-characterized mixtures of different types (see Fig. 7.1b). This is a rather common circumstance in pharmaceutical production. In this case, the process is subject to frequent startups and shutdowns to realize product changeover. The transient operating duration can be also compara-

ble to the production time, causing a considerable amount of the feed to be consumed in the transient phases. Obviously, in such case development of efficient startup and shutdown strategies is particularly relevant and of great practical importance. Some potential benefits are easy to recognize:

- Minimize off-spec production and thus enhance overall production capability. This is highly profitable for small-scale applications.
- Reduce or even avoid downstream recycling or reprocessing, lowering solvent, energy and other separation costs.
- Create more flexible production campaigns, which enables a quick response to market demands.

7.2 Previous work

Optimizing transient conditions to achieve an efficient and reliable transient operation has been subject to substantial research for chemical processes over the past few decades. A rather representative example is the startup of distillation columns, which is considered as one of the most difficult operations in the chemical industry. For this topic, Sørensen and Skogestad developed optimal startup procedures for a batch distillation process, and examined under which conditions the optimal startup time was significant compared to the total operating time. Wozny and coworkers not only successfully derived optimal policies for column startup using dynamic optimization strategies, but also verified their work experimentally (see for example [86], and the papers cited therein). Optimal startup of different types of reactors, such as batch, semi-batch and continuous, is another challenging task and has also gained great interest (see for example [87, 88, 89]). Recently, Haugwitz et

al. [90] have proposed a strategy that combines open-loop optimal startup and feedback control, and applied it to a novel plate reactor with an exothermic reaction to guarantee a safe, robust and efficient startup. Furthermore, in the area of fuel cell, Chachuat et al. [91] used numerical optimal control techniques to obtain an optimal startup policy for a microfabricated power generation system.

For conventional SMB and its derivatives, to the best of our knowledge, only very few attempts in the open literature have been made so far to explore the startup and shutdown issues. Lim and Ching [79] suggested pre-loading the columns with the feed to reduce the startup time. Xie et al. [80] further enhanced this approach by developing a detailed design procedure of pre-loading and pre-elution for their tandem SMB process for insulin purification. They also designed a shutdown procedure to recover the retained insulin. The startup and shutdown strategies were derived based on standing wave analysis [84]. Both numerical simulations and experimental validation showed satisfactory transient performance. Bae et al. [81, 82] examined effects of feed concentration and flow-rate ratio on startup and steady state behaviors of SMB. Abunasser and Wankat [20] performed both startup and shutdown analyses for their single-column chromatographic analogue to SMB, considering that the analogue would be useful in short campaigns. Rodrigues et al. [22] provided a fast model-based startup procedure for their single-column apparatus used for experimentally reproducing the periodic behavior of SMB, reducing the duration of each experimental run significantly. Nevertheless, as pointed out by the authors, the scheme was not directly applicable to a real multi-column SMB unit since such a process relies on the capability of artificially generating a prescribed inlet concentration profile. In addition, although the work by Zenoni et al. [83] was devoted to the development of

an on-line system to monitor the composition of the enantiomers of a chiral SMB unit, the authors emphasized the importance of optimizing startup and shutdown. However, it is worth noting that none of the aforementioned contributions explicitly touched on the optimal startup and shutdown operations of SMB.

8

Conventional startup and shutdown

Beginning with a short introduction regarding mathematical modeling of transient behavior, we provide a brief overview of various design methods developed for the SMB chromatography. We show that the design procedures represent a considerable asset to the steady state operation of the process. After highlighting the limitation of these design strategies, we next describe the conventional startup and shutdown approaches in detail and define one set of performance criteria used to evaluate them. The chapter ends with a qualitative discussion of advantages and drawbacks of the conventional operating regimes.

8.1 Modeling transient behavior

A rigorous mathematical model with ability to accurately capture the transient dynamics of SMB is necessary for investigating the startup and shutdown operations. The detailed model equations have been presented in Section 2.2 and are not reproduced in this section. Only relevant aspects are discussed here.

For the initial conditions given in Eq. (2.2), a few additional remarks are worth noting. If the model equations are used to characterize the startup behavior, the initial time t_0 denotes the starting time of a new separation campaign. When the shutdown process is described alternatively, it should be understood as the time instance at which the shutdown operation begins. For both kinds of problems, t_0 is assumed to be zero for convenience. Furthermore, it is assumed that the process is started up with clean columns and has reached CSS before shutdown. With this assumption, the initial concentration value $c_{i,0}$ can be specified conveniently. Note that the assumption applies both to the conventional and to our multistage operating regimes to be discussed in the next chapter.

8.2 Design methods for SMB processes

Development of effective and reliable design procedures for SMBs has gained considerable attention in the last decades. The most straightforward way is the trial-and-error approach, where dynamic simulations of an SMB process model are performed and operating parameters are adjusted manually after each simulation run. The procedure is repeated until the given separation specifications can be satisfied. In order to avoid this time-consuming process, some short-cut design procedures have been developed. The repre-

sentatives, among them, include the standing wave approach suggested by Ma and Wang [84] and the triangle theory introduced in Section 2.3. These design methodologies provide a valuable guide for SMB practitioners and are widely used in the practical development of SMB applications. However, both procedures are based on the equivalent TMB model. The triangle theory neglects the effects of axial dispersion and mass transfer resistances, as pointed out in Section 2.3. To overcome these limitations, alternative model-based mathematical optimization strategies have been proposed. They consider a detailed dynamic SMB model, involve a single or multiple objective functions, and employ efficient solution techniques well developed in the mathematical programming community. With the ability to exploit the full process potential, they have been extensively used to optimize not only the standard SMB, but also many non-standard operations and even the combination of different modes. In the first part of the thesis, our approach adopted to optimize the FF-SMB process also falls into this category. For a detailed discussion of this class of design methods, we refer to Section 4.3 and the references therein.

It should be noted that all the design methods reviewed above aim to determine the operating parameters conforming to the specified performance criteria only at CSS, and do not take the transient performance into account. For the sake of clarity, the conditions determined are referred to as the nominal (or reference) CSS operating conditions u^*, in order to distinguish them from the transient operating conditions. Furthermore, it is assumed that u^* consists of the nominal switching period t_s^* and four dimensionless m-factors [35] defined as

$$m_j^* = \frac{Q_j^* \, t_s^* - \epsilon V_{Col}}{(1-\epsilon) V_{Col}}, \quad j = I, II, III, IV \tag{8.1}$$

with Q_j^* being the nominal CSS flow-rate in zone j, and V_{Col} the column volume. In addition, the corresponding axial concentration profile established

at CSS is assumed to be unique. It exhibits a time-dependent but period-invariant behavior over each switching period. For convenience, such a steady periodic solution is denoted by $C^*(\tau) \in \mathbb{R}^{N_C}$, where the dimensionless time coordinate $\tau \in [0, 1]$ is obtained by normalizing t with respect to t_s^*. $C^*(\tau)$ is referred to as the nominal (or reference) concentration profile. It is also assumed that u^* and $C^*(\tau)$ are known a priori throughout this work.

8.3 Conventional startup operation

In the conventional operation, the SMB process is started up with clean columns and u^* is directly specified as the transient conditions, which remain constant over the entire startup stage (see Fig. 8.1a). One then waits until the axial concentration profile reaches its reference value. This process is schematically shown in Fig. 8.1b. Once at the end of some switching period, say $N_{startup}$, the corresponding axial concentration fulfills the following criterion

$$\left\| C_k|_{k=N_{startup}} - C^*|_{\tau=1} \right\|^2 \leq \epsilon_{startup} \tag{8.2}$$

the startup period is considered to be completed. Here $C_k \in \mathbb{R}^{N_C}$ is the axial concentration at the end of switching period k, $\epsilon_{startup}$ a pre-specified startup tolerance, and $\|\cdot\|$ the Euclidean norm. The resulting startup time can be easily calculated by

$$t_{startup} = N_{startup}\, t_s^* \tag{8.3}$$

and the total desorbent consumption follows

$$V_D^{startup} = t_{startup}\, Q_D^* \tag{8.4}$$

Two recovery vessels illustrated in Fig. 8.1b are used to contain the extract and raffinate products recovered from the outlets during the startup period.

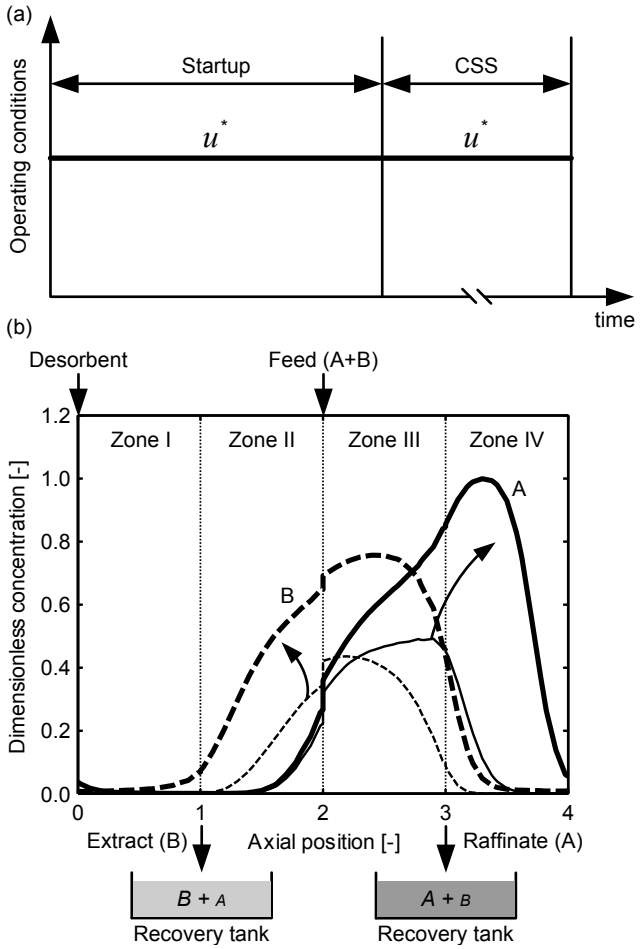

Figure 8.1: Conventional startup for SMB. (a) Operating conditions in conventional scheme, and (b) development of axial concentration profiles during startup (taken at the end of one switching period). Thin solid and dashed lines: dimensionless concentration profiles for component A and B, respectively; thick solid and dashed lines: dimensionless reference concentration profiles for component A and B, respectively.

The purities for the transient products can be defined as

$$Pu_E^{startup} = \frac{\sum_{k=1}^{N_{startup}} M_{B,k}^{startup,E}}{\sum_{k=1}^{N_{startup}} (M_{A,k}^{startup,E} + M_{B,k}^{startup,E})} \tag{8.5}$$

$$Pu_R^{startup} = \frac{\sum_{k=1}^{N_{startup}} M_{A,k}^{startup,R}}{\sum_{k=1}^{N_{startup}} (M_{A,k}^{startup,R} + M_{B,k}^{startup,R})} \tag{8.6}$$

where $M_{i,k}^{startup,E}$ and $M_{i,k}^{startup,R}$ represent the masses of component i collected over switching period k from the extract and raffinate outlets, respectively. The definitions of the above parameters used to evaluate the performance of the conventional startup are also summarized in Table 8.1.

Table 8.1: Definitions of performance parameters used to evaluate conventional startup and shutdown methods[a].

Parameter	Definition
t_{mode} [h]	$N_{mode}\, t_s^*$
V_D^{mode} [ml]	if $mode = startup:\ Q_D^*\, t_{startup}$
	if $mode = shutdown:\ (Q_D^* + Q_F^*)\, t_{shutdown}$
Product purity [%]	
Pu_E^{mode}	$\frac{\sum_{k=1}^{N_{mode}} M_{B,k}^{mode,E}}{\sum_{k=1}^{N_{mode}} (M_{A,k}^{mode,E} + M_{B,k}^{mode,E})}$
Pu_R^{mode}	$\frac{\sum_{k=1}^{N_{mode}} M_{A,k}^{mode,R}}{\sum_{k=1}^{N_{mode}} (M_{A,k}^{mode,R} + M_{B,k}^{mode,R})}$

[a]For startup, $mode = startup$; for shutdown, $mode = shutdown$.

8.4 Conventional shutdown operation

The shutdown operation simply flushes out the holdups in the columns. Thus, it can be more aggressive than the startup operation. For example, the

unit can be operated in the single-pass mode where the recycling line is cut open and the holdups are purged from the desorbent supply point to the outlet. If the products are expensive, however, recovery of the residuals becomes crucial and the process must be operated carefully. In such a case, a more "conservative" shutdown regime capable of maintaining product quality should be employed.

The simplest shutdown approach is to replace the original feed tank with a desorbent tank and all the operating conditions are kept the same as those at the CSS operation (see Fig. 8.2a). The column configuration at CSS is also held unchanged. The shutdown phase lasts until the components retained in the columns have eluted out from the extract and raffinate outlets, which is illustrated in Fig. 8.2b. In this scheme, the system actually involves two desorbent streams that purge the columns simultaneously. We restrict ourselves to this regime and refer to it as the conventional shutdown strategy. Similarly, two recovery tanks are also introduced to recover the components eluted during the shutdown stage. When the following recovery criteria for the two components are satisfied simultaneously, the shutdown process is defined to be concluded:

$$Re_i^{T,shutdown} = \frac{\sum_{k=1}^{N_{shutdown}} (M_{i,k}^{shutdown,E} + M_{i,k}^{shutdown,R})}{M_i^{Col}} \geq Re_{i,min}^{T,shutdown},$$

$$i = A,\, B \tag{8.7}$$

where $Re_i^{T,shutdown}$ represents the total recovery of component i achieved after shutdown, $M_{i,k}^{shutdown,E}$ and $M_{i,k}^{shutdown,R}$ the masses of component i recovered over switching period k from the extract and raffinate ports, respectively, M_i^{Col} the total mass amount of component i retained in the columns before shutdown, $Re_{i,min}^{T,shutdown}$ the pre-specified minimum recovery requirement for component i, and $N_{shutdown}$ the number of switching periods required to shut

down. A set of performance parameters for the conventional shutdown can be defined similarly and thus is presented in Table 8.1 directly. Note that in this case the total amount of desorbent consumption $V_D^{shutdown}$ should also take the amount supplied from the feed inlet into account.

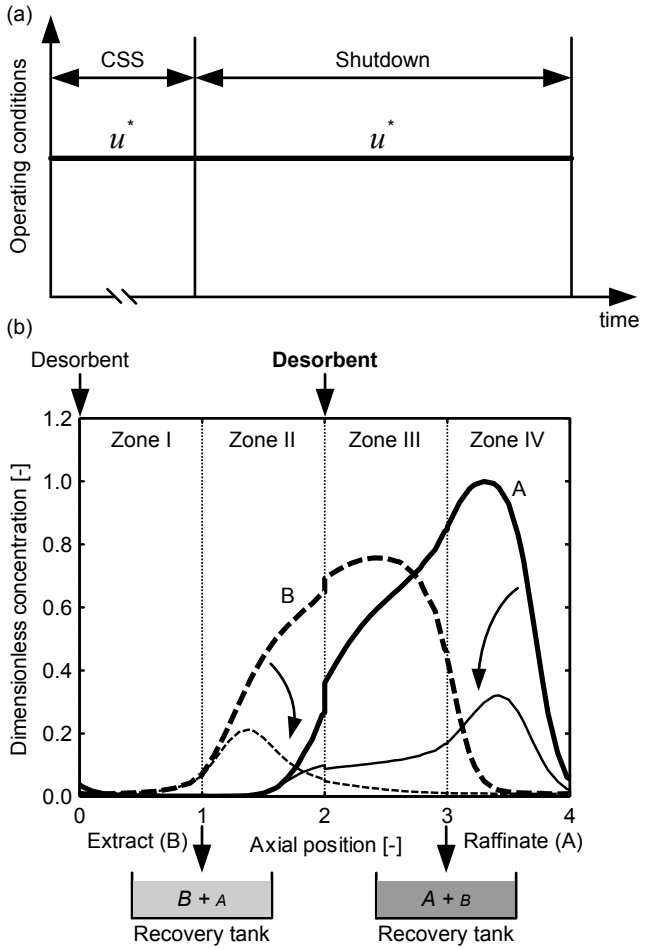

Figure 8.2: Conventional shutdown for SMB. (a) Operating conditions, and (b) development of axial concentration profiles over shutdown (taken at the end of one switching period).

The conventional strategies are often adopted in practical applications due to their simplicity of operation. However, simply using the CSS condi-

tions as the transient operating policies typically leads to long startup and shutdown duration and a large amount of desorbent consumption. Furthermore, these approaches also suffer from another drawback that the outlet streams collected may not be necessarily guaranteed to be on-spec. In the case of off-spec production, they have to be either discarded or reprocessed. The discard scheme, although simple, causes a waste of valuable feedstock materials, which must be avoided in particular in small-scale campaigns. On the other hand, reprocessing off-spec products consumes additional production time and separation costs, and could be highly undesired for some cases. Therefore, more efficient startup and shutdown strategies which can surmount these shortcomings need to be developed. They constitute the subject of the next chapter.

8.5 Nomenclature

c	liquid phase concentration [g/l]
C	liquid phase concentration state vector [g/l]
m	flow-rate ratio parameter [-]
M	mass amount [g]
N	number of switching periods [-]
N_C	number of concentration state variables [-]
Pu	purity [%]
Q	liquid phase flow-rate [ml/min]
Re	recovery [%]
t	time [min]
t_s	switching period [min]
u	vector of operating conditions
V	liquid phase volume [ml]
V_{Col}	column volume [cm^3]

Greek letters

ϵ	total column porosity [-]
$\epsilon_{startup}$	startup tolerance [-]
τ	dimensionless time coordinate [-]

Roman letters

I, II, III, IV	zone index

Subscripts and superscripts

$*$	CSS reference value
0	initial value
A	less retained component
B	more retained component
Col	chromatographic column
D	desorbent
E	extract
F	feed
i	component index, $i = A, B$
j	zone index, $j = I, II, III, IV$
k	switching period index
$mode$	operating mode, $mode = startup, shutdown$
R	raffinate
$shutdown$	shutdown
$startup$	startup
T	total quantity

9

Multistage optimal startup and shutdown

In this chapter, we first present a multistage optimal startup strategy proposed for SMB chromatographic processes. The new transient regime allows to adjust the startup operating conditions stage-wise and provides the capability of improving the startup performance and fulfilling product quality specifications. The optimal startup operation is then formulated as a dynamic optimization problem, for which a specially tailored decomposition solution algorithm is developed to ensure its computational tractability. We next generalize the proposed concept also to the shutdown process to enhance the shutdown performance. By examining the transient operation of a literature separation example characterized by nonlinear competitive isotherm, the feasibility of the solution approach is demonstrated, and the conventional and multistage optimal operating strategies are compared systematically in terms of one set of transient performance criteria. Furthermore, the effects of enforcing product quality constraints upon the optimal operating conditions and transient performance are examined.

9.1 Multistage optimal startup strategy

In order to overcome the limitations of the conventional startup operation, we propose a multistage startup approach which is schematically shown in Fig. 9.1. In this strategy, the startup period of interest is divided into P stages with $P \geq 1$. For the n-th stage over the time interval from $t_{n-1}^{startup}$ to $t_n^{startup}$, it is assumed that the process is operated with one set of time-invariant operating conditions denoted by $u_n^{startup}$, and undergoes $N_n^{startup}$ port switches ($N_n^{startup} \geq 1$), $n = 1, 2, \ldots, P$. In contrast to the conventional mode, the new startup regime allows to adjust the transient operating conditions in a stage-wise manner. Here the piece-wise constant approximation of the startup trajectory is used aiming to facilitate practical implementation, although more complex types of approximation, such as piece-wise linear or quadratic, are possible in principle. The condition $N_n^{startup} \geq 1$ guarantees the existence of stage n. Moreover, the conventional startup can be regarded as one special case of the multistage scheme, where only one stage exists with the operating conditions equal to the CSS conditions.

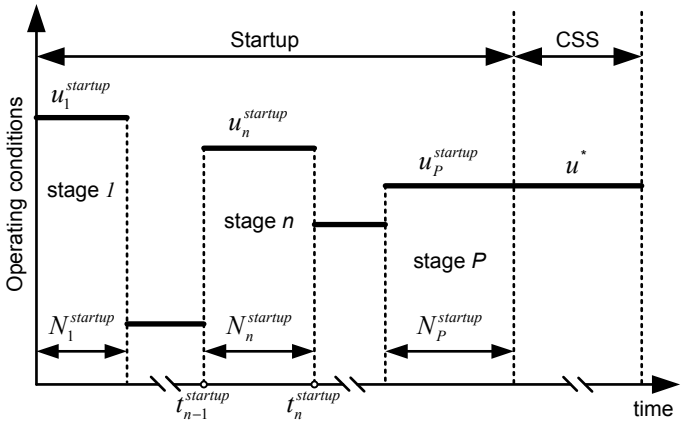

Figure 9.1: Illustration of multistage startup strategy.

The primary task of a multistage optimal startup procedure is to deter-

mine $u_n^{startup}$ and $N_n^{startup}$ $(n = 1, 2, \ldots, P)$ in such a way that the process can be driven from the initial conditions (i.e., clean columns) towards the reference concentration $C^*(\tau)$ in some optimum manner while respecting the constraints imposed during startup. To find the optimal startup policy, a dynamic optimization problem is required to be solved, for which the formulation and solution algorithm are detailed below.

9.1.1 Problem formulation

In stage n, the four dimensionless m-factors defined as

$$m_{j,n}^{startup} = \frac{Q_{j,n}^{startup}\, t_{s,n}^{startup} - \epsilon V_{Col}}{(1-\epsilon)V_{Col}}, \quad j = I, II, III, IV \tag{9.1}$$

and the switching period $t_{s,n}^{startup}$ are chosen as the operating conditions and thus $u_n^{startup} = \left[m_{I,\ldots,IV,n}^{startup},\, t_{s,n}^{startup} \right]^T \in \mathbb{R}^5$. Here $Q_{j,n}^{startup}$ is the flow-rate in zone j at stage n. A straightforward objective of a startup optimization problem is to minimize the startup time:

$$t_{startup} = \sum_{n=1}^{P} N_n^{startup}\, t_{s,n}^{startup} \tag{9.2}$$

subject to the steady state constraints. However, Wozny and Li [86] pointed out that this kind of formulation may lead to numerical expenses for the startup optimization of distillation columns. Chachuat et al. [91] mentioned potential problems of minimizing startup time directly when optimizing the startup operation of their portable power generation system. Such previous experience motivates us to employ an alternative objective function in this work. For convenience of defining this objective function, a local dimensionless time coordinate τ_n is introduced for stage n:

$$\tau_n = \frac{t - t_{n-1}^{startup}}{t_{s,n}^{startup}} \in [0, N_n^{startup}] \tag{9.3}$$

with $t \in [t_{n-1}^{startup}, t_n^{startup}]$ and $n = 1, 2, \ldots, P$. The coordinate transformation is illustrated in Fig. 9.2a. The objective function is then formulated as follows:

$$J = \sum_{n=1}^{P} t_{s,n}^{startup} \int_0^{N_n^{startup}} \| C^n(\tau_n) - C^*(\tau_n - \tau_n') \|^2 \, d\tau_n \tag{9.4}$$

where $\tau_n' = round(\tau_n)$. The round-to-integer function $round(\cdot)$ rounds its argument downwards to the nearest integer, and thus τ_n' represents the dimensionless starting time of a switching period where τ_n lies (see Fig. 9.2a). $C^n(\tau_n) \in \mathbb{R}^{N_C}$ is the concentration state vector of stage n. In the objective function, $\| C^n(\tau_n) - C^*(\tau_n - \tau_n') \|^2$ measures the quadratic deviation of the concentration profile from its reference value at τ_n. The development of such a deviation over the startup period is schematically illustrated in Fig. 9.2b by the gray line. It is easily checked that the objective function J represents the area of the shaded region in Fig. 9.2b. The area nicely reflects the convergence rate of the process towards the reference concentration profile. More precisely, if one set of startup conditions allows a smaller area, it implies a relatively shorter transient time and would be more preferable than others. Therefore, it is advisable to use J to characterize the startup behavior. A similar objective function was also adopted by [86, 87, 89, 91].

It is worth noting that although the reference concentration profile $C^*(\tau)$ is assumed to be known, evaluating J exactly remains non-trivial since it requires the knowledge of the nominal concentration value at every $\tau \in [0, 1]$. Alternatively, the exact integration in Eq. (9.4) can be approximated period-wise by the rectangles depicted in Fig. 9.2b, yielding an approximated version $\tilde{J}$:

$$J \approx \tilde{J} = \sum_{n=1}^{P} \tilde{J}_n = \sum_{n=1}^{P} t_{s,n}^{startup} \sum_{k=1}^{N_n^{startup}} \| C_k^n - C^*|_{\tau=1} \|^2 \tag{9.5}$$

where $\tilde{J}_n$ denotes the approximated integral value for stage n, $C_k^n = C^n|_{\tau_n = k}$,

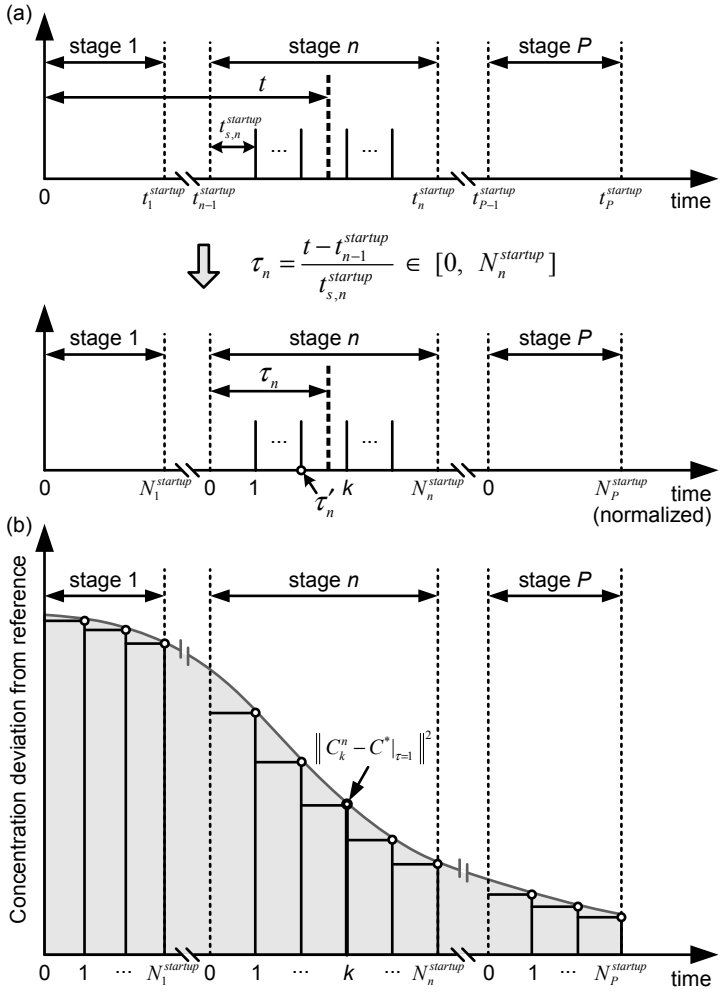

Figure 9.2: (a) Transformation of time t into a local dimensionless time coordinate τ_n for stage n, and (b) development of the quadratic deviation of axial concentration from reference value during startup and interpretation of the objective function J defined in Eq. (9.4) and its approximation.

is the value of the concentration state variables at the end of switching period k of stage n. The multistage optimal startup problem can then be formulated mathematically as follows:

$$\min_{u_n^{startup}, N_n^{startup}, n=1,\ldots,P} \tilde{J} \tag{9.6}$$

subject to:

$$\left\| C_{N_P^{startup}}^{P} - C^*|_{\tau=1} \right\|^2 \leq \epsilon_{startup} \tag{9.7}$$

$$Pu_E^{startup} \geq Pu_{E,min},\ Pu_R^{startup} \geq Pu_{R,min} \tag{9.8}$$

$$m_{j,P}^{startup} = m_j^*,\ t_{s,P}^{startup} = t_s^*,\ \ j = I, II, III, IV \tag{9.9}$$

$$Q_{I,n}^{startup} \leq Q_{max},\ Q_{III,n}^{startup} \leq Q_{max} \tag{9.10}$$

$$m_{I,n}^{startup} - m_{II,n}^{startup} > 0,\ m_{I,n}^{startup} - m_{IV,n}^{startup} > 0,$$

$$m_{III,n}^{startup} - m_{II,n}^{startup} > 0,\ m_{III,n}^{startup} - m_{IV,n}^{startup} > 0 \tag{9.11}$$

with $n = 1, 2, \ldots, P$. The inequality constraint in Eq. (9.7) requires the concentration profile at the end of stage P to approximate the reference profile within the given accuracy. The constraints in Eq. (9.8) impose the purity specifications on the products recovered over startup to explicitly guarantee them to be on-spec. $Pu_{E,min}$ and $Pu_{R,min}$ are the minimum acceptable extract and raffinate purity values respectively, which are assumed to be the same as those specified for the normal products. The set of equality constraints in Eq. (9.9) aims to force the transient conditions at the final stage to converge to the nominal CSS conditions. The inequality constraints in Eqs. (9.10)–(9.11) take into account the operational feasibility and restrictions that must be respected during startup. Q_{max} is the maximum allowable flow-rate in zones I and III, which is constrained typically by the capacity of the installed pumps or the pressure drop in the unit.

9.1.2 Solution strategy

Solving the problem formulated in Section 9.1.1 directly remains a significant challenge. First of all, in each stage besides the continuous operating parameters $u_n^{startup}$, an additional discrete decision variable $N_n^{startup}$ also exists because of the cyclic switching regime. This causes the original problem to be a large-scale mixed integer nonlinear programming (MINLP) problem. Furthermore, the fact that the total number of stages P is unknown a priori constitutes another serious difficulty for the direct solution approach. To deal with the numerical difficulties, a sequential decomposition algorithm has been proposed. The specially tailored solution strategy decomposes the overall problem into a sequence of stage-wise sub-problems each of which can be solved relatively easier. For each sub-problem, optimizing the discrete variable $N_n^{startup}$ simultaneously may lead to further improvements in transient performance, but considerably increases the complexity of the problem. Thus, in this work it is not treated as one degree of freedom but pre-specified to reduce solution complexity, leaving the potential of optimizing also this decision variable for future work.

For stage n, the startup optimization sub-problem $Prob_n^{startup}$ is stated as below:

$$Prob_n^{startup}: \min_{u_n^{startup}} J_n^{startup} = \tilde{J}_n + \epsilon_{reg} \left\| u_n^{startup} - u^* \right\|^2 \tag{9.12}$$

subject to:

$$Pu_{E,n}^{startup} \geq Pu_{E,min},\ Pu_{R,n}^{startup} \geq Pu_{R,min} \tag{9.13}$$

$$Q_{I,n}^{startup} \leq Q_{max},\ Q_{III,n}^{startup} \leq Q_{max} \tag{9.14}$$

$$m_{I,n}^{startup} - m_{II,n}^{startup} > 0,\ m_{I,n}^{startup} - m_{IV,n}^{startup} > 0,$$
$$m_{III,n}^{startup} - m_{II,n}^{startup} > 0,\ m_{III,n}^{startup} - m_{IV,n}^{startup} > 0 \tag{9.15}$$

Note that the equality constraints in Eq. (9.9) cannot be considered explicitly in the above formulation. Alternatively, an additional regularizing term with the coefficient ϵ_{reg} is introduced in the objective function $J_n^{startup}$, to guide the transient conditions towards the CSS conditions as the sub-problems are solved stage by stage. This is necessary due to the non-uniqueness of the optimal solution to the above problem. As the startup proceeds, the first term $\tilde{J}_n$ becomes non-dominant and the regularizing term takes effect, leading to convergence to u^*. Furthermore, the stage-wise purity requirements in Eq. (9.13) are alternatively imposed, considering that the original constraints (Eq. (9.8)) cannot be incorporated into this formulation directly. Here $Pu_{E,n}^{startup}$ and $Pu_{R,n}^{startup}$ represent the purities of the extract and raffinate products collected over only stage n, respectively, and are defined as

$$Pu_{E,n}^{startup} = \frac{M_{B,n}^{startup,E}}{M_{A,n}^{startup,E} + M_{B,n}^{startup,E}}, \; Pu_{R,n}^{startup} = \frac{M_{A,n}^{startup,R}}{M_{A,n}^{startup,R} + M_{B,n}^{startup,R}} \tag{9.16}$$

with $M_{i,n}^{startup,E}$ and $M_{i,n}^{startup,R}$ being the masses of component i obtained over this stage from the extract and raffinate outlets, respectively. It should be pointed out that the stage-wise purity constraints provide a sufficient rather than necessary guarantee for the quality of the final products, and thus are more restrictive than the original specifications (Eq. (9.8)).

Once the optimal solution of the sub-problem $Prob_n^{startup}$ is found, the resulting concentration profile can be determined. Its value at the end of the stage is required to initialize that at the beginning of the next stage. The subsequent new sub-problem can then be solved once again. Such a procedure is repeated, until at the end of stage P the criterion defined in Eq. (9.7) is fulfilled. The decomposition algorithm described is outlined in Fig. 9.3. It should be stressed that the solution obtained by the algorithm is only an approximation to that of the original problem. Exploring more

possibilities of refining the solution is left for our future work.

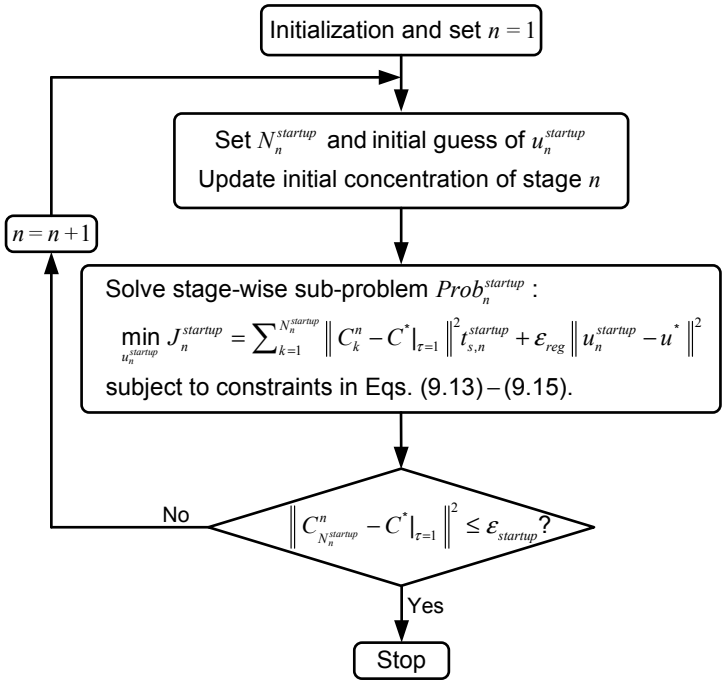

Figure 9.3: Decomposition solution algorithm developed for solving multistage optimal startup problem.

9.2 Multistage optimal shutdown strategy

We have extended the multistage concept to the shutdown process to enhance the shutdown performance, yielding a new shutdown scheme which is shown in Fig. 9.4. We also follow the same assumption that the SMB process has achieved a desired CSS before shutdown, as made for the conventional case discussed in Chapter 8. Once the shutdown begins, the original feed is replaced with a desorbent flow. The operating conditions are now allowed to be adjusted stage-wise as the shutdown proceeds. It is assumed that the shutdown process lasts P stages ($P \geq 1$). For the n-stage, the transient

conditions are $u_n^{shutdown}$ and $N_n^{shutdown}$ port switches are involved, $N_n^{shutdown} \geq 1$, $n = 1, 2, \ldots, P$. Finding optimal values for $u_n^{shutdown}$ and $N_n^{shutdown}$ with which the process can be shut down from the initial CSS to the final state of clean columns is the objective of a multistage optimal shutdown procedure.

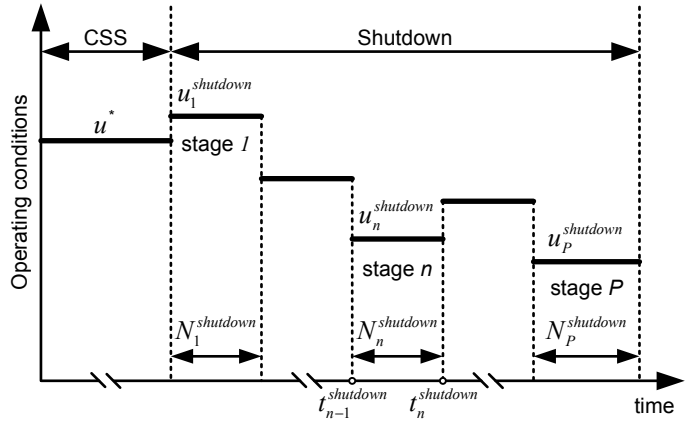

Figure 9.4: Illustration of multistage shutdown strategy.

The formulation of the optimal shutdown problem can be performed similar to that of the startup problem presented in Section 9.1.1 and is omitted here for the sake of brevity. The decomposition solution approach developed previously is also used to deal with the shutdown problem. In order to reduce the complexity of solving each sub-problem, the number of switching periods is fixed a priori, as treated in the startup problem. The n-th shutdown sub-problem is formulated as follows:

$$Prob_n^{shutdown} : \min_{u_n^{shutdown}} J_n^{shutdown} = \int_{t_{n-1}^{shutdown}}^{t_n^{shutdown}} \| C^n(t) \| \, dt \tag{9.17}$$

subject to:

$$Pu_{E,n}^{shutdown} \geq Pu_{E,min}, \; Pu_{R,n}^{shutdown} \geq Pu_{R,min} \tag{9.18}$$

$$Q_{I,n}^{shutdown} \leq Q_{max}, \; Q_{III,n}^{shutdown} \leq Q_{max} \tag{9.19}$$

$$m_{I,n}^{shutdown} - m_{II,n}^{shutdown} > 0, \; m_{I,n}^{shutdown} - m_{IV,n}^{shutdown} > 0,$$

$$m_{III,n}^{shutdown} - m_{II,n}^{shutdown} > 0,\ m_{III,n}^{shutdown} - m_{IV,n}^{shutdown} > 0 \tag{9.20}$$

The vector of operating conditions $u_n^{shutdown} \in \mathbb{R}^5$ consists of the dimensionless m-factors $m_{j,n}^{shutdown}$ $(j = I, II, III, IV)$ and switching period $t_{s,n}^{shutdown}$. The objective function $J_n^{shutdown}$ is aimed to minimize the stage-wise deviation of the concentration profile $C^n(t)$ with respect to the nominal value (i.e., a zero vector) over stage n that spans the time horizon from $t_{n-1}^{shutdown}$ to $t_n^{shutdown}$. The purity constraints in Eq. (9.18) are used to ensure the quality of the final shutdown products. The stage-wise purities $Pu_{E,n}^{shutdown}$ and $Pu_{R,n}^{shutdown}$ are similar to those defined in the startup case (Eq. (9.16)):

$$Pu_{E,n}^{shutdown} = \frac{M_{B,n}^{shutdown,E}}{M_{A,n}^{shutdown,E} + M_{B,n}^{shutdown,E}},$$

$$Pu_{R,n}^{shutdown} = \frac{M_{A,n}^{shutdown,R}}{M_{A,n}^{shutdown,R} + M_{B,n}^{shutdown,R}} \tag{9.21}$$

where $M_{i,n}^{shutdown,E}$ and $M_{i,n}^{shutdown,R}$ are the masses of component i collected during stage n from the extract and raffinate outlets, respectively. Moreover, the operational feasibility and restrictions should be also fulfilled during shutdown, which are considered in the remaining inequality constraints. The shutdown sub-problems are solved sequentially, until at the end of stage P, the total recoveries of both components reach their respective minimum threshold values:

$$Re_i^{T,shutdown} = \frac{\sum_{n=1}^{P}(M_{i,n}^{shutdown,E} + M_{i,n}^{shutdown,R})}{M_i^{Col}} \geq Re_{i,min}^{T,shutdown},\ i = A,\ B \tag{9.22}$$

In order to assess the performance of the new transient operations quantitatively, the same set of performance criteria as that of the conventional case can be defined. The definitions of these parameters are given in Table 9.1.

Table 9.1: Definitions of performance parameters used to evaluate multistage optimal startup and shutdown strategies[a].

Parameter	Definition
t_{mode} [h]	$\sum_{n=1}^{P} N_n^{mode}\, t_{s,n}^{mode}$
V_D^{mode} [ml]	if $mode = startup$:
	$\sum_{n=1}^{P} Q_{D,n}^{startup}\, N_n^{startup}\, t_{s,n}^{startup}$
	if $mode = shutdown$:
	$\sum_{n=1}^{P} (Q_{D,n}^{shutdown} + Q_{F,n}^{shutdown})\, N_n^{shutdown}\, t_{s,n}^{shutdown}$
Product purity [%]	
Pu_E^{mode}	$\frac{\sum_{n=1}^{P} M_{B,n}^{mode,E}}{\sum_{n=1}^{P} (M_{A,n}^{mode,E} + M_{B,n}^{mode,E})}$
Pu_R^{mode}	$\frac{\sum_{n=1}^{P} M_{A,n}^{mode,R}}{\sum_{n=1}^{P} (M_{A,n}^{mode,R} + M_{B,n}^{mode,R})}$

[a]For startup, $mode = startup$; for shutdown, $mode = shutdown$.

9.3 Results and discussion

9.3.1 Example process

A literature example of separation of two cycloketones, cycloheptanone (component A) and cyclopentanone (B) on silica gel using n-hexane:ethylacetate (85:15) as mobile phase [30] was taken to evaluate the conventional and multistage optimal startup and shutdown procedures. The adsorption behavior of the two cycloketones is characterized by the competitive Langmuir isotherm. The detailed parameters used to quantify the model process are listed in Table 9.2. For this laboratory-scale example, the feed concentrations of both components were fixed identically at 1.25 g/l. The maximum allowable flow-rate Q_{max} caused by the maximum pressure drop was restricted to

60 ml/min.

Table 9.2: Summary of parameters for the considered SMB process.

Column properties and operating parameters:			
Column configuration	1-1-1-1	c_i^F, $i = A, B$ [g/l]	1.25
Column dimensions [cm]	2×25	Q_{max} [ml/min]	60
ϵ [-]	0.83	N_p [-]	50
Adsorption isotherm coefficients:			
H_A [-]	5.72	K_A [l/g]	0.110
H_B [-]	7.70	K_B [l/g]	0.148

9.3.2 Determination of CSS operating conditions

As reviewed in Section 8.2, several well-established design procedures can be used to determine the CSS operating conditions u^*. In this work, u^* was obtained by solving the following feed throughput maximization problem:

$$\max_{u^*} \quad Q_F^* \tag{9.23}$$

subject to:

$$\| C_{k+1} - C_k \| \leq \epsilon_{css} \tag{9.24}$$

$$Pu_E^* \geq Pu_{E,min},\ Pu_R^* \geq Pu_{R,min} \tag{9.25}$$

$$Q_I^* \leq Q_{max},\ Q_{III}^* \leq Q_{max} \tag{9.26}$$

$$m_I^* - m_{II}^* > 0,\ m_I^* - m_{IV}^* > 0,\ m_{III}^* - m_{II}^* > 0,\ m_{III}^* - m_{IV}^* > 0 \tag{9.27}$$

where $u^* = [\, m_I^*, m_{II}^*, m_{III}^*, m_{IV}^*, t_s^* \,]^T$, C_{k+1} and C_k the axial concentration profiles at the end of switching period $k+1$ and k, Pu_E^* and Pu_R^* the nominal extract and raffinate product purities achieved at the end of each

CSS switching period, and ϵ_{css} the tolerance which controls the accuracy of CSS. The sequential solution algorithm equipped with the DAE integrator DASPK3.1 [33] and the SQP optimizer E04UCF from the NAG Library [74] was used to solve the CSS optimization problem. The standard dynamic simulation approach was adopted for the determination of CSS. The concentration profiles normalized with respect to the feed concentrations were used to check CSS numerically with $\epsilon_{css} = 1.0 \times 10^{-4}$. Both $Pu_{E,min}$ and $Pu_{R,min}$ were specified as 90%. The forward sensitivity analysis of the DAE system with respect to u^* was performed to evaluate the gradients of the purity constraints in Eq. (9.25) and the other gradients were determined analytically. The obtained CSS operating conditions for the model system are reported in Table 9.3, and the corresponding reference concentration profile established at the end of one CSS period is shown by the thick lines in Fig. 8.1b for both components.

Table 9.3: CSS operating parameters for the example process.

$m^*_{I,\ldots,IV}$	$[8.0485, 4.8930, 6.1933, 4.6167]$	t^*_s	2.8775
Q^*_D	15.92	Q^*_I	60.00
Q^*_E	14.64	Q^*_{II}	45.36
Q^*_F	6.03	Q^*_{III}	51.39
Q^*_R	7.32	Q^*_{IV}	44.08

Flow-rates are expressed in ml/min and t^*_s in min.

9.3.3 Startup strategies

For the reference process described in Section 9.3.1, we have examined the conventional method and multistage optimal startup with and without prod-

uct purity constraint. The sequential solution approach was also used to solve the decomposed sub-problems formulated in Section 9.1.2. The capability of sensitivity calculation of DASPK was employed again to obtain the gradients of the objective function and purity constraints that cannot be determined analytically. The optimum solution found by E04UCF from the preceding stage was chosen as the initial guess for the sub-problem of the next stage. The number of switching periods for each stage was fixed at 4 a priori in this illustrative study. In the scenario where purity specifications are taken into account, the same value of 90% as that required for the normal CSS products was enforced on both stage-wise extract and raffinate products. It should be pointed out that, for the example under consideration, it is infeasible for the first two stages to fulfill such high purity requirements, and both extract and raffinate streams obtained are highly diluted. Taking additional effort to guarantee reasonably good purities for these products might be feasible but is of little value, since a significant amount of evaporation cost is required. Thus, we imposed the constraints only from the third stage and discarded the outlet streams collected over the first two stages. For each startup strategy, the normalized concentration profiles were used to check the completion of startup with the same tolerance $\epsilon_{startup} = 1.0 \times 10^{-6}$. In addition, the coefficient ϵ_{reg} should be sufficiently larger than $\epsilon_{startup}$ to ensure the regularization term to be dominant before the startup ends. On the other hand, if ϵ_{reg} is too large, the optimizer would behave conservatively and the potential for finding more efficient startup regimes might be unexploited. In this work, for the case without purity constraint, we did not encounter any difficulty choosing ϵ_{reg} and a value of 1.0×10^{-3} was found to be appropriate. However, when dealing with the sub-problems with purity constraint, such value appears to be insufficient to force the operating conditions to converge

to u^*, and alternatively a larger value of 5.0×10^2 was used. Note that for both cases, ϵ_{reg} remains constant over stages. A more sophisticated strategy that allows ϵ_{reg} to vary stage-wise is also possible but not considered here.

Conventional method

Following the conventional startup policy, the process takes 84 switching periods to achieve the reference concentration profile within the given tolerance. The resulting startup time is more than 4 h and the desorbent consumption is 3849 ml. The final extract product purity $Pu_E^{startup} = 88.91\%$, which violates the acceptable purity threshold of 90%, and the raffinate purity $Pu_R^{startup}$, on the contrary, increases to 90.80%. The results can be perfectly rationalized by examining the development of the period-wise extract and raffinate purities shown in Fig. 9.5. In order to avoid confusing with $Pu_E^{startup}$ and $Pu_R^{startup}$, below we give the definitions of the period-wise purities for period k:

$$Pu_{E,k}^{startup} = \frac{M_{B,k}^{startup,E}}{M_{A,k}^{startup,E} + M_{B,k}^{startup,E}}, \; Pu_{R,k}^{startup} = \frac{M_{A,k}^{startup,R}}{M_{A,k}^{startup,R} + M_{B,k}^{startup,R}} \tag{9.28}$$

It is seen that although both extract and raffinate purities reach the desired value of 90% after startup, their transient behavior differs significantly from each other. For the raffinate, as time proceeds, the purity gradually converges towards the target with values obviously higher than 90%, except those of the initial very few periods. The on-spec raffinate startup product therefore results. By contrast, the extract purity is consistently lower than 90% over the startup stage, thus making it impossible to achieve an on-spec extract startup product.

The effect of feed concentration on the startup product purity has been also investigated for the conventional scheme. For this purpose, the feed con-

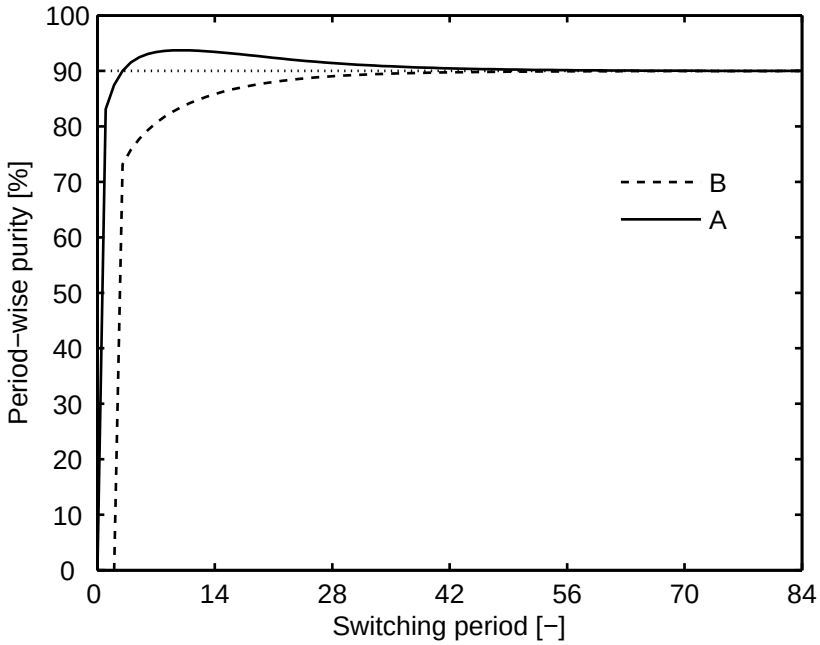

Figure 9.5: Development of period-wise extract (B) and raffinate (A) purities (see Eq. (9.28) for definition) during conventional startup. The dotted line marks the purity threshold of 90%.

centrations of both components were altered from those of the reference system and are summarized in Table 9.4. For each process of different feed concentrations, the optimization problem presented in Section 9.3.2 was solved to find the corresponding CSS operating conditions. The modified systems were then started up in the conventional way to reach their respective reference profiles. In each case, the purities of extract and raffinate products collected over the startup period are reported in Table 9.4. As expected, for the cases examined, although the raffinate purity remains higher than 90%, the extract purity, however, always deviates adversely from the desired value. The extent of such deviation becomes more significant at higher feed concentrations. For the system with the feed concentrations of 2.5 g/l, the

extract purity drops up to 88.79%. The results obviously reveal that the conventional scheme has no ability to ensure on-spec startup products.

Table 9.4: Purities of extract and raffinate products obtained during conventional startup for systems with different feed concentrations.

c_i^F, $i = A, B$ [g/l]	0.55	1.25	2.0	2.5
$Pu_E^{startup}$ [%]	89.12	88.91	88.83	88.79
$Pu_R^{startup}$ [%]	90.38	90.80	90.98	91.05

Multistage optimal operation

For the same process, when using the optimal startup procedure, the total number of switching periods required to reach the reference profile is reduced from 84 to 36 (9 stages with four switching periods per stage). If the purity constraint of 90% is imposed on both products from the third stage, the process needs 15 stages and totally 60 switching periods to complete the startup. A detailed comparison of the conventional and multistage strategies in terms of startup time, desorbent consumption and product purity is illustrated in Fig. 9.6a, b and c, respectively. The new startup regime without purity constraint allows the process to achieve a reduction of 58% in startup time and a saving of 63% in desorbent usage, compared to the normal mode. However, both product purities are below the specified requirements and even a bit lower than those of the conventional approach. By contrast, for the case with purity constraint, the on-spec production can be successfully performed over startup. But note that such a guarantee of product quality comes at the expense of a slight increase of startup time and desorbent consumption with respect to the case without quality constraint. In spite of this, however, significant benefits are still observed for both performance parameters from

Fig. 9.6a and b. In this case, the startup time and desorbent consumption can be reduced by 29% and 35%, respectively. The results also reflect that there exists a tradeoff between the rapidity of startup and product quality. It should be pointed out that the desorbent consumption is not explicitly included in the objective function. The achieved reduction in desorbent usage is a side benefit of minimizing startup time.

The optimal startup operating conditions for the two cases in terms of internal and external flow-rates are demonstrated in Figs. 9.7 and 9.8, respectively. Let us first take a closer look at the case without purity constraint. It is seen that the flow-rates Q_I, Q_{III} and Q_{IV} reach the upper bound of 60 ml/min simultaneously in the first stage (see Fig. 9.7a, c and d), whereas a relatively lower value of 37.48 ml/min is achieved by Q_{II} (Fig. 9.7b). Over the same stage, it results that $Q_D = Q_R = 0$ and $Q_E = Q_F = 22.52$ ml/min (see Fig. 9.8). From Fig. 9.8c, it is also noted that Q_F is more than 3.5 times higher than its CSS value of 6.03 ml/min. The above quantitative observations for Q_D and Q_F reveal the following interesting heuristics: the feed flow-rate should be operated at a higher value than the nominal one to load the fresh mixture into the columns quickly, while the desorbent must be shut off to avoid dilution. On the other hand, the results for the raffinate and extract flow-rates are also rather enlightening. For the reference process, it is found that the raffinate begins to elute out in the first switching period. By contrast, the extract cannot be withdrawn until a few periods have elapsed. Thus, $Q_R = 0$ aims to prevent the raffinate eluting out of the unit; a high value of Q_E implies that the process attempts to throw away the solvent residing in the system and to reduce dilution. The behavior observed for the external flow-rates is useful in fast building up the desired CSS profile.

Over the second stage, Q_{II} undergoes a dramatic increase up to 52.15

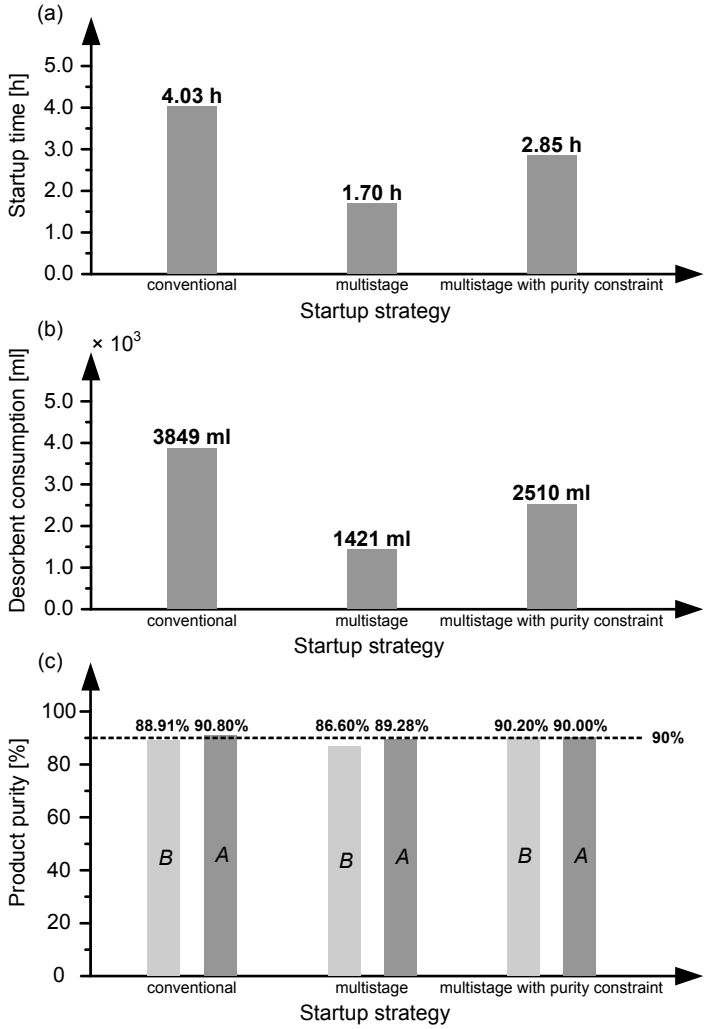

Figure 9.6: Comparison of performance of different startup strategies in terms of (a) startup time, (b) desorbent consumption, and (c) extract (B) and raffinate (A) product purities. The dashed line in (c) marks the minimum purity threshold of 90%.

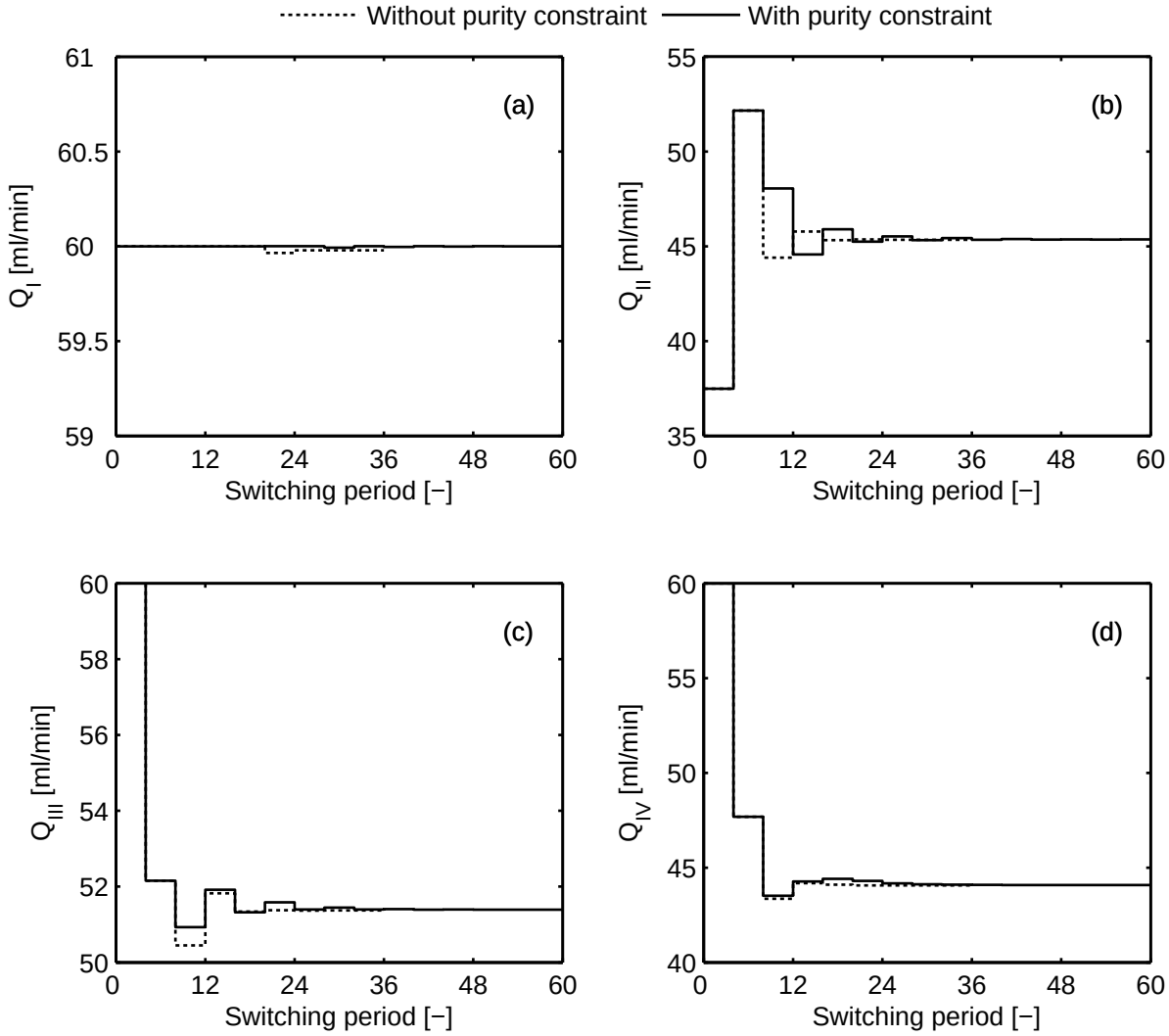

Figure 9.7: Optimal startup profiles (internal flow-rates) of multistage strategies with and without purity constraint.

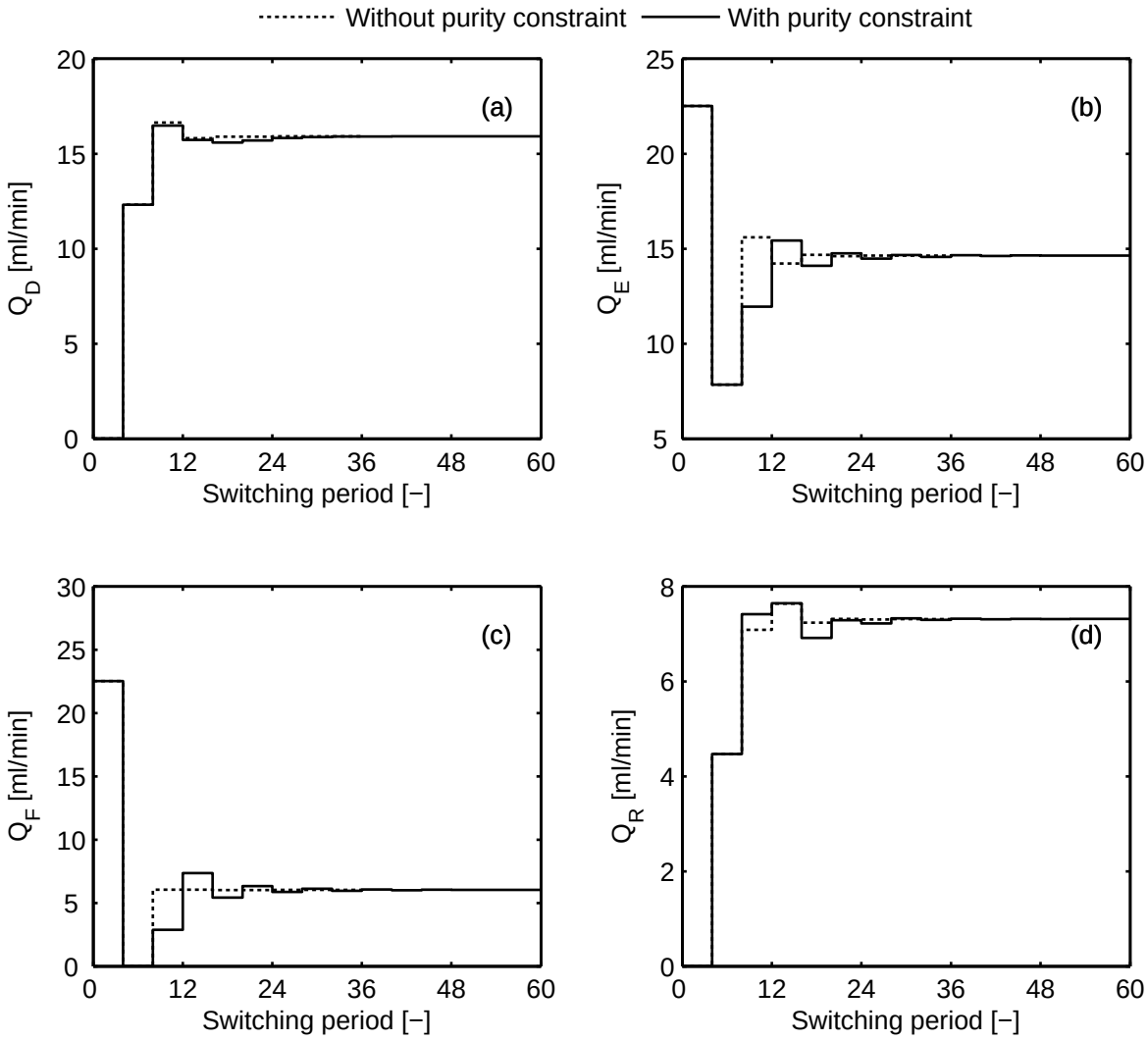

Figure 9.8: Optimal startup profiles (external flow-rates) of multistage strategies with and without purity constraint.

ml/min, and Q_{III}, on the contrary, quickly drops from 60 ml/min to the same value. This causes the feed flow-rate Q_F to decrease to zero. Such a control profile of Q_F can avoid the potential overload of the columns. Moreover, Q_D and Q_R rise from zero to 12.32 ml/min and 4.47 ml/min, respectively. As the stage further advances, the flow-rates shown in Figs. 9.7 and 9.8 gradually converge towards their CSS values. After about 5 stages they have almost reached the nominal values. Note that the flow-rate in zone I always remains at 60 ml/min during the entire startup process.

For the case with purity constraint, the optimal startup regime over the initial two stages is the same as that of the previous scenario. This is because no stage-wise purity requirements are specified on these stages, as already pointed out, and the same two startup optimization sub-problems were solved in this case. Once the extract and raffinate purity constraints are explicitly enforced from the third stage, the obtained optimal operating conditions exhibit a different behavior, as can be seen from Figs. 9.7 and 9.8. In the case of the internal flow-rates, for example, it is readily noted from Fig. 9.7 that such difference with respect to the previous case is particularly striking in Q_{II} and Q_{III}, but much less noticeable in Q_I and Q_{IV}. This can be explained as follows: typically, Q_{II} and Q_{III} have a more significant impact on the extract and raffinate purities, respectively. Therefore, when the purity constraints are imposed, the optimizer chooses to adjust them in order to avoid the violation of the constraints.

The optimal switching periods obtained for both cases are shown in Fig. 9.9. The profiles show a very similar tendency, implying that imposing the purity specifications has a weak effect on this operating variable. It is also observed that the switching period is obviously lower than its CSS setting of 2.8775 min over the initial two stages. This is helpful in shortening

the startup time. The switching period then undergoes a slight overshoot and finally rapidly settles down to the nominal value.

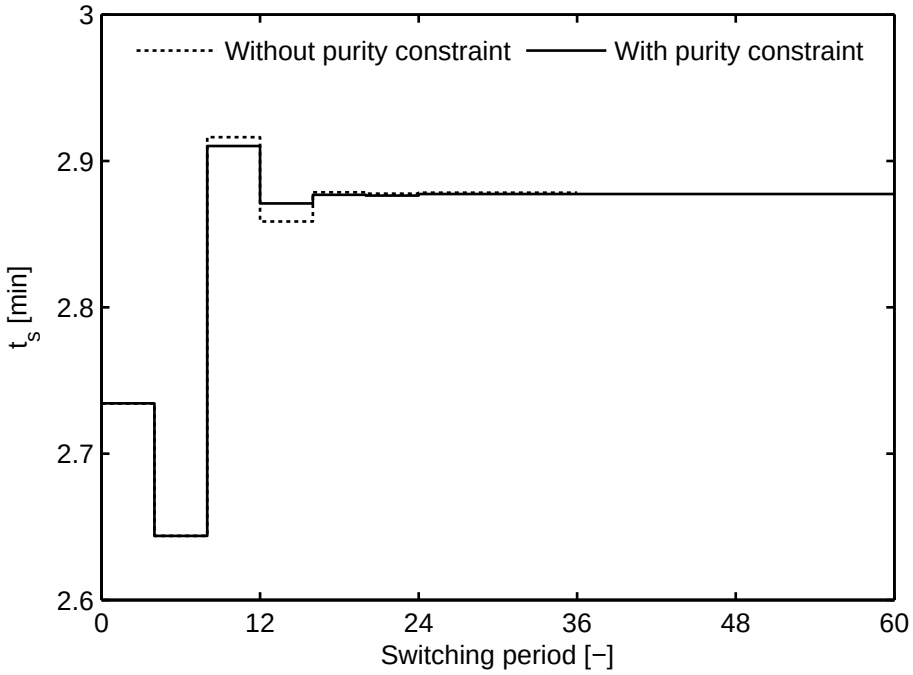

Figure 9.9: Optimal switching period of multistage startup strategies with and without purity constraint.

The development of axial concentration profiles for the multistage strategies over the first four stages is illustrated in the left column of Fig. 9.10. Note that for the scenario with purity constraint, since the profiles at the end of stages 1 and 2 are the same as those obtained without constraint, they were omitted for simplicity in Fig. 9.10a1 and b1, respectively. For comparison purposes, the results of the conventional startup at the end of switching periods 4, 8, 12, and 16 are also plotted in sequence in the right column of the same figure. To allow for fair comparison, the corresponding absolute time elapsed since the beginning of the startup operation is given

explicitly in each sub-graph of Fig. 9.10. It can be observed that the new startup regime without purity constraint enables the process to achieve the fastest convergence to the reference profile, although the case considering the quality constraints also clearly outperforms the conventional approach. At the end of stage 1, the multistage scheme allows to establish a concentration plateau more than two times higher than that of the normal startup (see Fig. 9.10a1, a2). In this case, the raffinate (A) concentration in zones II and III and extract (B) concentration in zones III and IV are even higher than the corresponding reference profiles. For both components, the axial profiles approximate the reference ones rather well at the end of the second stage (Fig. 9.10b1), and even better than those do at the end of switching period 16 in the conventional case (Fig. 9.10d2). Once the stage-wise purity of 90% is required from the next stage, the development of the profiles differs significantly from that without purity specifications. By the end of stage 4, the profiles in the previous case have already perfectly converged. However, fulfilling the purity requirements results in a relatively slower convergence rate, as can be seen in Fig. 9.10c1 and d1. In addition, it is noted from Fig. 9.10c1 that the concentration fronts of component A in zones II and III are shifted to the right relative to those of the previous case. This interesting observation can be elucidated as follows. In the previous discussion on the conventional startup, we have shown the period-wise purity profiles (see Fig. 9.5). The profiles, although obtained with the conventional method, to a certain extent also reflect that respecting the required stage-wise purity of 90% might be more non-trivial for the extract than for the raffinate. Such a variation of the shape of the front can reduce the impurity present in the extract product and help it satisfy the purity requirement.

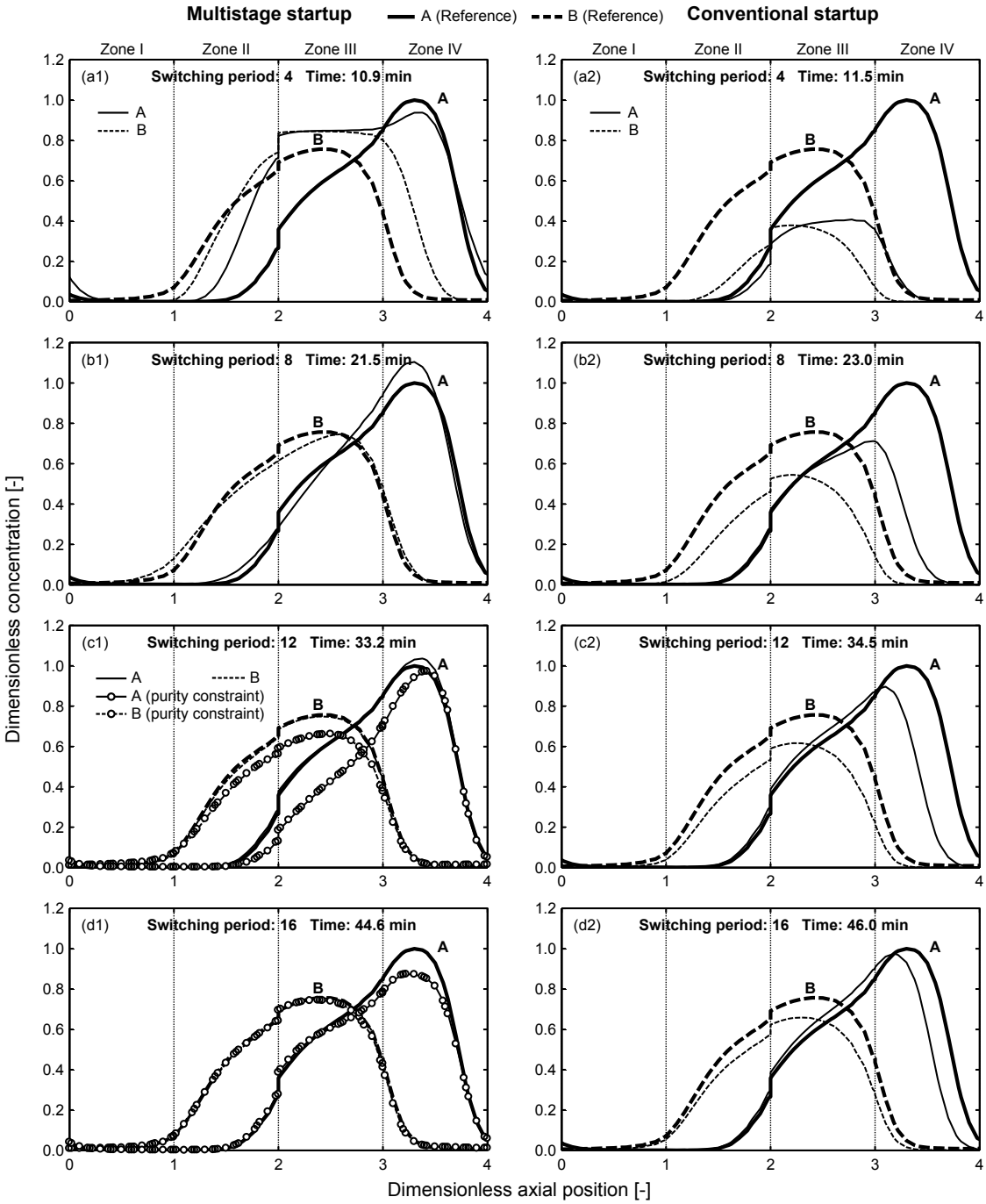

Figure 9.10: Comparison of development of axial concentration profiles with different startup strategies. The profiles are taken at the end of (a) stage 1 (switching period 4), (b) stage 2 (period 8), (c) stage 3 (period 12), and (d) stage 4 (period 16).

9.3.4 Shutdown strategies

To study the shutdown issue, the amount of each component accumulated in the columns at CSS is required, which also shows a periodic behavior. For convenience, the shutdown procedure is assumed to start only after some full CSS period is completed. With this assumption, the accumulated value can be readily calculated by subtracting the amount collected from both extract and raffinate outlets from the total amount supplied to the system until the end of this switching period. The conventional startup approach was used to determine the results. For the model separation, the total masses retained in the columns are 0.2258 g and 0.2293 g for component A and B, respectively. The primary goal of a shutdown procedure is to recover these holdups in an efficient way. For the multistage regime, a sequence of decomposed sub-problems presented in Section 9.2 was solved by the sequential approach. The number of switching periods involved in each stage was specified as eight. In the case that considers the purity specifications, the same requirement of 90% as in the startup case was imposed on the stage-wise shutdown products. For each shutdown scheme examined, once the total recoveries of both components defined in Eq. (9.22) reach the minimum threshold $Re_{i,min}^{T,shutdown} = 99.95\% \, (i = A, B)$, the shutdown phase is considered to be terminated.

A systematic comparison of performance of different shutdown strategies in terms of the shutdown time, desorbent consumption and product purity is demonstrated in Fig. 9.11a, b, and c, respectively. The conventional scheme needs 70 switching periods and 3.36 h to complete the shutdown process, during which the total amount of desorbent consumed is 4423 ml. In this case, it is observed from Fig. 9.11c that an off-spec extract product of purity of 85.03% is produced, although the raffinate purity is higher than 90%. The

fact can be well explained by examining the period-wise purity profiles shown in Fig. 9.12. It is readily noted that the extract purity suffers a dramatic drop from the initial CSS specification of 90% to a poor value of about 30% as the shutdown advances. The raffinate purity, however, develops obviously above the threshold over the most of the shutdown process. In summary, the quantitative results indicate that the conventional shutdown is not able to ensure the quality of the final products either. With the aid of the proposed shutdown regime, the same process takes only one stage (eight switching periods) and totally 0.20 h to shut down and the desorbent consumption can be saved by 68%. Such rapid shutdown is achieved at the sacrifice of the product quality. Both product purities are just around 55% and even lower than those of the conventional mode. Once the purity specification of 90% is required, an on-spec production of the extract and raffinate products can be obtained during shutdown, as can be seen from Fig. 9.11c. However, higher desorbent consumption and longer shutdown time result, compared to those of the previous case. In this last scenario, four stages and 1.82 h are spent to shut down the SMB unit. In contrast to that of the conventional operation, the total time is shortened by 45%. The amount of desorbent used, however, tends to be increased to some degree.

For the optimal operating conditions, it is found that in the case without purity constraint, both Q_I and Q_{III} touch the allowable upper limit of 60 ml/min, while $Q_{IV} = 0$ ml/min and Q_{II} also approaches zero (0.32 ml/min). As a result, $Q_D = Q_R = 60$ ml/min and $Q_E = Q_F = 59.68$ ml/min. The results well approximate one extreme case where $Q_I = Q_{III} = Q_D = Q_E = Q_F = Q_R = 60$ ml/min and $Q_{II} = Q_{IV} = 0$ ml/min, and mean that during the shutdown process, two purge paths are formed to clean the columns and to recover the retained components. The interesting purge regime identified

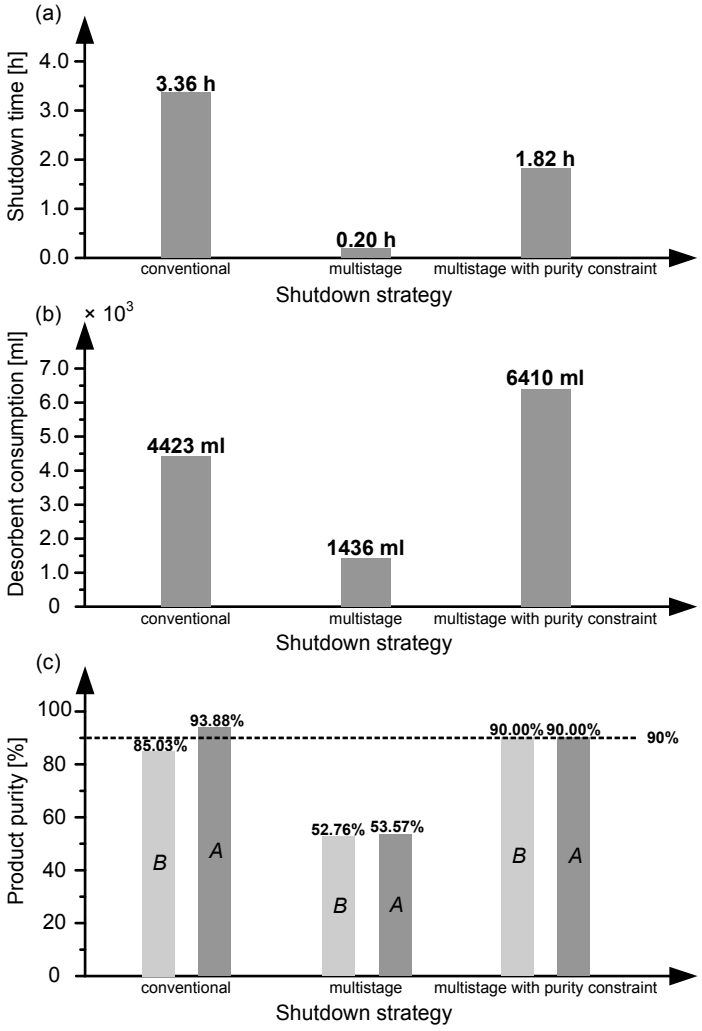

Figure 9.11: Comparison of performance of different shutdown strategies in terms of (a) shutdown time, (b) desorbent consumption, and (c) extract (B) and raffinate (A) product purities. The dashed line in (c) marks the minimum purity threshold of 90%.

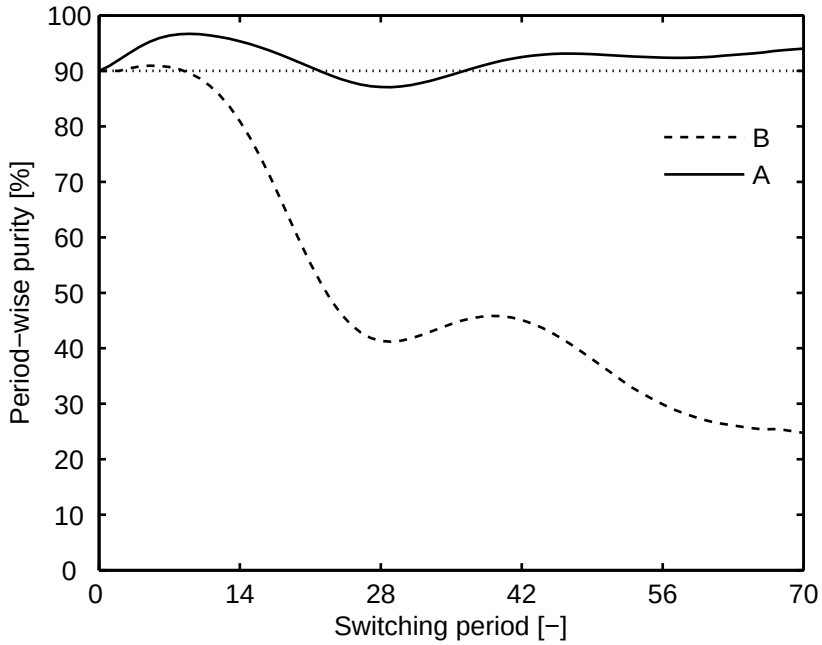

Figure 9.12: Development of period-wise extract (B) and raffinate (A) purities during conventional shutdown. The dotted line marks the purity threshold of 90%.

is shown schematically in Fig. 9.13. A zero flow-rate in both zones II and IV aims to isolate the columns being washed from those to be treated. The purge flows Q_D and Q_F operated at the maximum flow-rate value enable the process to wash the holdups out of the columns efficiently.

The optimal internal flow-rate profiles with purity constraint are illustrated in Fig. 9.14. It can be seen that although the optimal Q_I also remains at the upper bound, the other flow-rates exhibit different behavior in contrast to that without purity constraint. In particular, a significant variation in both Q_{II} and Q_{III} can be observed, which aims to fulfill the purity constraints enforced on each stage. Additionally, the optimal profile of Q_{IV} is not kept at zero as before, but drops from 21.66 ml/min to zero from the

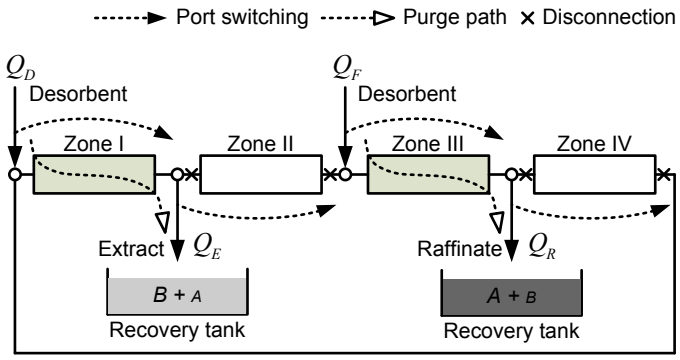

Figure 9.13: Illustration of the purge regime identified from the optimal shutdown operating conditions without purity constraint.

third stage. The external flow-rates also behave distinctly from those in the previous case. For the two purge flows, Q_D does not increase to 60 ml/min until at the third stage; Q_F ranges only from 6 to 11 ml/min and becomes significantly smaller compared to the previous result.

9.4 Rules of thumb

Development of practical and useful guidelines for the transient operation of SMB is of great value, although it is beyond the scope of the thesis. However, it should be noted that such heuristics depends on a number of factors, such as column and component properties, feed concentrations and transient performance criteria. For example, if we minimize the amount of desorbent consumed during startup rather than time, different startup profiles for the operating parameters can be expected. Thus, it is impossible to derive general rules that can be applicable to various cases. In this section, we present some rules of thumb that are summarized only from our previous case studies in Section 9.3. We restrict to the case where a fast startup or shutdown is

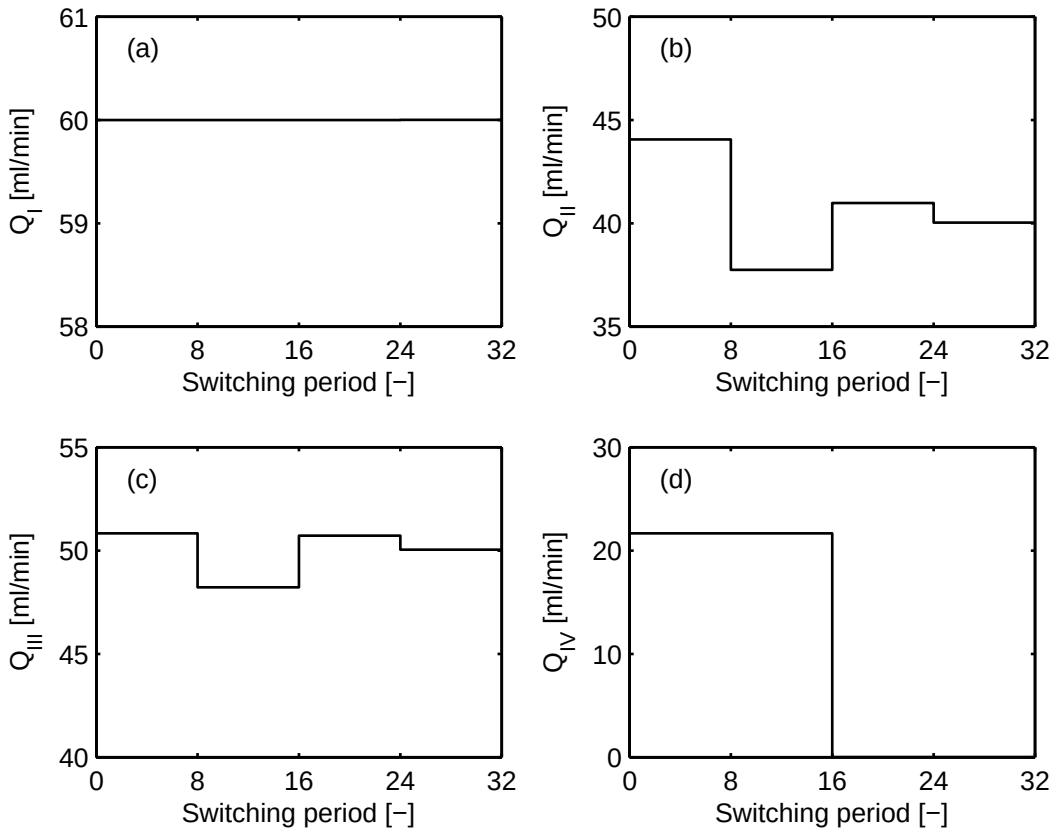

Figure 9.14: Optimal internal flow-rate profiles of the 4-stage shutdown strategy with purity constraint.

our primary concern while product quality is neglected. Furthermore, these rules might be subject to refinement in future as the research in this area advances further.

For the startup problem, it is noted from Figs. 9.7, 9.8 and 9.9 that the operating conditions show a dramatic variation during only the initial few stages, but become increasingly "conservative" as the startup proceeds. This reflects that the first several stages play a crucial role in improving the startup performance. The observation also inspires us to propose the

following reduced three-stage startup procedure:

- In the first stage, shut off both desorbent and raffinate flows (i.e., $Q_D = Q_R = 0$) by setting Q_I, Q_{III} and Q_{IV} to the allowed maximum flow-rate. Supply the mixture with the feed flow-rate several times higher than its nominal value, and at the same time withdraw only the extract stream. Note that here $Q_F = Q_E$ must be maintained in order to match mass balance. The switching period can be chosen to be smaller than its CSS value. This first step is aimed to fill the columns with the concentrated feed and thus the dilution should be avoided.

- Then turn off the supply of fresh feed and activate the desorbent pump to deliver desorbent into the system. Begin to draw off both raffinate and extract. In this stage, adjust Q_D, Q_E and Q_R to be close to but lower than the nominal settings. Their choice should also respect the balance $Q_D = Q_E + Q_R$. The same switching period as that in the preceding stage can be used. The intermediate stage is mainly intended to elute the loaded feed inside the columns.

- Finally, resume the feed supply and switch the operating conditions to their steady state values. The role of the last stage is to induce the process towards its CSS.

When the shutdown campaign begins, if one follows the simple approach discussed in this thesis and just wants to purge the columns quickly, the following heuristics might be advantageous:

- Tune the four external flow-rates together with Q_I and Q_{III} from their CSS values to the upper limit, forcing Q_{II} and Q_{IV} to be zero. The switching period can be kept the same as that at CSS for simplicity.

Then clean the columns with the two desorbent flows step by step until some pre-specified shutdown criterion is fulfilled.

9.5 Concluding remarks

The periodic behavior and complex nonlinear process dynamics of SMB chromatography poses a significant challenge for the formulation and solution of its optimal transient operation problems. In this chapter, the multistage optimal startup and shutdown schemes were suggested. A specially tailored decomposition solution strategy was employed to guarantee the numerical solvability of the resulting dynamic optimization problems. An existing literature separation example with nonlinear competitive Langmuir isotherm was considered as a case study. The feasibility of the developed solution algorithm was demonstrated and the performance achievable by the conventional and multistage operation regimes was evaluated in detail. It was shown that for the case without product quality constraints, the new policies not only drastically reduce transient duration, but also lead to significant savings in desorbent consumption. Another obvious advantage of our multistage approach lies in its ability to optimize transient performance while respecting product quality requirements. This strength enables on-spec production of both extract and raffinate products during the startup and shutdown periods, which cannot be guaranteed with the conventional methods. The result could be extremely attractive for the production of valuable chemical products where either discarding or reprocessing off-spec transient products is highly undesirable. The efficient startup and shutdown strategies presented in this chapter not only are advantageous for continuous large-volume purifications, but also allow SMB chromatography to perform short-term campaigns with

small batch sizes more flexibly and efficiently.

9.6 Nomenclature

c	liquid phase concentration [g/l]
C	liquid phase concentration state vector [g/l]
H	Henry coefficient [-]
K	adsorption equilibrium constant [l/g]
M	mass amount [g]
m	flow-rate ratio parameter [-]
N	number of switching periods [-]
N_C	number of concentration state variables [-]
N_p	number of theoretical plates [-]
P	number of startup or shutdown stages [-]
Pu	purity [%]
Q	liquid phase flow-rate [ml/min]
Re	recovery [%]
t	time [min]
t_s	switching period [min]
u	vector of operating conditions
V	liquid phase volume [ml]
V_{Col}	column volume [cm^3]

Greek letters

ϵ	total column porosity [-]
ϵ_{css}	CSS tolerance [-]
ϵ_{reg}	regularizing coefficient [-]
$\epsilon_{startup}$	startup tolerance [-]
τ	dimensionless time coordinate [-]

τ_n	local dimensionless time coordinate for stage n [-]
τ'_n	starting time of one switching period where τ_n lies [-]

Roman letters

I, II, III, IV	zone index

Subscripts and superscripts

$*$	CSS reference value
0	initial value
A	less retained component
B	more retained component
Col	chromatographic column
D	desorbent
E	extract
F	feed
i	component index, $i = A$, B
j	zone index, $j = I, II, III, IV$
k	switching period index
$mode$	operating mode, $mode = startup$, $shutdown$
n	stage index
R	raffinate
$shutdown$	shutdown
$startup$	startup
T	total quantity

10

Conclusions and future work

10.1 Thesis summary and contributions

This dissertation primarily addressed the steady state and transient optimization problems of SMB chromatography. For the first topic, we devoted our attention to a novel operating alternative, referred to as FF-SMB, which introduces the concept of outlet fractionation and feedback to the conventional SMB operation. Beginning with an in-depth overview of employing recycling techniques in preparative liquid chromatography, we considered a special case of FF-SMB where only one outlet is fractionized. A rigorous model-based mathematical programming approach was applied to optimize its steady state performance. With the aid of the developed optimization framework, the effectiveness of the single fractionation concept was demonstrated, and its optimal potential over the classical SMB process was evaluated systematically. The results revealed that the new operating regime significantly outperforms SMB in terms of the maximum feed throughput and minimum desorbent consumption for both linear and Langmuir isotherms.

The advantages obtained further motivated us to investigate the gener-

alized case characterized by the simultaneous fractionation of both extract and raffinate outlets. The model-based optimization strategy previously proposed was extended to consider this more flexible fractionation mode. To demonstrate its superiority over the existing single fractionation options and classical SMB, extensive optimization studies based on a specific separation problem were carried out for these process alternatives. The quantitative performance comparison substantiated that the double fractionation regime behaves most productively and each single fractionation scheme is clearly superior to conventional SMB chromatography. The potential of the extension was also assessed in terms of commonly used performance parameters. It was shown that FF-SMB presents significant improvements in productivity and product concentration and allows for substantial savings in eluent consumption, while maintaining a level of recovery comparable to that of SMB. The practical applicability of the advanced operating concept was then evaluated in detail by examining the effect of required product purity, adsorption selectivity, column efficiency etc., on its achievable relative advantages. The optimization results showed that FF-SMB has more potential for difficult separations characterized by high product purity requirements, low column efficiency, small selectivity and a small number of columns. For such kind of applications, FF-SMB can be a highly competitive alternative to conventional SMB and its other modifications.

Furthermore, we also explored the possibility of further exploiting the potential of FF-SMB by enriching the recycled fractions before feeding them back into the unit. By considering continuous solvent removal as example, the optimal performance of FF-SMB with enriched recyclates was compared to that of the non-enriched case and standard SMB, with the aim to evaluate the effectiveness of this new concept. It was found that the enrichment

regime allows to create more concentrated recyclates, and feeding back the resulting enriched version is proven advantageous for FF-SMB and leads to further performance enhancement. It was also demonstrated that as improving the extent of enrichment, the advantage over the normal case becomes more significant. Our contributions for the first part of the thesis can be summarized as follows:

- We applied a model-based optimization methodology to investigate FF-SMB. To the best of our knowledge, the thesis is the first work to systematically optimize this advanced operating mode. Compared to the simulation-based method adopted in the previous work [26], our strategy is more systematic and efficient, and allows to exploit the full potential offered by the new process alternative.

- The second major contribution lies in that we extended the single fractionation concept proposed in [26] to the general case which fractionizes both outlets simultaneously. The optimal performance of various fractionation policies was also compared systematically for the first time. Besides, we further introduced the concept of enriching recyclates to FF-SMB and evaluated it with the aid of the developed optimization tool.

- The evaluation of practical applicability performed for FF-SMB constitutes another significant achievement. Such an evaluation is of great importance since it not only gives more comprehensive and deeper insights into the process behavior, but also helps to identify strengths and limitations of FF-SMB. The conclusions drawn from the theoretical evaluation provide an extremely valuable guide for SMB practitioners.

The thesis then discussed the optimal transient operation problems of

SMB. We started this second part by providing an introductory overview on the transient operation of SMB chromatography. The relevance and benefits of developing efficient transient operating procedures were particularly highlighted. A literature survey which summarizes the previous work related to the challenging task was given. We showed that none of the recent research endeavors had explicitly optimized the startup and shutdown processes of SMB. We next briefly reviewed different design methods suggested for SMB. These approaches represent significant contributions to the steady state design and operation of the process, but they do not consider the transient performance. We then discussed the conventional startup and shutdown strategies, which simply specify the steady state operating parameters as the transient policies. The conventional methods, although being easy to implement, often suffer from long transient duration and a large amount of desorbent consumption. Furthermore, they cannot ensure that the products collected during the transient periods are on-spec. If off-spec production occurs, the transient products have to be discarded or subject to reprocessing, causing a significantly adverse impact on overall process economics and efficiency.

In order to overcome the shortcomings of the conventional operations and to improve the transient performance of the SMB process, we developed new multistage optimal startup and shutdown procedures. The proposed concept allows for a stage-wise modulation of the transient operating conditions and is able to conveniently take the product quality specifications into account. We then formulated the optimal transient operation as a dynamic optimization problem. The objective is to find the optimal operating conditions with which the process can be driven optimally towards the reference concentration profile, while fulfilling the constraints imposed during the tran-

sient phase. However, the inherent periodic nature of the process dynamics greatly complicates the direct solution of the original problem. To guarantee computational tractability, we presented a specially tailored decomposition algorithm. The solution approach decomposes the overall problem into a sequence of stage-wise sub-problems, each of which is of reduced complexity and thus easier to deal with. We then demonstrated the feasibility of the solution strategy, and systematically evaluated the performance of the conventional and multistage optimal schemes by examining a binary separation example with Langmuir isotherm. The results proved that the newly developed transient regimes not only obviously shorten the startup and shutdown time, but also drastically reduce the desorbent consumption. Another advantage which was also clearly revealed lies in that the multistage approach is capable of optimizing the transient performance, while respecting the product quality requirements. This strength allows the process to achieve the on-spec production of both extract and raffinate products over the startup and shutdown periods, which is infeasible with the conventional schemes. The contributions made in this part of the dissertation are outlined as below:

- Optimal transient operation is not a new topic in the field of process engineering, and has been studied for a variety of process systems, in particular for those of continuous dynamics. However, for the periodically operated SMB process, as far as is known to the author, the work is the first contribution to address in a systematic manner its optimal startup and shutdown problems.

- Our multistage strategy outperforms the conventional operation and significantly enhances the transient performance. This improvement is of great value to applications of different production scales. In particular, the efficient startup and shutdown procedures developed can

expand the applicability of SMB chromatography to short-term campaigns with small batch sizes, and allow SMB to carry out these kinds of separations more efficiently and flexibly.

- We suggested some rules of thumb based on our theoretical optimization results. These qualitative operating heuristics, although somewhat coarse, can serve as helpful guidelines for efficient transient operations of practical SMB units.

10.2 Recommendations for future work

Exploring the two interesting topics of the thesis has also helped us to identify many potential directions for improvement as well as challenging problems that are worth further investigating. Below we summarize the recommendations for future work of each topic.

10.2.1 FF-SMB

The focus problem in the future is to practically implement the fractionation and feedback regime to SMB units and to validate the conclusions drawn in this work experimentally. Since the additional hardware investment of the new system is rather low, its practical implementation may not take much effort. Firstly validating the simple concept of fractionating one outlet, and then extending to more flexible cases realizing double fractionation and recyclate enrichment would be a reasonable path for practitioners to follow. Obviously, our optimization studies together with the previous work [26] have laid a solid theoretical foundation for the successful achievement of this goal.

As far as the theoretical research of FF-SMB concerned, there still exists some interesting aspects that are not examined in the thesis and deserve a

detailed study in the future:

- When optimizing FF-SMB, we restrict our consideration to the case where each buffer vessel neither overflows nor "runs dry" but exhibits a stable periodic behavior. However, it is also interesting to relax the restrictions imposed on the liquid levels of the vessels. For example, one can assume that the buffer tanks have a sufficiently large volume and a gradual increase of the liquids is allowed during operating FF-SMB.

- In addition, coupling the fractionation and feedback approach with other advanced SMB operating modes, such as those reviewed previously in Chapter 1, is also very appealing. It can be expected that the resulting hybrid scheme will provide more advantages than each single regime.

Another relevant topic that was not explored in the thesis is regarding the control of FF-SMB. Since model uncertainties and disturbances exist inevitably in practice, operating the process close to its optimal operating point remains a challenge. This calls for the development and implementation of efficient control algorithms for FF-SMB, which can improve the process robustness and allow for the full exploitation of its advantages. During examining the new concept, we have noted that the production periods ($\tau^{E}_{Production}$ and $\tau^{R}_{Production}$) have a most significant impact on the product purities. Thus, a simple control approach is to manipulate the two operating variables directly to guarantee the purity specifications in the presence of disturbances. This can be easily implemented by two standard single-loop proportional-integral-derivative (PID) controllers. Our preliminary simulation results have demonstrated the feasibility of this control scheme. Other advanced optimization based strategies, such as model predictive control (MPC) suggested for con-

ventional SMB [31, 92], can be also extended to the FF-SMB process. These schemes can exploit the full degrees of freedom and conveniently handle the operational and product quality constraints, while online optimizing some given performance criterion. However, they need much computational effort compared to the previous method, and thus the real-time feasibility for FF-SMB is a key issue that is worth evaluating. In addition, for the experimental validation of both kinds of control concepts, a reliable and accurate purity measurement is critical and deserves much attention.

10.2.2 Transient operation of SMB

Compared to the steady state optimization of SMB, the optimal transient operation of such periodic adsorption process still remains largely unexplored. We summarize the potential directions for future work for this challenging research field as follows:

- The encouraging results presented in this work motivate us to evaluate the new transient operating strategies experimentally in the future. For this purpose, the detailed characterization of the system under examination and its steady state studies are necessary.

- We optimize only the continuous operating conditions and fix a priori the number of switching periods when dealing with each stage-wise sub-problem. However, treating also this parameter as one decision variable allows for the full exploitation of the degrees of freedom, and is expected to produce further improvement in transient performance. In this case, the original problem can be formulated as an MINLP problem, for which efficient and reliable solution algorithms are needed.

- In this thesis we restrict our discussion to two typical transients. In

the future, our work can be easily extended to optimize the grade transition operation of SMB, where the plant is required to transfer from one CSS to another in some optimal way to produce different grades of products. Furthermore, although we demonstrate the multistage approach only for the conventional SMB process, the proposed concept is quite generic and can be generalized to various advanced SMB variants and other classes of periodic adsorption systems, such as pressure swing adsorption (PSA) processes.

- Development of efficient solution algorithms for the optimal transient operation problems of SMB remains an open question so far. The suggested decomposition algorithm can guarantee only the stage-wise optimality. The resulting solution is only an approximation and might be suboptimal for the original problem. The model and parameter uncertainty is also neglected in the problem formulation. These limitations motivate us to explore alternative solution approaches that can avoid decomposition, and to take uncertainties into account in the future. They constitute the most challenging issues that need be addressed.

- The ultimate objective of our theoretical studies is to transfer specific transient optimization results to practically applicable operating rules, since the latter are of significant interest for SMB practitioners. Thus, refinement of existing rules of thumb and experimental validation of their effectiveness need to be carried out with high priority in the future.

Bibliography

[1] D.B. Broughton, C.G. Gerhold, Continuous sorption process employing fixed beds of sorbent and moving inlets and outlets, US Patent 2,985,589 (1961). 2, 11

[2] M. Juza, M. Mazzotti, M. Morbidelli, Simulated moving-bed chromatography and its application to chirotechnology, Trends Biotechnol. 18 (2000) 108-118. 2

[3] M. Negawa, F. Shoji, Optical resolution by simulated moving-bed adsorption technology, J. Chromatogr. 590 (1992) 113-117. 2

[4] E.R. Francotte, P. Richert, Applications of simulated moving-bed chromatography to the separation of the enantiomers of chiral drugs, J. Chromatogr. A 769 (1997) 101-107. 2

[5] S. Imamoglu, Simulated moving bed chromatography (SMB) for application in bioseparation, Advances in Biochemical Engineering/Biotechnology, 76 (2002) 211-231. 2

[6] M. Schulte, J. Strube, Preparative enantioseparation by simulated moving bed chromatography, J. Chromatogr. A 906 (2001) 399-416. 2

[7] A. Seidel-Morgenstern, L.C. Keßler, M. Kaspereit, New developments in simulated moving bed chromatography, Chem. Eng. Technol. 31 (2008) 826-837. 3

[8] A. Rajendran, G. Paredes, M. Mazzotti, Simulated moving bed chromatography for the separation of enantiomers, J. Chromatogr. A 1216 (2009) 709-738. 3, 17

[9] M. Mazzotti, G. Storti, M. Morbidelli, Supercritical fluid simulated moving bed chromatography, J. Chromatogr. A 786 (1997) 309-320. 2

[10] C. Migliorini, M. Wendlinger, M. Mazzotti, M. Morbidelli, Temperature gradient operation of a simulated moving bed unit, Ind. Eng. Chem. Res. 40 (2001) 2606-2617. 2

[11] D. Antos, A. Seidel-Morgenstern, Application of gradients in the simulated moving bed process, Chem. Eng. Sci. 56 (2001) 6667-6682. 2

[12] O. Ludemann-Hombourger, R.M. Nicoud, M. Bailly, The "VARICOL" process: a new multicolumn continuous chromatographic process, Sep. Sci. Technol. 35 (2000) 1829-1862. 3

[13] Z. Zhang, M. Mazzotti, M. Morbidelli, PowerFeed operation of simulated moving bed units: changing flow-rates during the switching interval, J. Chromatogr. A 1006 (2003) 87-99. 3

[14] H. Schramm, M. Kaspereit, A. Kienle, A. Seidel-Morgenstern, Simulated moving bed process with cyclic modulation of the feed concentration, J. Chromatogr. A 1006 (2003) 77-86. 3, 13, 49

[15] G. Hotier, Physically meaningful modeling of the 3-zone and 4-zone simulated moving bed processes, AIChE J. 42 (1996) 154-160. 3

[16] W. Jin, P.C. Wankat, Two-zone SMB process for binary separation, Ind. Eng. Chem. Res. 44 (2005) 1565-1575. 3

[17] X. Wang, C.B. Ching, Chiral separation of β-blocker drug (nadolol) by five-zone simulated moving bed chromatography, Chem. Eng. Sci. 60 (2005) 1337-1347. 3

[18] R. Wooley, Z. Ma, N.-H.L. Wang, A nine-zone simulating moving bed for the recovery of glucose and xylose from biomass hydrolyzate, Ind. Eng. Chem. Res. 37 (1998) 3699-3709. 3

[19] N. Abunasser, P.C. Wankat, Y.-S. Kim, Y.-M. Koo, One-column chromatograph with recycle analogous to a four-zone simulated moving bed, Ind. Eng. Chem. Res. 42 (2003) 5268-5279. 3

[20] N. Abunasser, P.C. Wankat, One-column chromatograph with recycle analogous to simulated moving bed adsorbers: analysis and applications, Ind. Eng. Chem. Res. 43 (2004) 5291-5299. 3, 121

[21] J.P.B. Mota, J.M.M. Araújo, Single-column simulated-moving-bed process with recycle lag, AIChE J. 51 (2005) 1641-1653. 3

[22] R.C.R. Rodrigues, J.M.M. Araújo, M.F.J. Eusébio, J.P.B. Mota, Experimental assessment of simulated moving bed and varicol processes using a single-column setup, J. Chromatogr. A 1142 (2007) 69-80. 3, 121

[23] Y. Zang, P.C. Wankat, SMB operation strategy–Partial feed, Ind. Eng. Chem. Res. 41 (2002) 2504-2511. 3

[24] Y.-S. Bae, C.-H. Lee, Partial-discard strategy for obtaining high purity products using simulated moving bed chromatography, J. Chromatogr. A 1122 (2006) 161-173. 3, 36, 44

[25] L.C. Keßler, A. Seidel-Morgenstern, EU Patent 07,007,765 (2007). 37

[26] L.C. Keßler, A. Seidel-Morgenstern, Improving performance of simulated moving bed chromatography by fractionation and feed-back of outlet streams, J. Chromatogr. A 1207 (2008) 55-71. 3, 5, 13, 37, 52, 54, 55, 60, 65, 91, 175, 178

[27] G. Guiochon, Preparative liquid chromatography, J. Chromatogr. A 965 (2002) 129-161. 13

[28] G. Guiochon, A. Fellinger, S.G. Shirazi, A.M. Katti, Fundamentals of preparative and nonlinear chromatography, 2nd ed. Academic Press, Boston, 2006. 13, 14

[29] C. Migliorini, A. Gentilini, M. Mazzotti, M. Morbidelli, Design of simulated moving bed units under nonideal conditions, Ind. Eng. Chem. Res. 38 (1999) 2400-2410. 13

[30] H. Schramm, S. Grüner, A. Kienle, Optimal operation of simulated moving bed chromatographic processes by means of simple feedback control, J. Chromatogr. A 1006 (2003) 3-13. 13, 146

[31] G. Erdem, S. Abel, M. Morari, M. Mazzotti, M. Morbidelli, J.H. Lee, Automatic control of simulated moving beds, Ind. Eng. Chem. Res. 43 (2004) 405-421. 13, 180

[32] G.F. Carey, B.A. Finlayson, Orthogonal collocation on finite elements, Chem. Eng. Sci. 30 (1975) 587-596. 16

[33] S. Li, L. Petzold, Design of new DASPK for sensitivity analysis, Technical Report, University of California, Santa Barbara, CA, USA, 1999. 16, 59, 84, 148

[34] G. Storti, M. Mazzotti, M. Morbidelli, S. Carrá, Robust design of binary countercurrent adsorption separation processes, AIChE J. 39 (1993) 471-492. 17

[35] M. Mazzotti, G. Storti, M. Morbidelli, Optimal operation of simulated moving bed units for nonlinear chromatographic separations, J. Chromatogr. A 769 (1997) 3-24. 17, 18, 20, 22, 125

[36] A. Gentilini, C. Migliorini, M. Mazzotti, M. Morbidelli, Optimal operation of simulated moving-bed units for non-linear chromatographic separations: II. Bi-Langmuir isotherm, J. Chromatogr. A 805 (1998) 37-44. 17

[37] M. Mazzotti, Equilibrium theory based design of simulated moving bed processes for a generalized Langmuir isotherm, J. Chromatogr. A 1126 (2006) 311-322. 17

[38] M. Kaspereit, A. Seidel-Morgenstern, A. Kienle, Design of simulated moving bed processes under reduced purity requirements, J. Chromatogr. A 1162 (2007) 2-13. 17

[39] A. Rajendran, Equilibrium theory-based design of simulated moving bed processes under reduced purity requirements: linear isotherms, J. Chromatogr. A 1185 (2008) 216-222. 17

[40] K.J. Bombaugh, W.A. Dark, R.F. Levangie, High resolution steric chromatography, J. Chromat. Sci. 7 (1969) 42-47. 30

[41] A. Seidel-Morgenstern, G. Guiochon, Theoretical study of recycling in preparative chromatography, AIChE J. 39 (1993) 809-819. 30, 31

[42] C. Heuer, A. Seidel-Morgenstern, P. Hugo, Experimental investigation and modelling of closed-loop recycling in preparative chromatography, Chem. Eng. Sci. 50 (1995) 1115-1127. 30

[43] M. Bailly, D. Tondeur, Recycle optimization in non-linear productive chromatography–I Mixing recycle with fresh feed, Chem. Eng. Sci. 37 (1982) 1199-1212. 31, 36

[44] M. Bailly, D. Tondeur, Reversibility and performances in productive chromatography, Chem. Eng. Process. 18 (1984) 293-302. 32

[45] F. Charton, M. Bailly, G. Guiochon, Recycling in preparative liquid chromatography, J. Chromatogr. A 687 (1994) 13-31. 32, 33

[46] C.M. Grill, Closed-loop recycling with periodic intra-profile injection: a new binary preparative chromatographic technique, J. Chromatogr. A 796 (1998) 101-113. 33, 35, 36

[47] C.M. Grill, L. Miller, Separation of a racemic pharmaceutical intermediate using closed-loop steady state recycling, J. Chromatogr. A 827 (1998) 359-371. 33

[48] I. Quiñones, C.M. Grill, L. Miller, G. Guiochon, Modeling of separations by closed-loop steady-state recycling chromatography of a racemic pharmaceutical intermediate, J. Chromatogr. A 867 (2000) 1-21. 35

[49] C.M. Grill, L. Miller, T.Q. Yan, Resolution of a racemic pharmaceutical intermediate: A comparison of preparative HPLC, steady state recycling, and simulated moving bed, J. Chromatogr. A 1026 (2004) 101-108. 36

[50] J.H. Kennedy, M.D. Belvo, V.S. Sharp, J.D. Williams, Comparison of separation efficiency of early phase active pharmaceutical intermediates by steady state recycle and batch chromatographic techniques, J. Chromatogr. A 1046 (2004) 55-60. 36

[51] T.Q. Yan, C. Orihuela, Rapid and high throughput separation technologies–Steady state recycling and supercritical fluid chromatography for chiral resolution of pharmaceutical intermediates, J. Chromatogr. A 1156 (2007) 220-227. 36

[52] T. Sainio, M. Kaspereit, Analysis of steady state recycling chromatography using equilibrium theory, Sep. Purif. Technol. 66 (2009) 9-18. 36

[53] G. Dünnebier, K.-U. Klatt, Optimal operation of simulated moving bed chromatographic processes, Comput. Chem. Eng. 23 (1999) S195-S198. 53, 57

[54] G. Dünnebier, J. Fricke, K.-U. Klatt, Optimal design and operation of simulated moving bed chromatographic reactors, Ind. Eng. Chem. Res. 39 (2000) 2290-2304. 53, 57

[55] A. Toumi, F. Hanish, S. Engell, Optimal operation of continuous chromatographic processes: Mathematical optimization of the VARICOL process, Ind. Eng. Chem. Res. 41 (2002) 4328-4337. 53, 57

[56] A. Toumi, S. Engell, O. Ludemann-Hombourger, R.M. Nicoud, M. Bailly, Optimization of simulated moving bed and Varicol processes, J. Chromatogr. A 1006 (2003) 15-31. 53, 57

[57] Z. Zhang, K. Hidajat, A.K. Ray, M. Morbidelli, Multiobjective optimization of SMB and varicol process for chiral separation, AIChE J. 48 (2002) 2800-2816. 53, 59

[58] Z. Zhang, M. Mazzotti, M. Morbidelli, Multiobjective optimization of simulated moving bed and Varicol processes using a genetic algorithm, J. Chromatogr. A 989 (2003) 95-108. 53, 59

[59] Z. Zhang, M. Mazzotti, M. Morbidelli, Continuous chromatographic processes with a small number of columns: Comparison of simulated moving bed with Varicol, PowerFeed, and ModiCon, Korean J. Chem. Eng. 21 (2004) 454-464. 53, 54, 59

[60] H.J. Subramani, K. Hidajat, A.K. Ray, Optimization of reactive SMB and Varicol systems, Comput. Chem. Eng. 27 (2003) 1883-1901. 53, 59

[61] M. Amanullah, M. Mazzotti, Optimization of a hybrid chromatography-crystallization process for the separation of Tröger's base enantiomers, J. Chromatogr. A 1107 (2006) 36-45. 53, 54, 59

[62] Y. Kawajiri, L.T. Biegler, Large scale nonlinear optimization for asymmetric operation and design of simulated moving beds, J. Chromatogr. A 1133 (2006a) 226-240. 58

[63] Y. Kawajiri, L.T. Biegler, Optimization strategies for simulated moving bed and PowerFeed processes, AIChE J. 52 (2006b) 1343-1350. 58

[64] Y. Kawajiri, L.T. Biegler, Nonlinear programming superstructure for optimal dynamic operations of simulated moving bed processes, Ind. Eng. Chem. Res. 45 (2006c) 8503-8513. 58

[65] J. Hakanen, Y. Kawajiri, K. Miettinen, L.T. Biegler, Interactive multi-objective optimization for simulated moving bed processes, Control and Cybernetics 36 (2007) 283-302. 53

[66] Y. Kawajiri, L.T. Biegler, Comparison of configurations of a four-column simulated moving bed process by multi-objective optimization, Adsorption 14 (2008) 433-442. 53, 58

[67] J.M.M. Araújo, R.C.R. Rodrigues, J.P.B. Mota, Use of single-column models for efficient computation of the periodic state of a simulated moving-bed process, Ind. Eng. Chem. Res. 45 (2006) 5314-5325. 58

[68] J.M.M. Araújo, R.C.R. Rodrigues, J.P.B. Mota, Optimal design and operation of a certain class of asynchronous simulated moving bed processes, J. Chromatogr. A 1132 (2006) 76-89. 54, 58

[69] G. Ziomek, D. Antos, Stochastic optimization of simulated moving bed process: Sensitivity analysis for isocratic and gradient operation, Comput. Chem. Eng. 29 (2005) 1577-1589. 54, 59

[70] L. Jiang, L.T. Biegler, V.G. Fox, Simulation and optimization of pressure-swing adsorption systems for air separation, AIChE J. 49 (2003) 1140-1157. 58

[71] A. Toumi, S. Engell, M. Diehl, H.G. Bock, J. Schlöder, Efficient optimization of simulated moving bed processes, Chem. Eng. Process. 46 (2007) 1067-1084. 58

[72] F.G. Cauley, S.F. Cauley, N.-H.L. Wang, Standing wave optimization of SMB using a hybrid simulated annealing and genetic algorithm (SAGA), Adsorption 14 (2008) 665-678. 59

[73] E. Kloppenburg, E.D. Gilles, A new concept for operating simulated moving-bed processes, Chem. Eng. Technol. 22 (1999) 813-817. 58

[74] The NAG Fortran Library Manual. Mark 18, Vol. 5, NAG Ltd., Oxford, 1997. 59, 84, 148

[75] L. Hascoët, V. Pascual, TAPENADE 2.1 user's guide, INRIA Sophia-Antipolis, Cedex, France, 2004. 60

[76] H. Kniep, Vergleich verschiedener verfahrenstechnischer Konzepte zur Durchführung der präparativen Flüssigchromatographie, PhD Thesis, Otto-von-Guericke-Universität Magdeburg, Germany (1997). 60

[77] M. Bailly, R.-M. Nicoud, A. Philippe, O. Ludemann-Hombourger, Method and device for chromatography comprising a concentration step, U.S. Patent Application No. WO2004039468, 2004. 108

[78] J. Siitonen, T. Sainio, M. Kaspereit, Theoretical analysis of steady state recycling chromatography with solvent removal, Sep. Purif. Technol. 78 (2011) 21-32. 108

[79] B.G. Lim, C.B. Ching, Modelling studies on the transient and steady state behaviour of a simulated counter-current chromatographic system, Sep. Technol. 6 (1996) 29-41. 121

[80] Y. Xie, S.Y. Mun, N.-H.L. Wang, Startup and shutdown strategies of simulated moving bed for insulin purification, Ind. Eng. Chem. Res. 42 (2003) 1414-1425. 121

[81] Y.-S. Bae, J.-H. Moon, C.-H. Lee, Effects of feed concentration on the startup and performance behaviors of simulated moving bed chromatography, Ind. Eng. Chem. Res. 45 (2006) 777-790. 121

[82] Y.-S. Bae, K.-M. Kim, J.-H. Moon, S.-H. Byeon, I.-S. Ahn, C.-H. Lee, Effects of flow-rate ratio on startup and cyclic steady-state behaviors of simulated moving bed under linear conditions, Sep. Purif. Technol. 62 (2008) 148-159. 121

[83] G. Zenoni, M. Pedeferri, M. Mazzotti, M. Morbidelli, On-line monitoring of enantiomer concentration in chiral simulated moving bed chromatography, J. Chromatogr. A 888 (2000) 73-83. 121

[84] Z. Ma, N.-H.L. Wang, Standing wave analysis of SMB chromatography: Linear systems, AIChE J. 43 (1997) 2488-2508. 121, 125

[85] E. Sørensen, S. Skogestad, Optimal startup procedures for batch distillation, Comput. Chem. Eng. (20) 1996 S1257-S1262.

[86] G. Wozny, P. Li, Optimisation and experimental verification of startup policies for distillation columns, Comput. Chem. Eng. 28 (2004) 253-265. 120, 137, 138

[87] D.R. Hahn, L.T. Fan, C.L. Hwang, Optimal startup control of a jacketed tubular reactor, AIChE J. 17 (1971) 1394-1401. 120, 138

[88] J.W. Verwijs, H. van den Berg, K.R. Westerterp, Startup strategy design and safeguarding of industrial adiabatic tubular reactor systems, AIChE J. 42 (1996) 503-515. 120

[89] L. Luperini-Enciso, H. Purón-Zepeda, L. Pedraza-Segura, A. Flores-Tlacuahuac, Optimal startup/shutdown operating policies with a recombinant strain continuously stirred bioreactor, Ind. Eng. Chem. Res. 49 (2010) 308-316. 120, 138

[90] S. Haugwitz, J. Åkesson, P. Hagander, Dynamic startup optimization of a plate reactor with uncertainties, Journal of Process Control 19 (2009) 686-700. 121

[91] B. Chachuat, A. Mitsos, P.I. Barton, Optimal startup of microfabricated power generation processes employing fuel cells, Optim. Control Appl. Meth. 31 (2010) 471-495. 121, 137, 138

[92] A. Toumi, S. Engell, Optimization-based control of a reactive simulated moving bed process for glucose isomerization, Chem. Eng. Sci. 59 (2004) 3777-3792. 180